# FUNCTIONAL NEAR INFRARED SPECTROSCOPY (FNIRS) IMAGING FOR RESTING STATE FUNCTIONAL CONNECTIVITY IN POST STROKE RECOVERY

**ARUN K M**

PHD THESIS

2020

THE SREE CHITRA TIRUNAL INSTITUTE
FOR
MEDICAL SCIENCES AND TECHNOLOGY, TRIVANDRUM

# FUNCTIONAL NEAR INFRARED SPECTROSCOPY (FNIRS) IMAGING FOR RESTING STATE FUNCTIONAL CONNECTIVITY IN POST STROKE RECOVERY

A THESIS PRESENTED BY

**ARUN K M**

TO

THE SREE CHITRA TIRUNAL INSTITUTE FOR
MEDICAL SCIENCES AND TECHNOLOGY, TRIVANDRUM

IN PARTIAL FULLFILMENT OF THE REQUIREMENTS

FOR THE AWARD OF

**DOCTOR OF PHILOSOPHY**

2020

# Certificate

I Arun K M hereby certify that I had personally carried out the work depicted in the thesis "Functional Near Infrared Spectroscopy (FNIRS) imaging for resting state functional connectivity in post stroke recovery". No part of the thesis has been submitted for the award of any degree or diploma prior to this date.

Date: Arun K M

# Certificate By Guide

Name of the guide : Dr C Kesavadas

Division/Department : Imaging Sciences and Interventional Radiology

This is to certify that Mr. Arun K M in the Department of Imaging Sciences and Interventional Radiology, Sree Chitra Tirunal Institute for Medical Sciences and Technology, Trivandrum has fulfilled the requirements prescribed for the Ph.D. degree of Sree Chitra Tirunal Institute for Medical Science and Technology, Trivandrum.

The thesis entitled “Functional Near Infrared Spectroscopy (FNIRS) imaging for resting state functional connectivity in post stroke recovery ” was carried out under my direct supervision. No part of this work has been submitted for the award of any other degree or diploma prior to this date.

Clearance was obtained from the Institutional Ethics Committee for carrying out the study.

Signature :

Date:

**Approval of Thesis**

The thesis entitled

**FUNCTIONAL NEAR INFRARED SPECTROSCOPY (FNIRS) IMAGING FOR RESTING STATE FUNCTIONAL CONNECTIVITY IN POST STROKE RECOVERY**

Submitted by

**Arun K M**

for the degree of

Doctor of Philosophy

of

SREE CHITRATIRUNAL INSTITUTE

FOR

MEDICAL SCIENCE AND TECHNOLOGY, TRIVANDRUM

Thiruvananthapuram

Is evaluated and approved by

Name of the Guide

Name of thesis Examiner

# Acknowledgements

I am greatly indebted to my Ph.D. supervisor **Dr. C. Kesavadas**, Professor and Head of the department of Imaging Sciences and Interventional Radiology, SCTIMST, for his constant support and invaluable insights of high standards which helped to improve the quality of research work and scientific thinking through out the duration of the study. I am fortunate to get immense moral support from him during the hardships.

I express my sincere gratitude to my Doctoral Advisory Committee members, **Dr. Bejoy Thomas**, Professor, Department of Imaging Science and Interventional Radiology, SCTIMST, **Dr. Sylaja P. N**, Professor, Department of Neurology, SCTIMST, for their valuable suggestions , corrections and constant encouragement. Dr. Bejoy have always given a critical assessment of the work and helped in improving the quality of the work. Dr Sylaja was kind enough to help me in the patient recruitment and provided me with vital clinical details required for the study.

I express my special thanks to **Dr Ranganatha Sitaram**,Associate Professor and Director of Brain Machine Interfaces and Neuromodulation Laboratory, Catholic university of Chile and VAJRA faculty to SCTIMST, who has been instrumental in giving me opportunity to get trained in the optical imaging modality.

I am thankful to all DM Resident doctors, Radiographers and DAMITS of the Dept. of Imaging Science and Interventional Radiology of SCTIMST for their constant words of encouragement and clearing my doubts all throughout the duration of my research.

I express my sincere gratitude to **Department of Biotechnology, Government of India** for the financial assistance and **Indian Council for Medical Research** for the awarding me the Senior Research Fellowship to conduct this research study.

Special thanks to my dearest colleagues, Dr Sujesh S, Dr. Smitha K.A, Rajesh P.G, Dr.Sheela Nair,Anuvitha Chandran,Diljith Singh Kajal, Subramaniom A ,Anu Sundar, Maha Laxmi, Vijay Yanamala,Mashal P K, Darshana Regunath, Shania Soman, Gautami Nair, Priya Ajayaghosh and Josline for their timely help and good company ensuring the progress of the study.

It would not have been possible without the support from the family and in-laws. I would like to acknowledge their constant support.I would like to thank all the mentors who have taught me in life from school days till now for the knowledge transferred to me and I see GOD in those souls.Once again I wish to thank all those people who made this thesis possible.

# Dedication

The thesis is dedicated to my wife Mrs.Sivapriya Devidas K. The undying persistence and support from her was second to none other reason for the completion of the thesis.

# Table of Contents

# List of Figures

# List of Tables

# SYNOPSIS

Several neurological functions are impaired by stroke. The most common deficit is for motor functions of the body. A stroke lesion on the left hemisphere of the brain will cause a deficit in the opposite side of the body. Many rehabilitation techniques based on motor learning paradigms have been developed to expedite the recovery of compromised movement in patients with stroke. Early stroke rehabilitation is critical for enhancing motor recovery, but the optimal time window for specific neuro-rehabilitation has yet to be developed. The concept of brain plasticity has been shown to us in various studies wherein some brain regions in the adult brain can change in structure and function during the process of learning. This very idea is utilized in the recovery from deficits due to stroke through rehabilitation techniques over time.

Neuroimaging studies help to understand the functioning of various brain regions. Functional Magnetic Resonance Imaging (fMRI), Positron Emission Tomography (PET), Electroencephalogram (EEG), Functional Near Infrared Spectroscopy (fNIRS), etc. are the techniques used for evaluating functional aspects of the brain. Recovery from stroke is attributed to the reorganization of the motor cortex and associated areas in the brain. The cortical reorganization is of interest to various neuroimaging study groups as the insight into the recovery process will help to formulate the rehabilitation strategies for respective deficits. fMRI and PET studies have reported the functional reorganization of the motor cortex. The concern with these imaging modalities is the requirement for the subject to be lying in the scanner for a considerable amount of time even during their distress due to stroke. fNIRS, an optical imaging tool which is completely portable is an alternative to study functional brain activities barring from the fact that it is limited to investigating the brain, not beyond cortex.

Studies have reported promising approaches to elucidate on functional components of the reorganization of affected brain regions after stroke using fNIRS. The approaches until recently were to study the motor response of the brain based on the task given as stimulus. The motor cortical activations were studied using fMRI to a larger extent and fNIRS to a very little extent. Compensatory motor activation of cortical regions in patients recovered from hemiparesis

after cortical infarction has been evaluated successfully using fNIRS in comparison with functional magnetic resonance imaging fMRI. The changes in cortical activations during motor recovery after stroke were studied. Resting state functional connectivity investigates the spontaneous cerebral hemodynamic fluctuations that reflect neuronal activity at rest. Connectivity studies using habitual neuroimaging techniques like fMRI has been started a few decades ago. Recent pieces of the literature suggest remarkable interest in resting state cerebral hemodynamic fluctuations. This thesis hypothesizes a disruption in the motor cortical network due to stroke and reorganization of the network owing to recovery that can be identified using the resting state analysis. The motivation for this thesis comes from this fact of using fNIRS, which is a low cost, portable and reliable neuroimaging modality for understanding brain functions about cortical depth. In this thesis, we have attempted to evaluate the resting state data acquired using fNIRS for functional connectivity analysis of the motor cortical area to study the changes in the network organization of the motor cortex in the process of recovery

Thus the main objectives of this thesis are to:

- Establish the role of cortical functional connectivity in the reorganization of the motor cortex in post-stroke recovery using fNIRS.
- Study the correlation between task-based and resting state fNIRS

The study was designed as a case-control study wherein twenty patients were recruited from the stroke clinic of the institute and an equal number of control subjects were included in the study. The recruitment of the patient group was under the supervision of the consultant neurologist with strict inclusion and exclusion criteria. The study was carried out after getting approval from the Institute Ethics Committee. Informed consent was obtained and the information sheet was provided for all the subjects. The study included a longitudinal data acquisition design for the patient group. The first set of data was collected from the patients on an average of 23 days after the onset of the stroke. The second set of data was collected on their follow up to the clinic (mean of 90 days).The mean age of the patient group was 54.4±11 years.

The data acquisition was performed using NIRSport system (NIRx Medical Technologies LLC, Berlin, Germany) having 8 sources and 8 detectors at a sampling rate of

7.825Hz. The device emits light at 2 distinct wavelengths, 760 and 850 nm, for discrimination of two oxygenation states of tissue. Four sources and four detectors were used to cover areas of interest in one hemisphere. The fNIRS signal was recorded bilaterally over the premotor area and supplementary motor area (10-20 EEG locations corresponding areas FC3, FC1, FCz, FC2, and FC4) and over the primary motor cortex (10-20 EEG locations corresponding areas C4, C2, Cz, C1 and C3), as combinations of these areas were likely to be active in response to the motor paradigm. A total of 20 channels were analysed to infer data from the motor cortex and associated areas. The inter optode distance was maintained at 30 mm. The acquisition was carried out in a relatively darker room in a relaxed environment. The device was calibrated for each subject before the acquisition for gain settings. A paradigm was designed using NIRSTIM software for task-based acquisition. It included a rest block followed by an active block of left-hand movement. This is followed by another block of rest phase and subsequent active block of right-hand movement. Data analysis was carried out using nirsLAB software and FC-NIRS software along with tailor-made scripts in Matlab.

The study initially focussed on the use of fNIRS modality for studying the task-based activations in which the left-hand movement task and right-hand movement task were analysed. The healthy control group data showed unilateral activation pattern for the tasks given. The dominant hand movement (right hand) showed significant contralateral activation in the primary motor areas (M1) and supplementary motor areas (SMA) ($p<0.05$). Deactivation of the ipsilateral primary motor area was observed for the dominant hand task indicating a possible inhibition by the contralateral M1 as reported by earlier studies. The patient group was subdivided based on the location of the infarct into right-hemispheric and left hemispheric groups. Studies using fMRI have suggested that the sub-acute stroke patients show bilateral activation of the motor cortex in response to motor tasks. Evaluation of the left hemispheric stroke for the affected hand (right hand) illustrates a bilaterally activated M1 areas, premotor and supplementary motor areas which are statistically significant ($p<0.05$). The recruitment of contra-lesional (right hemisphere) M1 and supplementary areas are important for the management of the stroke in the subacute phase.

The non-affected hand (left hand) showed significant activation in the contralateral (right) hemisphere (M1 area, premotor and SMA).

The same set of subjects were evaluated for the second time in which the subjects have undergone physiotherapy intervention and the data were analysed for studying the changes in the activation over time. The left hemispheric stroke group showed increased activation in the premotor and sensory-motor areas when compared to the contra-lesional area for the affected hand (right hand). For the left-hand movement, significant contralateral activation of M1 and premotor area was observed ($p<0.05$). A decrease in contra-lesional activation is observed. The unilateral pattern was observed in the post-recovery session when compared to the bilateral activations during the pre-recovery session. The right hemispheric group showed a significant contralateral increase in M1 and premotor area for the affected hand movement (left hand) during the pre-recovery session ($p<0.05$). The non- affected hand (right-hand activation) also showed contralateral activation in the pre-recovery session. More contralateral areas were activated for the affected hand movement and non-affected hand movement during the post-recovery session.

Resting state data was analyzed for both pre-recovery and post-recovery sessions for the patient group. The resting state functional connectivity (RSFC) pattern for the healthy group was obtained using Pearson correlation for each channel. The coefficient was Fischer transformed to obtain the Z values for obtaining normalized values. For the healthy group the motor cortices and supplementary areas were correlated (mean $r=0.59$ for left hemisphere and mean $r= 0.43$). The inter-hemispheric functional connectivity was observed between the right premotor and left association cortex. The connectivity values were thresholded with a sparsity threshold of 0.4 for uniformity in comparing between the groups. The left-hemispheric affected group showed a disruption in the ipsi-lesional network between the motor cortex and supplementary areas. The contra-lesional hemisphere has shown to have recruited more connections when compared to the healthy controls. The intra-hemispheric connections have decreased significantly when compared to the healthy group. The RSFC analysis of the post-recovery data showed a reappearance of the network in the left hemisphere along with strong inter-hemispheric connections between SMA of both hemispheres and association cortices of both hemispheres as well.

The right hemisphere affected group, on the other hand, had disruption of the normal network of M1, SMA and Premotor in the affected hemisphere. The group showed an inter-hemispheric connection between premotor areas of the left hemisphere and right hemisphere. The post-recovery analysis of the RSFC of this group has shown improvement in the disrupted network of the M1, SMA and premotor areas of the right hemisphere. The inter-hemispheric connections between M1, association cortices and SMA were observed in the post-recovery session. Further, the RSFC data was utilized to study network properties using graph theory. The healthy group and the patient groups showed significant differences ($p<0.05$) for the measures of segregation such as clustering coefficient and local efficiency. The patient group showed lesser values for the measures of segregation in the pre-recovery session signifying the loss of dense interconnection with the neighbouring regions.

In conclusion, the task-based activations for the healthy controls presented a unilateral engagement of the cortical areas and the results using fNIRS are in line with previous fMRI studies. The patient group responses gave a bilateral pattern of activation for the pre-recovery session which was shifted to unilateral activation of motor areas over time. Previous fMRI studies have shown that during recovery a normalized hemispheric balance between the two sides of the motor cortex could be re-established given the evidence that activation for most well-recovered stroke patients shifts from a bilateral to a unilateral pattern. The functional connectivity analysis also showed a change in pattern between the healthy control group and the patient group. Significant improvements in the connections were observed for the patient group when comparing the pre-recovery and post-recovery data. Since RSFC studies of stroke recovery using fNIRS are few this thesis will show more light into the cortical networks and its disruption due to stroke and its reorganization during recovery from stroke.

## *Thesis Outline*

Chapter 1:

**The introduction** gives background information about the study. It explains the principle behind the modality used (fNIRS) for the study, problem statement and motivation for the study.

Chapter 2:

**Literature Review** reviews the relevant literature about the task-based neuroimaging of stroke recovery and longitudinal studies on the recovery from stroke. The chapter also focuses on the research work using fNIRS modality in studying stroke recovery and resting-state fNIRS in general.

Chapter 3:

**Materials and Methods,** section discusses in detail about the experimental design, inclusion criteria, data acquisition, different pre-processing steps and software used for the analysis of the data. The chapter also discusses the task-based and resting-state fNIRS data analysis steps in detail.

Chapter 4:

**Results,** section presents the major results from the study including the task-based results for healthy controls, left hemisphere affected patient group and right hemisphere affected patient group. It also presents resting-state results for healthy controls and

patients.

Chapter 5:

**Discussion,** section describes the interpretation of the results in context to the relevant existing reported studies and tries to explain the individuality of the study. It also explains the limitations of the study and future directions.

Chapter 6:

**Conclusion and Summary,** section summarizes the results from the different experiments/ trials in the study and concludes the results.

# Chapter 1

# Introduction

## *1.1 Background*

In-vivo studies of human brain functions are made possible by neuroimaging techniques. These techniques allow us to produce detailed images of the structure (anatomical imaging) as well as capture images of the physiology associated with different processes (functional imaging). The field of medical imaging is expanding its clinical application and capabilities. In such a scenario newer and safer methods are being sought. There is an urge for the development and practice of non-invasive techniques, which are relatively safer to handle and use. For the functional understanding of the brain, different modalities of brain imaging are followed around the globe like Electroencephalography (EEG), functional Magnetic Resonance Imaging (fMRI), Positron emission tomography (PET) and Magnetoencephalography (MEG). Understanding how the brain acts under normal conditions and altered conditions have stern clinical repercussions. Each modality used has its own pros and cons. The optimal choice of modality is a trade-off between applicability to the population and neurological condition being studied. This study utilizes the method called functional near-infrared spectroscopy (fNIRS) for the measurement of brain activity during the recovery from stroke.

### 1.1.1 Stroke - Neuro-vascular condition.

Stroke is defined as a neurological dysfunction that happens when the blood supply to part of the brain is cut-off either due to cerebral infarction, intracerebral hemorrhage, or subarachnoid hemorrhage (Stormtrooper, 2014). It is the foremost reason of frailty and death worldwide. Stroke broadly includes two major types: a) ischemic, mainly due to the formation of a clot in the blood vessel causing a reduction in cerebral blood flow, and b) hemorrhagic, due to rupture of the blood vessel in the concerned area. During ischemic stroke cerebral blood supply is disrupted by narrowing of the vessels due to atherosclerosis or embolism. In the case of hemorrhagic stroke hypertension or ruptured aneurysm causes reduced blood flow due to direct blood loss or vessel compression. In both cases, a substantial drop in blood supply could be observed which results in the injury of the neurovascular unit. Like all cells lack of oxygen supply causes neurons to die and hence decreases the neuronal activity. Treatment to the stoke victim depends on the type of stroke and the location of the insult.

### 1.1.2 Recovery from stroke

The damage to the brain caused by a stroke can lead to extensive and continuing complications. But the concept that the brain is not hard-wired and in particular cortex has the capability to change in both structure and function is globally accepted. This change in structure over time with a resultant change in function is termed as the plasticity of cortex or brain itself. This helps in planning recovery from stroke through

various rehabilitation strategies according to the nature and location of the deficit. The extent of recuperation depends on various factors. The intensity and dose of rehabilitation play an important role in recovery. Recent studies confirm that recovery occurs mainly due to neuro-plastic reorganization. This, in turn, happens only when the rehabilitation activity surpasses a certain threshold(MacLellan et al., 2011).

This thesis focuses on the modality of fNIRS and its use for studying the motor cortex in the recovery phase of patients from stroke. It also describes the technique of resting-state fNIRS measurement, different analysis techniques and interpretation of data.

## *1.2 Functional near-infrared spectroscopy (fNIRS)*

FNIRS is an optical neuroimaging tool for noninvasive measurement of the brain activity and monitoring of regional cerebral hemodynamics. This is done by sensing light absorption and scattering mainly associated with measurable chemicals called chromophores (water, hemoglobin, cytochrome, etc.) through the skull. Frans Jöbsis who is considered to be a pioneer in the application of optical techniques to the study of intact organs in situ is credited to the discovery of NIRS (LaManna, 2007). The method works by illuminating two wavelengths of near-infrared light through the scalp and recording intensity variations resulting from the metabolic changes within brain tissue. Each wavelength of light is absorbed by the oxygenated and de-oxygenated species of hemoglobin differently. This allows concentration changes in each of them to be estimated.

The brain endures various electrophysiological and neuro-chemical reactions in response to external stimuli. These responses are the result of the concordant communications of neurons and non-neuronal cells in the brain. The increase in local neuronal activity is supplemented by the intake of glucose and oxygen, which in turn tips to an increase in local blood flow and blood volume through the vessels. This will eventually lead to the entry of oxygen-bound hemoglobin into the region. The above description defines neurovascular coupling. During this reaction to stimuli, the amount of oxygen supplied is typically more than that consumed locally, resulting in a substantial increase in oxygenated hemoglobin and a slight reduction in deoxygenated hemoglobin in the region (Fox et al., 1988; Villringer and Dirnagl, 1995). Since the magnitude and location of both oxy- and deoxy-hemoglobin are tightly linked to the extent and location of neuronal activity, the hemodynamic response is often measured as an alternative marker of neuronal activity as in case of fMRI (Chance et al., 1993; Ogawa et al., 1990; Villringer and Chance, 1997).NIRS allows us to measure relative changes in cortical hemoglobin concentration, coupling this concentration to brain functioning is what designates fNIRS.

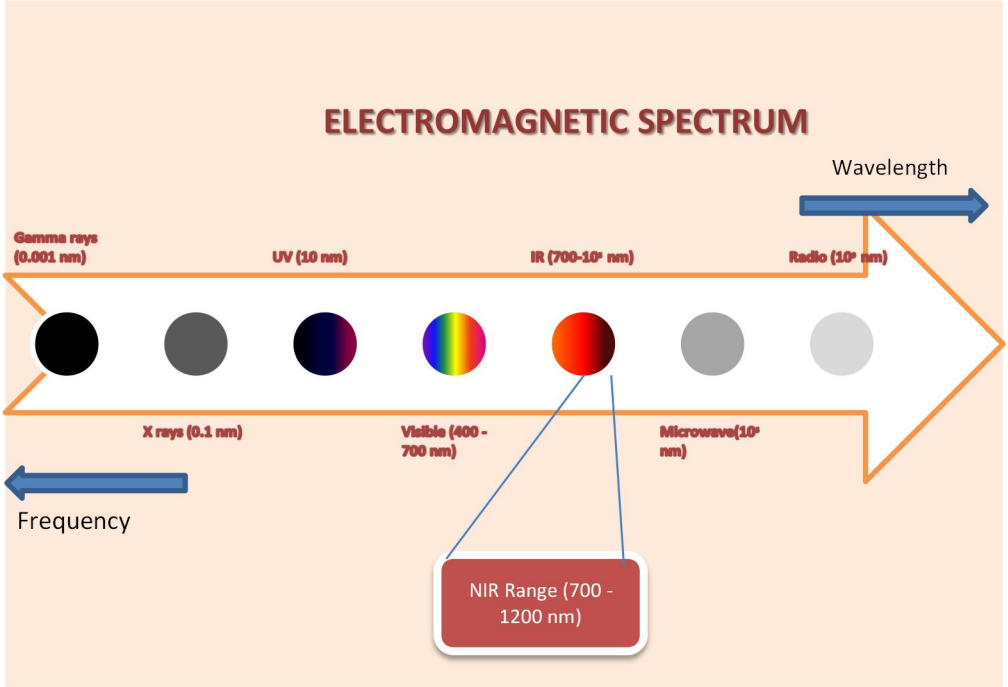


Figure1.1: Represents the Electromagnetic spectrum showing Near-infrared sub spectrum ranging from 700 nm to 1200 nm

### 1.2.1 Comparison of fNIRS with other neuroimaging techniques

Neuroimaging scientists have always encountered the question of the modality to be used for the study. The existing modalities offer advantages of one another and some of them when used simultaneously compliment the method to arrive at a solution to the problem being studied upon. Techniques like EEG and MEG, allow researchers to observe the direct manifestations of brain electromagnetic activity with temporal resolution on the order of milliseconds. However, these technologies have limited spatial resolution due to the presence of multiple dipoles contributing to the signal. On the other hand, methods such as PET and fMRI indirectly monitor the hemodynamic and

metabolic changes associated with neural activity with remarkable spatial resolution. However, these methods are limited in temporal resolution and are associated with neuronal activity through the neurovascular coupling function. The use of radioisotope limits the application of PET. FMRI, being non-invasive is the most popular functional neuroimaging technique available. The disadvantages of fMRI are that it is physically compelling, vulnerable to motion artifacts, exposes participants to loud noises, and is expensive. FNIRS, an emerging neuroimaging technique, offer relatively non-invasive, safe, portable, low-cost methods of both direct and indirect monitoring of brain activity. The summary of the comparison of fNIRS with other modalities is given in table 1.1.

**Table 1.1 Comparison among brain imaging techniques**

| Technique | Target | TR | SR | Merits | Demerits |
|---|---|---|---|---|---|
| MEG | Neural electric | 1 ms | 5 mm,3D | High Temporal | Difficulty in measuring some regions |
| EEG | Neural electric activity | 1 ms | 10-15 mm, 3D | Low cost, high exp. Flexibility | Low Spatial resolution |
| PET | HR, metabolic response | 10-45 s | 4 mm,3D | Quantitative measurement | High cost, invasiveness |

| | | | | | |
|---|---|---|---|---|---|
| fMRI | Hemodynamic Response | 0.5-5 s | 1-5 mm, 3D | Structural data availability | High cost, low exp. flexibility |
| fNIRS | Hemodynamic Response | 0.1-1 s | 10-30 mm | Low cost, high exp. Flexibility | Measurement limited to the lateral cortex surface |

### 1.2.2 Light Transport in Tissue

The human brain is relatively transparent to light in a small window of near-infrared range, which is capitalized in NIRS. The scientific basis of NIRS heavily relies on the physics of light transport in brain tissue. Absorbing characteristics of hemoglobin are distinctive and this helps for oxygenation-dependent quantification of NIR light absorption("fNIRS Analysis," n.d.). The relative change in concentrations of oxyhemoglobin (HbO) and deoxyhemoglobin (HbR) is calculated using the modified Beer-Lambert law.

When light enters the brain tissue the major interactions of light are absorption and scattering in varied proportions depending upon the optical properties of the medium. Absorption is the process in which the energy of the photon being transmitted to a

molecule. Such a molecule that can absorb light is called Chromophore. The energy of the photon absorbed by the chromophore can be converted to other forms such as heat, fluorescence or dissipated by non-radiated processes like metabolic pathways. The absorptivity of the chromophores in the tissue can be characterized by the absorption coefficient ($\mu_a$). For an ideal medium with no scattering the concentration of chromophore could be derived easily from Beer-Lambert's law as given below:

$$I = I_o e^{-\in cL}$$

Where, ( Eq 1.1)

I = intensity of the light passed through the medium

$I_o$= intensity of the incident light

ε - Molar extinction coefficient

c - Concentration of the chromophore

L – distance travelled by light in the medium

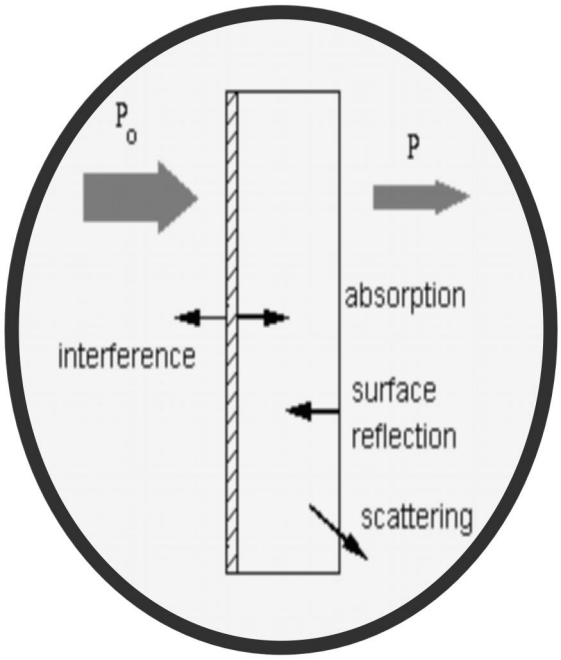


Figure 1.2 Represents the different types of interactions of the light ($P_o$) entering a medium

Scattering occurs elastically within the medium and the degree of which is a function of the difference in refractive index between regions within the cellular material and the angle of incidence. The scattering properties of a medium are described by its scattering coefficient $\mu_s$. Scattering is a broad term used to report a variety of light-matter interactions that hold back the state of the incoming photon but which may modify its path of motion (Cooper, 2010). The anisotropy (g) is a measure of the number of forwarding direction rays retained after a scattering event.

A fundamental consideration in optical imaging is maximizing the depth of light dissemination into the tissue, which is limited by absorption and scattering of light. Because absorption and scattering declines as wavelength increases, the detection of fluorescent dyes and proteins having absorption below 700 nm are difficult. In the NIR

region, the absorption coefficient of tissue is at its minimum and hence light can pierce to depths of few centimeters. Above 900 nm, light absorption by water causes interference. Auto-fluorescence is also an important consideration. Naturally-occurring compounds in animal tissue can cause considerable auto-fluorescence all over the visible range up to ~700 nm, which can mask the desired signal.

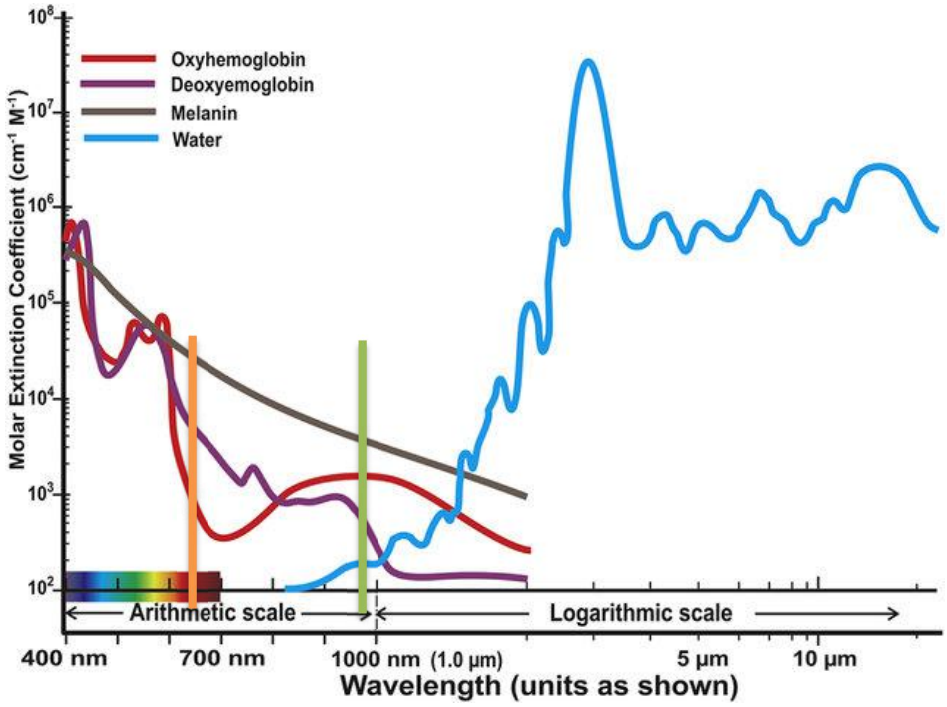


Figure 1.3 Absorption spectra of biological chromophores (hemoglobin, melanin, and water). The orange and green vertical lines represent the boundaries of the optical window in the spectrum which is used for NIR optical imaging

For a medium like a brain tissue, the light incident is partially absorbed and partially scattered. The concentration of chromophores then cannot be determined by the Beer-Lambert law as it is defined for a non-scattering medium. In such cases, the path length is not merely equal to the width of the medium-light passing through. Instead light takes a longer path inside the medium due to dispersion. This leads to the introduction of a

new factor called differential path length factor (B). Also, there is a loss of photon energy due to this phenomenon and to account for that another factor (G) is introduced in the equation as given below (Eq1.2). This modified Beer-Lambert law is used to find the change in concentration of chromophore in a continuous wave NIRS.

$$A = \log_{10}(I_o / I) = \in cLB + G$$
$$\Delta A = \log_{10}(I_o / I) = \in \Delta cLB \qquad \text{(Eq 1.2)}$$

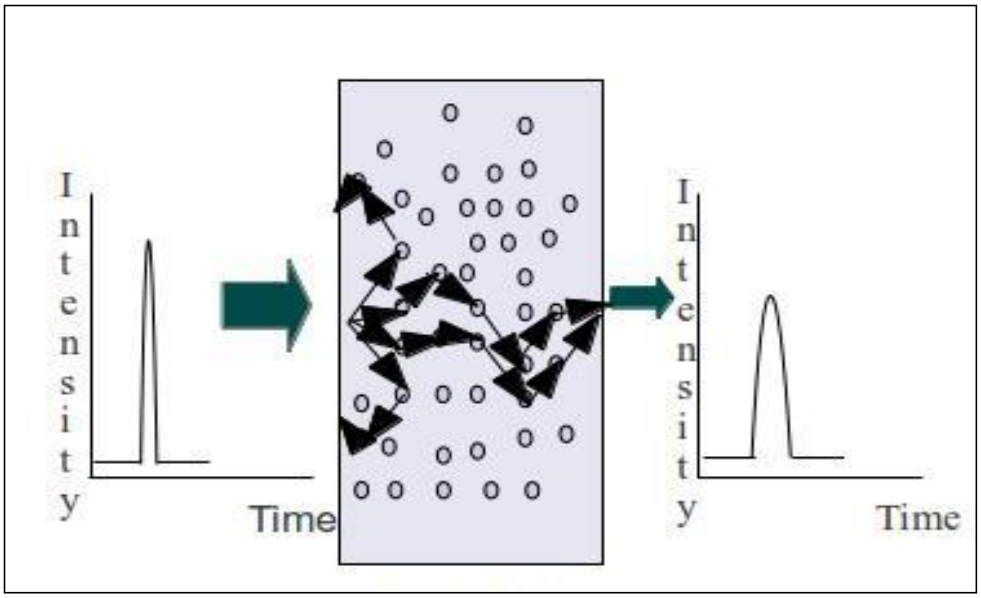


Figure 1.4 The photon entering a living tissue undergoes multiple scattering before emerging out. The zig-zag path taken by the photon increases the total path traveled by it. The concept of differential path length factor accounts for this extra path taken by the photon

Generally, a model is needed to determine the tissue optical parameters $\mu_a$, $\mu_{s,}$ and $_g$ from a set of measurements. Conversely, with knowledge of these parameters, a model can be used to predict useful measures like the absorbed dose and the light distributions in tissue, and the light fluxes emerging from the tissue, for a given light source and

tissue geometry. As NIR photons are applied to the turbid liquid (similar to tissue), the photons follow a trajectory similar to the shape of a 'banana' and exit the liquid to meet the detector surface as shown in the fig1.5. The depth resolution of the NIRS technique is under investigation and from the studies till now, it has been formulated that the penetration depth of photons in NIRS is almost half of the source-detector distance. Hence the general understanding is that when the distance between the source and the detector increases, penetration also increases. In natural tissue, the scattering particle density is such that the interaction of scattered waves between neighboring particles cannot be ignored and multiple scattering is bound to occur.

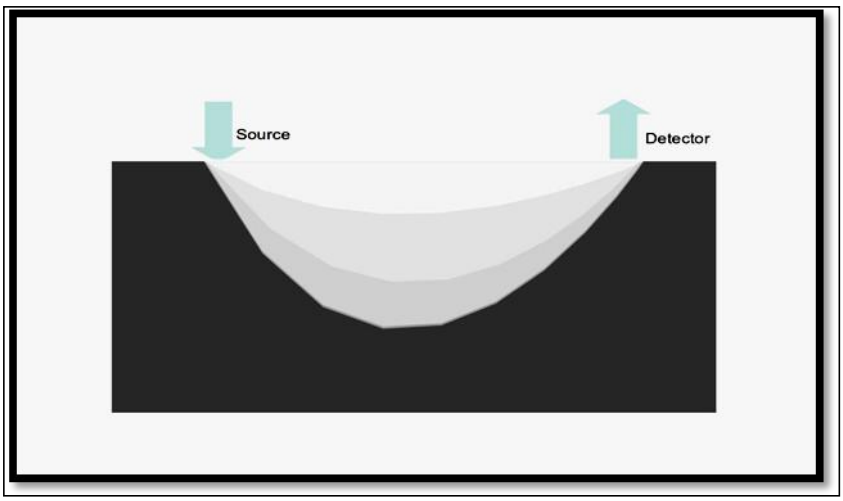


Figure 1.5 ‘Banana’ shape photon path pictorially depicted from source to detector inside a tissue.

### 1.2.3 Hemodynamic response function

The brain signal measured using fNIRS is the hemodynamic response which is coupled with the neuronal activation. This gives an indirect measure of the neuronal activation in response to the stimuli. The sequence of events is as follows: A neuronal activation is caused in response to a stimulus. This is followed by the increased utilization of HbO around the specific region. It induces an increase in blood flow to the region, improving the HbO concentration which is accompanied by a decrease in HbR concentration. Fig 1.6 depicts an optimal response to the stimulus activation. This vascular response to activation is known as the hemodynamic response function (HRF).

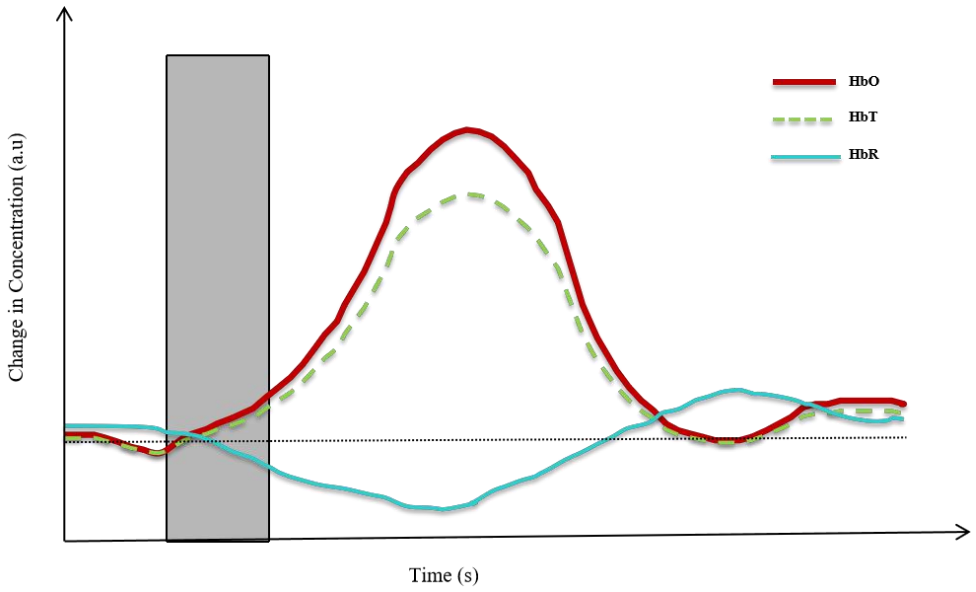


Figure 1.6 The hemodynamic response function to a stimulus (onset of stimulus shown in the grey rectangle). The red curve represents oxy hemoglobin response, the green dotted line represents total hemoglobin and the blue line represents deoxyhemoglobin.

This HRF is studied for many disorders using the specific stimulus to the brain and is

called task-based fNIRS studies. Researchers have started using fNIRS is understanding a variety of brain functions (Strangman et al., 2006). The initial research was focused on the neonates and with improved instrumentation, people started using fNIRS for adult studies. The application ranges of fNIRS include motor tasks, visual tasks, cognitive tasks, aging, and psychiatric disorders and rehabilitation. Several studies have proved the worth of fNIRS in the functional neuroimaging realm by comparison of results with that of fMRI studies.

### 1.2.4 Resting State functional connectivity using fNIRS

The interest in functional connectivity has been increasing ever since the discovery of synchronous neurophysiological activity of spatially remote brain regions were identified using fMRI. The correlated functional activity has been identified in various systems in brain-like sensorimotor, visual, auditory and language. The reliability and repeatability of the technique for RSFC measures have been established. The limited spatial resolution of fNIRS never stopped it being used in RSFC measurement as a complementary technique to fMRI. The common neurophysiologic basis of fMRI and fNIRS modalities is thought to be the reason for the high consistency of the RSFC measurement between them. More studies using fNIRS for RSFC assessment are discussed in Chapter 2. The concept of resting-state fNIRS based brain network analysis is possible with the help of extending graph theory to the brain network analysis. Resting-state fNIRS has proved to demonstrate characteristics of topological attributes

of human brain networks consistent with rs-FMRI studies. Further techniques of resting-state fNIRS are discussed in session 3.5.2.

## *1.3 Motivation and Objectives*

This thesis hypothesizes that fNIRS could detect the disruption in the motor cortical network due to stroke and the reorganization of the network during the course of recovery. The motivation for this thesis comes from this fact of using fNIRS, which is a low cost, portable and reliable neuroimaging modality for understanding brain functions about the depth of cortex. The portable nature of the modality in data acquisition helps to achieve a patient-centric approach. A bedside measurement for the patients who are unable to move around and who have difficulty in getting the fMRI scan done is a major shift in the paradigm. The use of such modality also makes a way forward towards brain-computer interfaces that can be used for the rehabilitation approaches in stroke recovery. In this thesis, we have attempted to evaluate the task-based and resting-state data acquired using fNIRS. Functional connectivity analysis of the motor cortical area is studied longitudinally. The change in the network organization of the motor cortex in the process of recovery is assessed using both task-based and connectivity measurements. Cortical connectivity changes in the stroke patients during recovery are hypothesised here. Thus the main objectives of this thesis are to a) Establish the role of cortical functional connectivity in the reorganization of the motor cortex in post-stroke recovery using fNIRS. b) Study the correlation between task-based and resting-state fNIRS

# Chapter 2

# Literature Review

## *2.1 fNIRS: Technique and Analysis*

The potential of fNIRS imaging is widespread in the research level as well as at the translational application level. The technique was initially used in the early ’90s by four different research groups to measure brain function (Chance et al., 1993; Hoshi and Tamura, 1993; Kato et al., 1993; Villringer et al., 1993). The field of fNIRS research has grown much faster and much advancement has been reported over the years. Technology-wise, the lion share of the fNIRS systems in the market is based on the continuous wave instrumentation which is simplest and less expensive. They can measure changes in oxy and deoxyhemoglobin (Scholkmann et al., 2014). Another type of fNIRS instrumentation is based on the time domain technique utilizing a short pulse of laser light. Such devices measure the time-spread function of the pulse. A better spatial and depth resolution is obtained with this method. The method though is expensive to build and hence not used by many groups (Torricelli et al., 2014). The third technique of frequency domain fNIRS measures a shift in phase along with light intensity attenuation. The emitted light is modulated at a particular frequency (Davies et al., 2017).

## *2.2 Task based Functional neuroimaging of stroke recovery:*

Functional recovery is seen to happen in stroke patients from weeks to months following the insult. Suggestions have come from non-human studies that cerebral reorganization is causative of the recovery. It is therefore important to have an understanding of the neuro-physiological processes fundamental to this reorganization in the human brain (Baron et al., 2004). Positron emission tomography (PET) and functional magnetic resonance imaging (fMRI) have been used reliably to reveal motor-related brain activations during movement of the stroke-affected upper limbs. Additional task-related recruitment in the unaffected hemisphere has often been reported with these modalities. The knowledge about recovery from stroke has been from the observational studies prior to the introduction of functional imaging modalities (Calautti and Baron, 2003).

The normal patterns of movement with hands were studied by many research groups. The areas identified typically include contralateral supplementary motor area (SMA), Primary motor cortex (M1) and sensorimotor cortex (SM1) and ipsilateral cerebellum for a normal self-paced or cue-based task with a dominant hand. But for a non- dominant hand the pattern remains the same except for the addition of dorsolateral prefrontal cortex (DLPFC), posterior parietal cortex and insular activations(Kim et al., 1993; Rao et al., 1993; Remy et al., 1994). Though the trans-callosal inhibition was evidenced by animal and clinical studies, fMRI studies involving unilateral motor tasks were conducted to establish the inter-hemispheric interactions (Reddy et al., 2000). Cao Y et

al hypothesized that the ipsilateral activation will be more in the primary sensorimotor cortex of the non-infarcted hemisphere in comparison with normal subjects. They used fMRI modality to study the motor function of the hemiparetic subjects who suffered a unilateral ischemic stroke (Cao Y. et al., 1998).

The researchers, with the introduction of fNIRS, started looking at it as an alternative to the existing modalities. The major reason for this is that the identified areas for motor-related activities are optically available for probing. Also with the advantage of portability, discreteness and good insulation from motion artifacts, the modality offers to delineate cortical correlates of real-world tasks. Many investigators used simple motor tasks like finger tapping, hand grasping, and thumb opposition to understand the fNIRS signal corresponding to brain activation and to monitor the neuro-vascular coupling (Franceschini et al., 2003; Hirth et al., 1996; Obrig et al., 1996). NIRS is considered as an effective monitoring tool for stroke recovery, including upper limb, lower limb recovery, motor learning and cortical function recovery (Mihara and Miyai, 2016).

fNIRS studies have described the role of the SM1, M1 and the PFC in tasks of daily activities such as upholding attention and concentration required for running in healthy subjects. Consistent results have been obtained with fNIRS studies, suggesting impaired contralateral M1 activations, up-regulation of ipsilateral motor activations, and longitudinal improvements in laterality toward contralateral M1 activation following rehabilitation (Leff et al., 2011). The research by Arenth, Ricker, and Schultheis

described the various applications of Functional Near-Infrared Spectroscopy (fNIRS) to Neurorehabilitation of cognitive disabilities. They focussed on the areas of Motor and Visual Tasks, cognition, aging and psychiatric population, stroke and traumatic brain injury. Keeping in line with the present study, the integration between fNIRS and rehabilitation in the area of Stroke was given significance. Upper limb and lower limb functional recovery, motor learning and balance control (gait) are the areas studied using fNIRS (Arenth et al., 2007). Miyai and colleagues evaluated six non-ambulatory patients with severe hemiplegia following stroke. The fNIRS system was utilized during the treadmill-walking task under partial body weight support. The performance of the gait activity was linked with increases in oxy-hemoglobin (HbO) in the medial primary sensorimotor cortex. Also, a greater increase in the HbO was noted in the unaffected hemisphere, as compared to the affected hemisphere. In another study, cortical activities of patients with stroke were measured during hemiparetic gait longitudinally during inpatient rehabilitation. They were eventually able to arrive at the conclusion that recovery of locomotion after stroke may be associated with improved asymmetry in the medial primary sensory cortex (SMC) activation and enhanced premotor cortex activation in the affected hemisphere(Miyai et al., 2002, 2001). Kato et al. did a study that compared fNIRS and fMRI to examine six patients who experienced a stroke, specifically within the distribution of the middle cerebral artery (MCA), who exhibited left hemiparesis, and recovered to the point that they had minimal or mild residual hemiparesis. The Subjects were studied by administering a hand movement task of both the unaffected and affected hand. The authors were able to communicate the conclusion

that fNIRS was useful for the study of post-stroke alterations in motor functioning(Kato et al., 2002, 2001).

### 2.2.1 Longitudinal study of motor recovery after stroke

The researchers initially studied comparison between the stroke affected subject and normal controls or fully recovered subject at a single time point alone. These functional studies would give the idea about the differences in activation patterns for the damaged brain with a lesion when compared to the normal brain. But for a study that focuses on the changes during the recovery process, it is inept. So there have been longitudinally designed studies that allow people to acquire data from one subject multiple times during the recovery phase. Such studies help us to determine the dynamic changes in the activation patterns. The selection of simple motor tasks could circumvent the learning effect often seen in longitudinal studies (Seidler et al., 2010). A few published longitudinal neuroimaging studies have shown that neural activity in cortical motor areas during movements of the paretic hand is enhanced in both the hemispheres two weeks post-stroke and subsequently decreases toward levels observed in healthy subjects concomitant to motor recovery(Tombari et al., 2004; Ward et al., 2003). One study reported that the gradually increasing activity in the contralesional primary motor and premotor cortex correlated with improved functional recovery in severely affected patients. They focussed on the role of the contralesional motor cortex using fMRI in the recovery process during the early days after stroke (Rehme et al., 2011). Further other researchers studied the contralesional motor areas and suggested that these activations

will impact the extent of motor function of the paretic limb in the subacute and chronic phase post-stroke and may serve as a new target for rehabilitation treatment strategies(Buetefisch, 2015). Grefkes et al reported that after four months of the patient recovery the contralesional activation disappears (Grefkes and Fink, 2011).fNIRS was useful for observing changes in hemodynamics and oxygenation in various types of rehabilitation interventions (Saitou et al., 2000).

Functional motor recovery of upper limb studies using fNIRS has been reported by Yang et al in a recent review. There have been only a handful of studies that focussed on the recovery of upper limbs. Upper limb functional recovery has been attributed to the ipsilateral motor cortex activation. All the studies concentrated on the longitudinal task-based activations for the analysis (Brunetti et al., 2015; Gobbo et al., 2017; Hara et al., 2013; Kato et al., 2002; Takeda et al., 2007).

## *2.3 Resting-state functional neuroimaging of stroke*

The intrinsic activity of brain regions in the resting state has been shown to be having a synchronous nature. fMRI research community has put more effort, time and money into analyzing the brain at rest during recent times for obvious reasons. This resting-state functional connectivity (RSFC) is observed in different brain systems including language, motor, visual, etc. The technique of RSFC has been applied to study various neurological and psychiatric conditions(Bharat Biswal et al., 1995; Fox and Raichle, 2007). Studies have reported both anatomical and functional connectivity changes during stroke in various conditions (Jang, 2011; Mukherjee, 2005; Son et al.,

2009). Considerable differences occur across the patient group due to lesion location, stroke onset time, the severity of impairment, etc (Jiang et al., 2013).

The motor system which controls the motor function will be disturbed whenever the motor deficit occurs due to stroke. The knowledge of brain structure and alteration in function doesn't essentially tell us how the regions interacted together to modulate the functions. Connectivity based studies are sought for the demonstration of structural and functional changes after stroke Since resting state acquisition does not require explicit task execution, it allows random assessment of functional connectivity within various neuronal networks in a single experiment(Meer et al., 2010). The advantage of these analyses is that more understanding of network dysfunction and functional reorganization are provided (Carter et al., 2012). The conceptual assumption for such analysis is that the brain is considered to be anatomically segregated into distinct brain regions and at the same time functionally integrated through a set of network architecture. RSFC measures the temporal correlation between signals from spatially remote brain regions(K. Smitha et al., 2017; K. A. Smitha et al., 2017). It has been shown RSFC using fMRI is consistent among the healthy population with aberrant results for different age groups (Damoiseaux et al., 2006). Park et al reported that the functional connectivity was seen more lateralized to the ipsilesional M1 at the onset when compared to the healthy subjects. This asymmetry was highest after a month and later starts to restore to asymmetrical connectivity after three months (Park Chang-hyun et al., 2011). Rs-fMRI studies have concentrated on motor cortex functional connectivity for reporting cerebral reorganization during stroke recovery. The importance of the

primary sensory cortex has been given its due along with the motor cortex as the results suggested inter-hemispheric asymmetry reduction with chronicity as in the case of the motor cortex(Carter et al., 2010; H. Xu et al., 2014). Inter-hemispheric disruption of RSFC occurs between sensory areas apart from motor cortices. A significant loss of sensory interconnection has been reported recently when studied using fMRI. This could be useful when combined with anatomical measures of the lesion in describing stroke outcomes (Frías et al., 2018).

### 2.3.1 Resting state fNIRS

In spite of the limited spatial resolution when compared to fMRI, fNIRS is a promising imaging modality for RSFC assessment. This can be used complementary to the resting-state fMRI studies (Boas et al., 2004). Recent studies have shown the potential of RSFC using fNIRS as the acquisition modality (Niu et al., 2011; Niu and He, 2014; White et al., 2009). FNIRS could be used to describe the topological organization of the brain network in the resting state up to the cortical depth. As in fMRI analysis of functional connectivity, the signals from predefined seed regions are utilized in research to identify the interaction of different brain regions. Study groups have observed strong connections between bilateral sensorimotor, auditory and visual systems in adults (Lu et al., 2010; White et al., 2009). Connectivity changes were observed in neurological disorders and developmental studies of early infancy by some groups (Homae et al., 2010; Imai et al., 2014; Nakano et al., 2009; White et al., 2012). The assessment of RSFC using fNIRS has definite advantages due to the portability and practicality of the

applications in neuroscience. The ease of translating the research into the clinical domain is also another advantage (Duan et al., 2012). Zhang et al have established the validity of RSFC results using both seed-based and independent component analysis methods from resting fNIRS data (Zhang et al., 2010).

# Chapter 3

# Materials and Method

## *3.1 Inclusion and Exclusion Criteria*

The study was designed as a case-control study wherein twenty patients were recruited from the stroke clinic of the institute and an equal number of healthy volunteers were included in the study. The recruitment was under the supervision of the consultant neurologist. The inclusion and exclusion criteria for the study are given in table 3.1

**Table 3. 1 Inclusion and exclusion criteria for the selection of patients/subjects for the study**

| *Inclusion Criteria* | *Exclusion Criteria* |
|---|---|
| ***Patients with Mild stroke*** | Patients with Cognitive impairment who cannot comprehend the commands for task-based study |
| ***Patients with Modified Rankin Score of 4 or less*** | Patients with a strong motor impairment who cannot perform the task |
| ***The onset of Stroke: 4 weeks to 8 weeks*** | Acute stroke and patients who are not able to cooperate under the scanner |
| ***Healthy Volunteers who have no history of stroke or other functional impairments*** | Healthy volunteers from the same lab who might be biased in performing the study |

## *3.2 Experiment Design*

The study was conducted as three segments. The first segment involved a simple hand grasping task. Both the healthy subject group and the patient group performed the hand grasping task. The task was designed in blocks of rest and active sessions. The active trial lasted for 20 seconds and the rest trial for 25 seconds. Five trials were repeated for a session. The second segment of data collection involved the resting state measurement of three minutes.It is followed by another trial of task measurement. The subject was instructed to be relaxed without any movement of the limbs. A fixation point was displayed on the screen during the measurement time. Figure 3.1 depicts the experimental design and set up

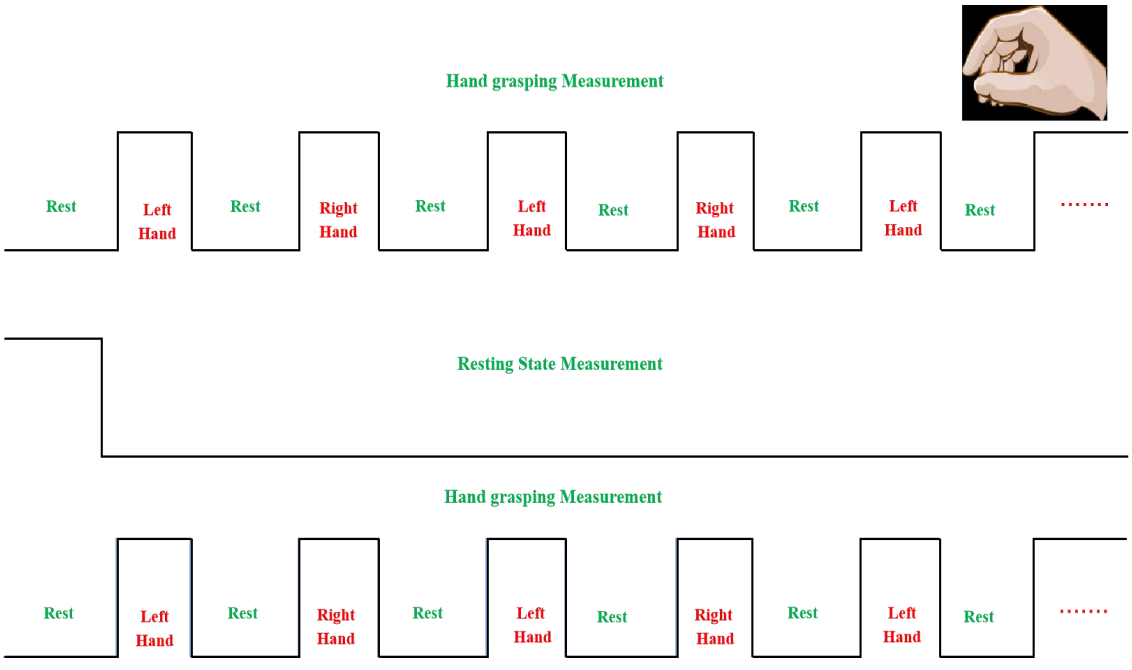


Figure 3- 1 Experimental block design paradigm used for the study.

## *3.3 Paradigm Design*

The task-based measurement using fNIRS was acquired with the help of a paradigm designed using NIRSTIM 4.0 software provided by NIRX LLC. As represented in Figure 3-1, the study was divided into blocks of active and rest phases. During the active phase, the subject was instructed to perform the simple hand grasp of the left hand initially followed by the rest phase for a specified duration. This is followed by the right hand in succession and continued for five trials for each hand. The instruction should be clearly conveyed to the subject for the best performance of the task. For close to accurate analysis of the activation in the brain we needed a synchronized paradigm delivery. This is achieved using the NIRSTIM software. The software has a modular and hierarchical organization. The advantage of using this proprietary software is that it can be launched from the acquisition software. This ensures the synchronization of the paradigm with the data acquired.

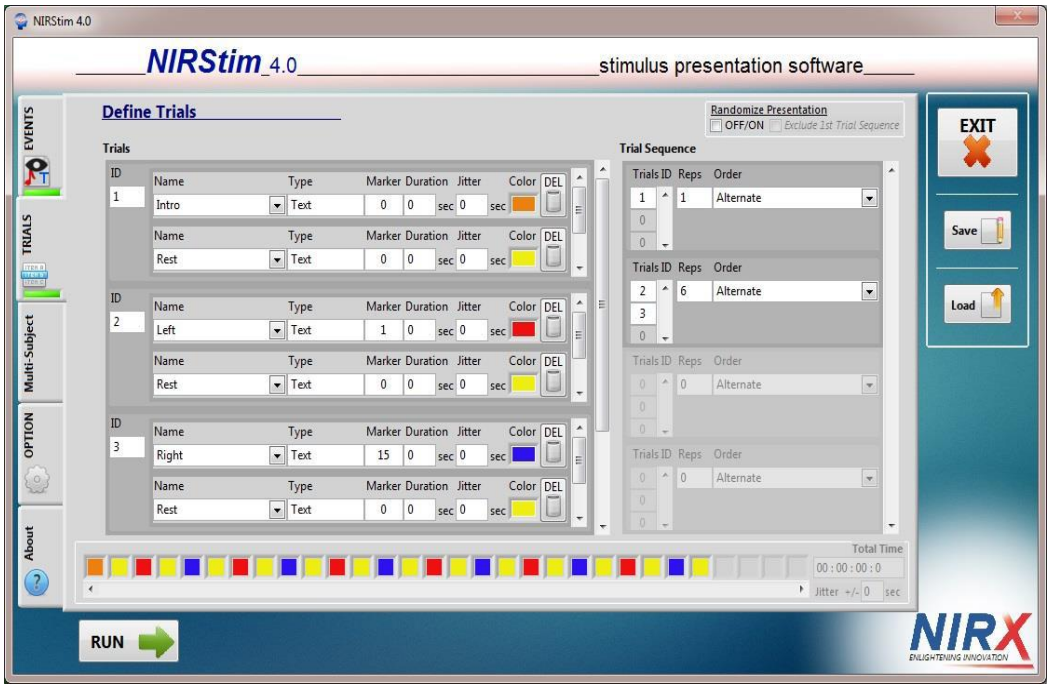


Figure 3-2 The GUI of the stimulus design and presentation software.

The task-based paradigm has three main events namely LEFT, REST and RIGHT. These events represent the left and right-hand grasp and resting block. The first step is to add the events in the paradigm. Events can be of different types like text, picture, sound, etc. After declaring types of the event, marker index and color should be defined. These event markers are eventually used for the analysis of active and rest block averages. We can also define other events like introduction text which may display the instructions for the subjects, helping to perform the task better. In the next step, we need to define the number of trials and the duration of the trials. This study has three main events and one introductory text event. Here the introduction text should be shown once to subject for ten seconds duration. So the introduction text can be given as 'Trial ID 1'. Similarly for the LEFT, RIGHT and REST events trials are defined for a duration of 20 seconds. The

subject is also given an auditory cue to perform the task, such that the sound stops at the end of the 'active' period.

Once the trials are defined, a sequence shall be generated to display the paradigm. In this study, there are five trials for each hand grasp. A hand grasp task was used in previous studies to obtain motor cortex response effectively (Kato et al 2002 ). So while generating the sequence 'introduction text' is given one repetition and 'LEFT', 'RIGHT' and 'REST' is given five repetitions alternatively.

## *3.4 Data Acquisition*

### 3.4.1 Equipment

The acquisition was performed using the NIRSport system (NIRx Medical Technologies LLC, Berlin, Germany) having 8 sources and 8 detectors at a sampling rate of 7.825Hz. The device emits light at two distinct wavelengths, 760nm, and 850 nm, for discrimination of two oxygenation states of tissue. The system facilitates the illumination of multiple targets in a time-multiplexed scanning method. Four sources and four detectors were used to cover areas of interest in each hemisphere. NIRSport is a portable, multi-channel, continuous-wave fNIRS platform that measures hemodynamic neuro activation via oxy-, deoxy-, and total hemoglobin changes in the cerebral cortex. NIRSport can measure both topographic and tomographic NIRS data from the entire cortex, yielding 3-Dimensional depth-discriminating brain activation. NIRSport system has to be connected to the laptop loaded with the acquisition software.

### 3.4.2 Subject preparation

The degree of subject tolerance needed is low, considering the modality's non-invasive and light-weight nature, as well as its fast setup and preparation times. The subject is seated comfortably in a chair for the data acquisition. The circumference of the subject's head is measured using a measuring tape. According to the circumference NIRScap size is determined. NIRScap is a specially designed fabric cap with provision for placing the optode holders. The optode holders are placed on the cap in the standard EEG electrode arrangement. This makes it is easy to define probe locations with respect to one another, head anatomy and brain regions of interest. If the NIRScap is placed properly, the optodes will have good optical contact with the skin and the whole setup will be robust to motion. This way, high signal quality is ensured.

Figure 3.3 The picture shows the NIRscap used for the study. The holes seen in the picture are the optode holders

Once the suitable sized cap is selected, the next step is to make sure optode holders are placed according to the montage required. The cap may be populated fully or partially in regard to the requirement of the study. There are stabilization links provided to keep the holders within the stipulated distance of 3 cm to obtain optimal signal quality. While placing the cap on the subject, start from the forehead and make sure it is perfectly centered. This is important for the anatomical positioning of the optodes. As shown in fig 3.3 the optode holder corresponding to the EEG electrode position Cz should be positioned centrally both in the left-right direction as well as in the anterior-posterior direction. Once it is fixed pull the chin strap and fit the cap tightly on to the head.

Hair is the main obstacle that precludes light penetration. Since signal quality depends on how good the interface is, it is very important to dedicate enough care to hair preparation. The goal is to minimize light blockage, by parting any hair such that direct contact with the scalp is achieved. A wooden applicator, a headlamp and preparation gel may be used for achieving this and clearing the scalp. Now that the NIRScap preparation is over, the subject can be given the instructions for a task-based paradigm. Once the instructions are given optodes are placed in the optode holders according to the montage used for the study.

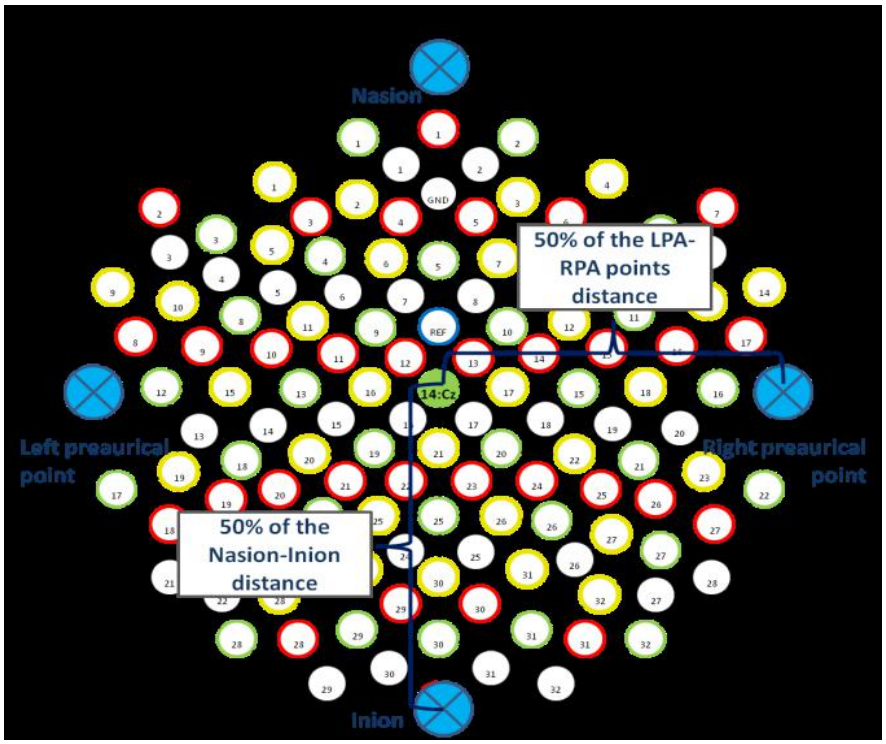


Figure 3- 4 The standard EEG locations depicted on the NIRScap for placement of the optodes

### 3.4.3 Acquisition Software

The fNIRS data acquisition is done with the help of 'NIRStar' software. In the software initial setup has to be completed prior to the start of the measurement. The first step is to configure the hardware which will help to recognize the equipment settings used for measurement. Hardware configuration involves different steps. We have to define the montage we use for the study. Here we use a motor 8x8 montage provided by the software. This montage helps with the placement of the optodes in the cap conforming to 128 standard EEG positions. The 2D representation of the montage used for acquisition is shown in fig 3.5. The sources are shown in pink shade numbers S1 up to S8. The detectors are shown in the green shaded circles which are numbered D1 to D8.

The purple interconnection shows the channels. The fNIRS signal was recorded bilaterally as shown in the 3D representation in figure 3.6. The combination of 8 sources and 8 detectors form twenty measurement channels. It is spread over the premotor area and supplementary motor area (10-20 EEG locations corresponding areas FC3, FC1, FCz, FC2, and FC4) and over the primary motor cortex (10-20 EEG locations corresponding areas C4, C2, Cz, C1 and C3). We used fNIRS Optodes Location Decider (fOLD) which helps to automatically decide optodes positions based on 10–10 and 10–5 systems according to a set of brain regions of interest. It works on the basis of sensitivity profile from photon transport simulations run on two head atlases. The inter optode distance was maintained at 30 mm. Anatomical locations of the channels are listed in table 3.3.

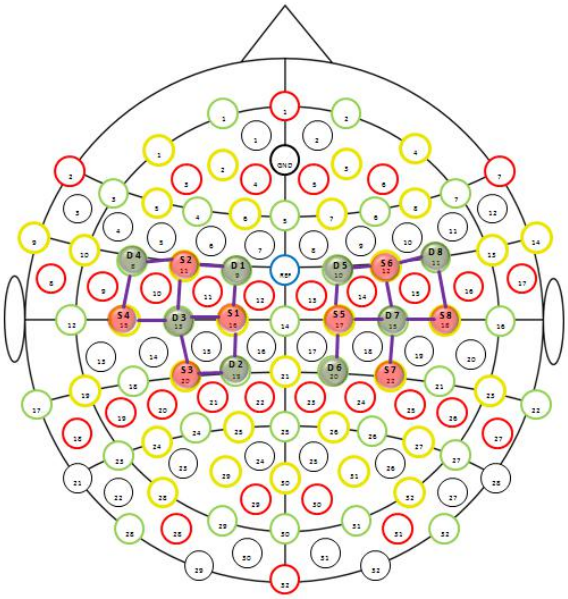

Figure3.5: Two-dimensional representation of the montage used for the study

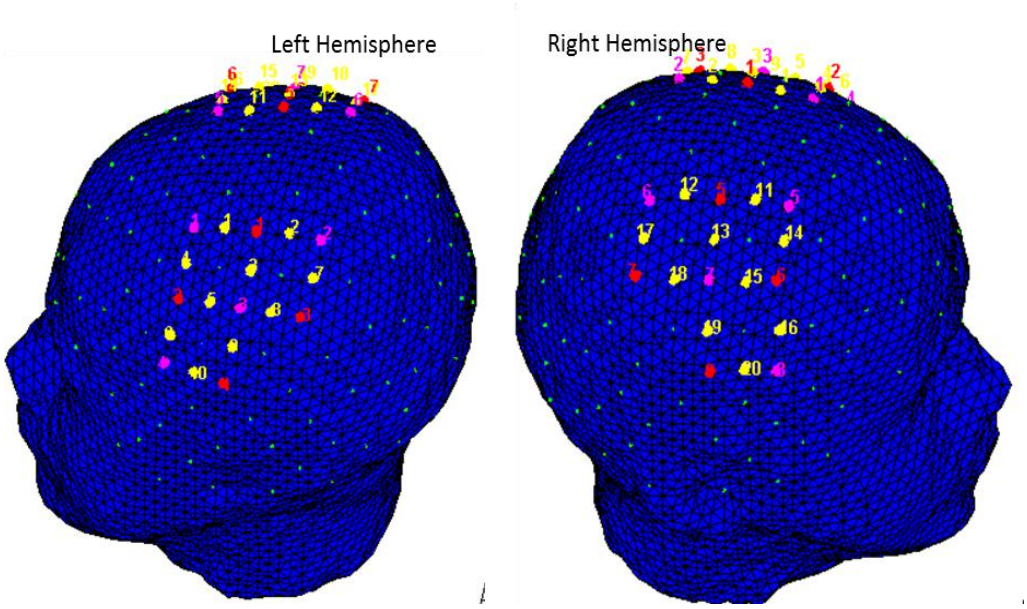


Figure 3.6: Shows the arrangement of optodes in the montage used for acquisition. Red dots represent sources and the pink dot represents detectors. Yellow dots represent the channels. Channel 1 to 10 is placed on the left hemisphere and 11 to 20 is placed on the right hemisphere.

**Table 3.2: Anatomical locations corresponding to channels used in the subject.**

| *Hemisphere* | *Channel* | *Anatomical Area* |
|---|---|---|
| ***Left*** | C1 | Premotor and Supplementary Cortex |
| | C2 | Somato sensory Association cortex |
| | C3 | Primary Motor Cortex |
| | C4 | Premotor and Supplementary Cortex |
| | C5 | Premotor and supplementary Cortex |
| | C6 | Premotor and supplementary Cortex |
| | C7 | Somato Sensory Cortex |
| | C8 | Somato Sensory Cortex |
| | C9 | Somato Sensory Cortex |
| | C10 | Primary Sensory |
| ***Right*** | C11 | Premotor and supplementary Cortex |
| | C12 | Somato sensory Association cortex |

| | | |
|---|---|---|
| | C13 | Primary Motor Cortex |
| | C14 | Premotor and supplementary Cortex |
| | C15 | Premotor and supplementary Cortex |
| | C16 | Premotor and supplementary Cortex |
| | C17 | Somato Sensory Cortex |
| | C18 | Somato Sensory Cortex |
| | C19 | Somato Sensory Cortex |
| | C20 | Primary Sensory |

Once the montage is defined, the setup is ready for acquisition. All the optodes in the montage are placed in position. The next step is calibration. The device needs to be calibrated prior to every acquisition. During this process, the software automatically assigns the appropriate amplification level (gain) for each of the detectors. After calibration, the optimal signal quality for each channel is displayed. The indication is given in four levels of color gradation. The green color indicates excellent signal quality, yellow indicates acceptable signal quality, red indicates the critical level and white represents no signal at all. A channel may fall into 'red' or 'white' level because of a lack of good contact between the skin and tip of the optode. This can be fixed by identifying the channel by using 'Show Topo Labels' function and removing the corresponding optodes to try and improve the contact. Once this is done a re-calibration is performed to analyze the signal quality. If the signal quality is acceptable, we can proceed to 'PREVIEW' of the data. This option helps us to visually inspect the data prior to recording. The next step is to record the data for the required duration according to the task. The stimulus presentation software is invoked from this software and runs

parallel to the acquisition for the synchrony. Once the paradigm is complete the recording can be stopped and the data will be saved in the predefined location.

## *3.5 Data Analysis*

### 3.5.1 Task-based fNIRS data Processing

Task-based data was processed using a Matlab based versatile software analysis environment called NirsLab software (NIRx Medical Technologies LLC) developed to support the study of time-varying near-infrared measurements of tissue (Y. Xu et al., 2014). The software interface is divided into sections like - Experimental Conditions and Data, Data pre-processing, Hemodynamic states, Data Viewer, Data Analysis, and Utilities.

#### *3.5.1.1 Loading Data*

The data acquired from NIRSport can be loaded in two different ways. One is to load the experiment configuration file, comprising details of the experiment conditions such as the duration of the experiment, source-detector arrangement, etc. This will initiate a 'nirsinfo' file which is a Matlab variable. The second option is to load the 'nirsinfo' file directly. We also need to add/ cross-check the information regarding the event markers and the probe setup. After each step, the 'nirsinfo' file will be updated and saved.

### *3.5.1.2 Raw Data Quality Check*

Data pre-processing starts with checking the quality of the raw data acquired. Initially, during the acquisition, we ensured the data quality by calibrating the equipment and checking for the optimal signal quality. The data quality was analyzed for bad/noisy channels and then such channels were excluded from further analysis. Electronic gain that is used to amplify the signal for each channel and the coefficient of variation (CV) of each channel were the criteria for the signal quality. As a rule, the signal-to-noise ratio of data decreases as the gain factor increases. Consequently, nirsLAB identifies the channels that have gain factors higher than a threshold value of 8, and exclude them from consideration in the subsequent processing and analysis steps. For each wavelength, we compute a CV which is given by the equation 3.1

$$\text{CV}=100 * \frac{Standard\ Deviation\ of\ the\ signal}{Mean\ of\ the\ signal} \qquad (3.1)$$

If the data has a high noise level, a considerable long-term drift, or cut-offs resulting from poor skin-optode contact, then the standard deviation, and due to that the CV would be significantly greater. The threshold value was kept at 7.5 for the CVs. The 'check raw data' option thus check for gain and CVs of the raw data and give the 'good' and 'bad' channels based on the thresholding of the values.

### *3.5.1.3 Data Pre-processing*

Pre-processing involves four steps: Truncating, Spike removal, Discontinuities removal, and Filtering. The data needs to be truncated generally if a) the baseline period

prior to the first event is substantially long b) a continuous recording of trials is done with a cool-down period in between c) you need to isolate a particular event type d) need to remove the time while the subject was given instructions, practice sessions, etc. The raw data was truncated for a uniform baseline period of 30 seconds before the first marker for every subject.

The data is then cleaned for discontinuities and jumps. It is extremely important to remove artifacts of this nature. In the absence of any correction, significant artifacts can remain in block averages. These residual artifacts can bring significant biases in results obtained from subsequent statistical analyses such as GLM computations. The data acquired during the study very rarely showed such a 'jump' artifact. The algorithm working behind discontinuity removal and spike removal computes the standard deviation ($S_d$) of the time series first. The difference between two successive time points ($T_d$) is calculated and the ratio of this difference to the $S_d$ is found out. The ratio (J) is compared to a threshold value to identify the discontinuity or spike in the time series.

$$J = \frac{T_d}{S_d} \qquad (3.2)$$

Once the jump artifact is identified a constant value is subtracted from the remaining time series so the discontinuity is removed.

The spikes in the time series could be identified and selected manually in the spike removal window. Once the time window is selected using the mouse, the time series within the selected time window is imputed with either nearest values or random

values. The algorithm computes the difference (D) between maximum ($d_{max}$) value and minimum value ($d_{min}$) within the selected time window and divides the difference with the $S_d$ to compute the ratio K. If K is greater than the threshold set then the data points are to be replaced. If the nearest signal option is selected the algorithm identifies the two nearest neighboring channels with clean data (iteratively) in the same time interval of the selection. The raw data values from this time interval of the two channels are averaged and those values are assigned for the identified spikes

Till now we have removed the different type of data artifacts and drifts in the data which were data values that changes over time in a manner not related to the experimental design. Such artifacts were limited to time intervals. But there may be artifacts that are distributed over the entire measurement duration. Such fluctuations can be removed by applying frequency filtering to the raw data.

A bandpass filter is used to filter out the fluctuations which are physiologic in origin. Higher cut off frequency of the band-pass filter is chosen in a way that physiological noises such as respiration (~0.5 Hz), heart rate-blood pressure (~1 Hz) are being filtered out. In the task-based fNIRS studies, the higher cut off frequency is chosen as 0.2 Hz as it is lower than 0.5 Hz. The frequency of stimulation must be in the range of filtering. The tasks are created based on the fact that the hemodynamic response of the brain changes very slowly. The task used in the study lasts about 25 seconds duration i.e the frequency of stimulation will be 0.04 Hz. The lower cut-off frequency was set at 0.01 Hz in order to suppress slow drifts and physiological noise contamination in the signal.

#### *3.5.1.4 Computing Hemodynamic states*

The pre-processed data is converted to the relative changes of hemodynamic states like oxyhemoglobin (HbO), deoxyhemoglobin (HbR) and total hemoglobin (Hbt). As explained in Chapter 1, we employ Modified Beer Lambert's Law (MBLL) for the calculation of the hemodynamic states. Initially set of parameters for MBLL are defined. a) Wavelengths b) Source –detector distance c) Baseline duration d) Background hemoglobin content in μM and mean venous oxygen saturation value e) Differential path length factor (DPF) which accounts for the additional path traversed by the due to scattering. Baseline duration is identified with the time before the first event marker where the subject is under rest condition. DPF values are essentially obtained from the literature(Kohl et al., 1998). After setting up all the parameters the hemodynamic states are computed. The data can be visualized in different ways to review the analysis. The block average can be displayed for different conditions of the task and different hemodynamic states. The signal variation in HbO and HbR has been reported in many studies. HbO signal variation shows higher amplitude than the HbR signal.

#### *3.5.1.5 GLM Analysis*

The task-related features from the hemodynamic time series data are extracted using the general linear model (GLM) analysis. The GLM has traditionally been the standard method to analyze data in functional magnetic resonance imaging (fMRI), which is a widely used functional imaging technique with standardized methods of analysis. Similar to fNIRS, fMRI measures changes in blood flow due to neurovascular coupling,

so the GLM can also be used to analyze fNIRS data (Ye et al., 2009). Comparisons among different channels of measurement within a single subject are performed using Level 1and comparisons across multiple subjects are done with Level 2 of GLM analysis. We employed Statistical Parametric Mapping (SPM) freeware package to perform this subject level and group level analysis. The GLM approach uses a regressor created from the convolution of a standard HRF and a boxcar function, which indicates whether or not the stimulus is present. We analyze the changes in HbO to determine in which cortical regions have significantly higher amplitude hemodynamic fluctuations compared to background fluctuations occurring during the resting period. The GLM expresses a dependent variable, in this case, changes in HbO over time, as a linear combination of reference functions. The basic GLM equation is given below in equation 3.3 (Jenkinson and Chappell, 2017).

$$Y = X\beta + \varepsilon \tag{3.3}$$

where Y is the m x n matrix containing HbO time series for each m time points and n channels. X is the m x p regressor matrix containing m regressors which tries to model the HbO time series in Y.β is the p x n matrix of beta value which indicates the weights of the regressors which is used to match the HbO time series in Y. ε is the model error term, which is the variation in the HbO time-series not explained by the regressors.

In the present study we have HbO time series and a boxcar design for the experiment involving Left-hand task( LHT), Right-hand task(RHT), and resting phase. Therefore the X matrix will have three columns as three models for each task are

designed as shown in fig 3.8. The Beta values are computed from equation 3.4 by using ordinary least square estimation. Once the beta values have been computed they are used in a t-test to determine if significant activation is present in the individual channels for any of the experimental conditions. To determine if either of the regressors explained a statistically significant amount of the variance in any of the channels, t-values were calculated using the following equation

$$t = \frac{c'\mathrm{B}}{\sqrt{Var(\varepsilon)c'(X'X)^{-1}c}} \qquad (3.4)$$

where c is the contrast vector which has the weights corresponding to the experimental conditions.

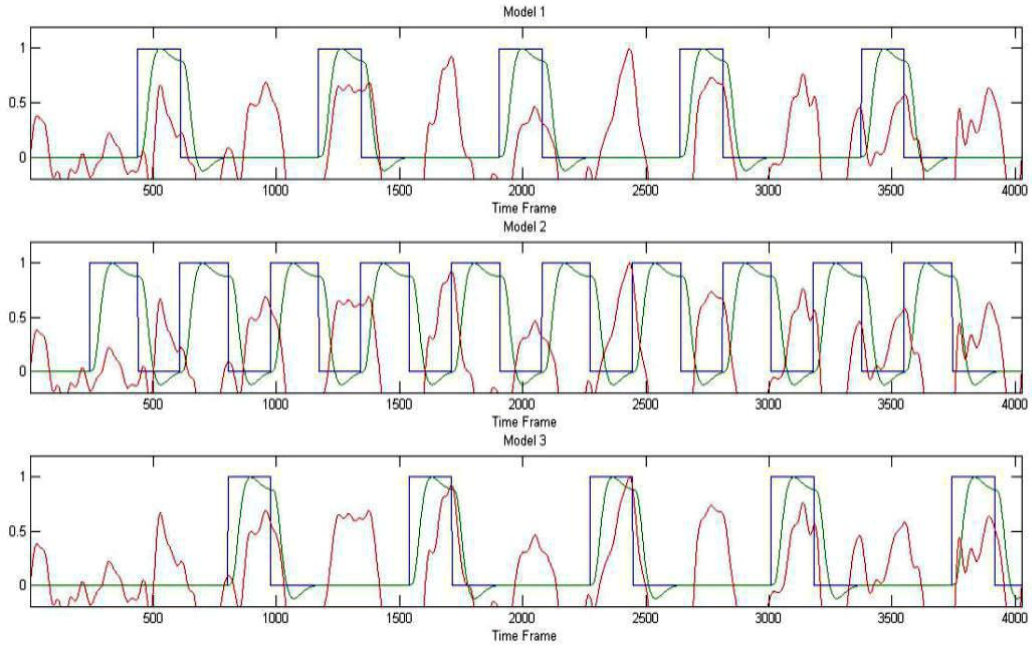


Figure 3.7 The three models created for GLM analysis. Boxcar design is indicated in black color. The ideal response is indicated in green color and the obtained response is represented in red color. Model 1is for LHT, Model 2 is for rest and Model 3 is for LHT.

Individual subject data were arranged for three different groups for analysis. The groups were defined as the healthy control group (HC), right hemisphere stroke affected group (RHS), and left hemisphere stroke affected group (LHS) on the basis of the stroke-affected side of the brain. Each subject data were analyzed for multi-condition comparisons like

a) LHT vs RHT

b) LHT vs Rest

c) RHT vs Rest

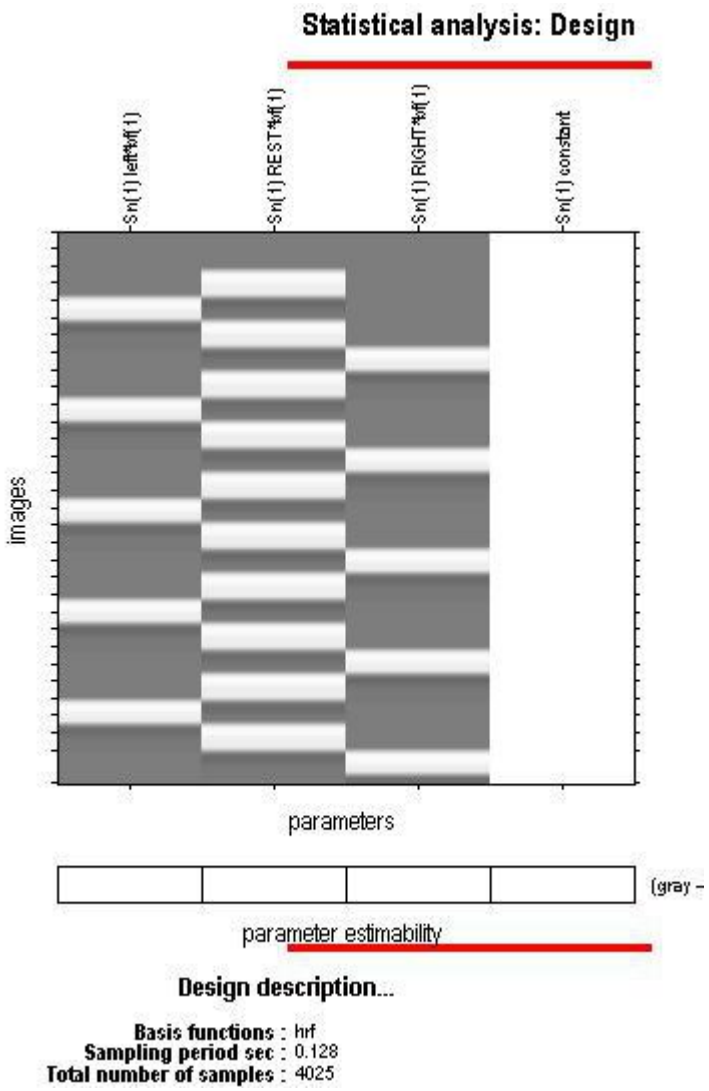


Figure 3.8: The Design matrix generated after the GLM design for the task-based analysis.

Healthy group data were analyzed for the typical motor lateralization pattern. The task was split into two different runs of LHT and RHT. Both hemoglobin and deoxyhemoglobin data were examined for the changes. For the HC group, the hemoglobin concentration changes during both LHT and RHT from the left hemisphere and right hemisphere channels were separately averaged

### 3.5.2 Resting State fNIRS Analysis

The resting-state fNIRS data preprocessing analysis was performed using a Matlab based freeware called FC-NIRS v1.0 developed by the *McGovern Institute for Brain Research, Peking University* (Xu et al., 2015). Further, the functional connectivity analysis was conducted using the Brain Connectivity toolbox developed in Matlab by Rubinov and Sporns. The visualization of the network properties was done with BrainNet Viewer (Xia et al., 2013)

#### *3.5.2.1 Data Pre-processing*

The resting-state data collection is done as explained in section 3.2 and 3.4. FC-NIRS software reads the fNIRS data in the universal format of '.nirs'. There are two options to get the data in the '.nirs' format. One option is to directly convert the data using the acquisition software 'NIRSTAR' and save the raw data in the desired format. The second option is to convert the data obtained using a custom made Matlab code. Once the data is in the '.nirs' format it can be loaded using the interface. The raw data can be displayed channel by channel by selecting the links in the montage.

The software provides a bunch of options for the pre-processing of the raw data. The preprocessing steps used for the analysis are depicted in fig 3.9 The first step is to cut down the time series length to the desired time. This is important for the group analysis as the measurement time may involve the extra length due to personal errors

and delays. The study was designed for three minutes of resting-state acquisition. So the data is cut to make sure 180 seconds of data is available uniformly across the subject. The second step is to convert the raw intensity values to optical density values. An optional step of detrending the data can be used if the data has long trends. The Optical density values are converted to the concentration of HbO and HbR using the modified Beer-Lambert law. A third-order Butterworth digital filter is used for bandpass filtering. A band-pass range from 0.01 to 0.1Hz, which represents the frequency range of hemodynamic signals that are thought to come up from instinctive neural activity, is used for filtering.

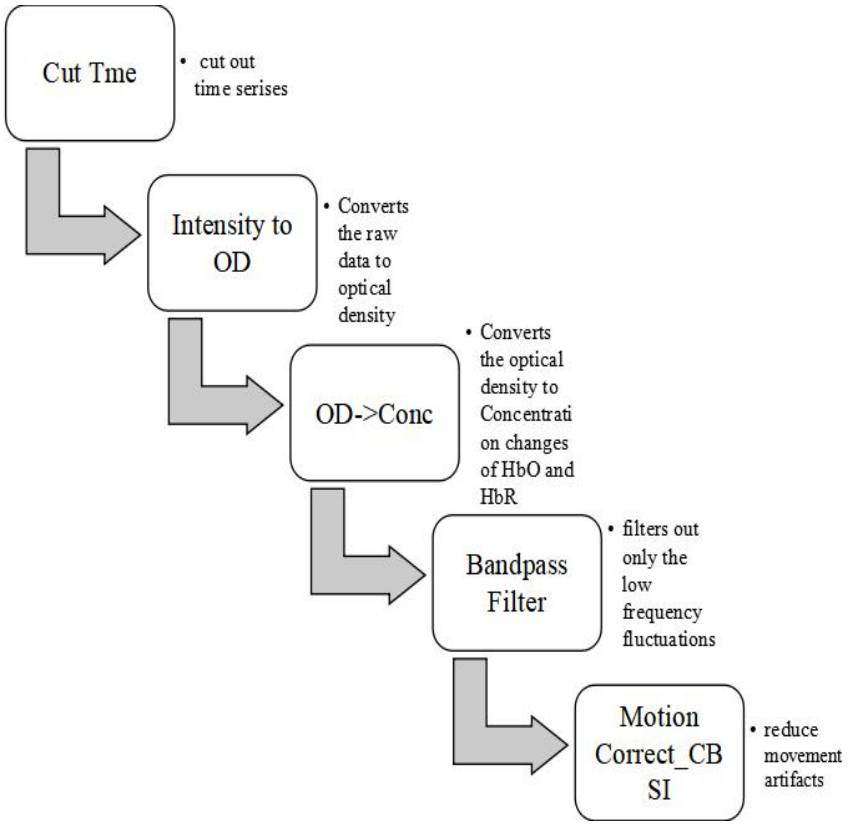


Figure 3.9 Diagrammatic representation of the steps involved in the processing of resting-state data.

### *3.5.2.2 Quality control*

For motion artifact correction a correlation-based signal improvement (CBSI) method is used. It is a channel-by-channel method based on the hypothesis that HbO and HbR will be negatively correlated during functional activation, while at the same time they should be more positively correlated when a motion artifact occurred. These approaches have demonstrated an improvement in the data quality through reducing motion artifacts. For the SNR check of the hemodynamic signal, FC-NIRS primarily examined the signal quality from the SNR optical intensity values and the signal correlation values in the concentration signal among all of the measurement channels.

### *3.5.2.3 Functional Connectivity*

A seed-based correlation approach and whole brain correlation approach is used to calculate functional connectivity. Seed based approach estimates the strength of the pairwise Pearson's correlation between the selected seed regions and all other channels in the montage. It is defined as

$$r_{xy} = \frac{\mathrm{cov}_{xy}}{Sd_x . Sd_y} \tag{3.5}$$

where x and y represent time series from two channels, $Sd_x$ and $Sd_y$ are the standard deviations and $cov_{xy}$ is the covariance of the time series.

The whole brain approach, on the other hand, gives the correlation strength between any two measurement channels. The group-level analysis is performed and a T map consisting of uncorrected t values after one-sample t-test is obtained.

### 3.5.3 Network Analysis

Real-world complex systems like the brain can be represented mathematically using networks which are a collection of nodes and links connecting the nodes. For brain networks, the different brain regions are considered as nodes and the links represent the connectivity between them. The network analysis is performed using the Brain Connectivity toolbox. The toolbox provides the opportunity to explore different complex connectivity measures defined using graph theory. Individual measures in a brain network may characterize different aspects of local and global brain connectivity. The connectivity data from the FC-NIRS is used for the network analysis. Here the nodes represent the individual channels in the montage which in turn represent the anatomical regions underlying them as in table 3.3. The links or edges are representative of the correlation strength between those channels calculated by the Pearson correlation method using FC-NIRS.

Functional connectivity studies, in general, try to understand two main concepts i.e Functional segregation and Functional integration. Functional segregation is the concept of having specialized processing groups within interconnected brain regions. Such measures of segregation denote the presence of clusters or modules within the network of interest. It is suggestive of an organized segregated neural processing within the

network. The measures of segregation are based on the number of interconnected nodes that forms clusters. The ability of the brain to combine information from distributed brain regions is explained by measures of integration. The estimate of the communication ability of brain regions is based on the concept of path. The study focuses on the measures of segregation such as the clustering coefficient and modularity as well as the measures of integration such as global efficiency and local efficiency.

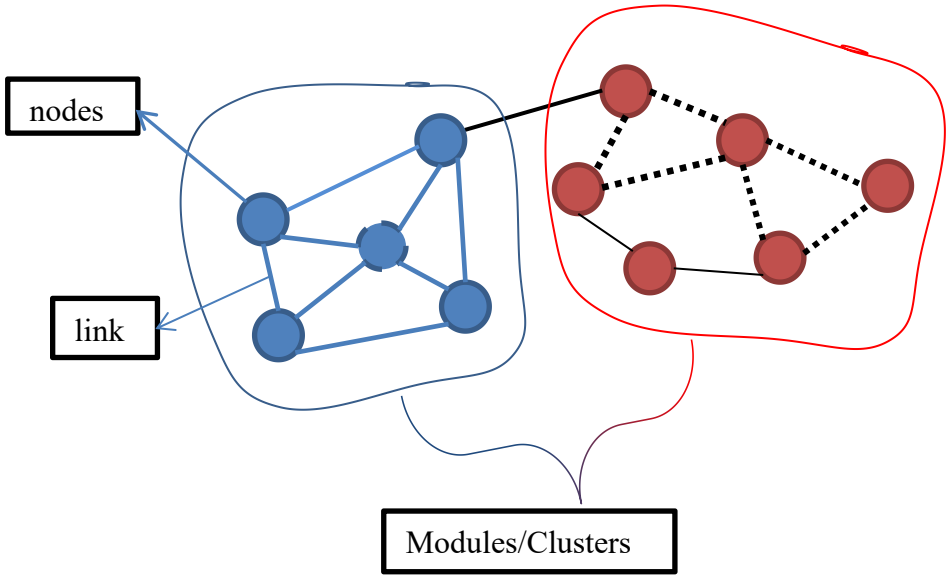


Figure 3.10 A representation of the brain network having two modules ( blue and red). Nodes are colored blue and orange in respective clusters.

The clustering coefficient of a node represents the ability to cluster together with the neighboring nodes (Watts and Strogatz, 1998). It is defined by the proportion of links between the nodes within its neighborhood divided by the number of links that could possibly exist between them.

$$C_i = \frac{1}{n}\sum_{i \in N} \frac{2t_i}{k_i(k_i - 1)} \qquad (3.6)$$

Where n is the number of nodes and N is set of all the nodes in the network, $t_i$ is the number of triangles around a node i and $k_i$ is the degree of the node i denoting the number of links connected to the node. As shown in fig 3.10 the central node in the blue cluster has the highest clustering coefficient where a maximum number of triangles are formed.

The clustering coefficient for the network is given by the mean of all the individual clustering coefficients of the nodes in the network.

$$Clustering\ Coefficient, C = \frac{1}{n}\sum_{i \in N} C_i \qquad (3.7)$$

Efficiency is the network measure that indicates the ability to transmit information at a global and local level. Global efficiency is considered as the inverse of the average shortest path length. The shortest path length is calculated by the minimum number of edges that are linked between any two nodes of the network. For a network, the mean of shortest path length is considered and is known as Characteristic path length. It is interpreted as an indication of parallel information processing within a network. Local efficiency is defined for a local subgroup of the nodes which is confined to the immediate neighboring nodes. For a node, efficiency (ε) is calculated as

$$\varepsilon = \frac{1}{L_{path}} \qquad (3.8)$$

Where $L_{path}$ is the shortest path length of the node.

Another measure of segregation which gives the composition and degree of clustering is the modularity. The modular or community structure indicates the division of the network into subgroups having maximum within-group links and minimum inter-group links. The modularity gives quantitative data of the degree of the division into non-overlapping groups. The demerit of this measure is that it is calculated by optimization algorithm which may compromise accuracy for computational speed. The method is a greedy optimization that tries to optimize the modularity of a partition of the network. The optimization is performed first by looking for local communities by optimizing modularity locally. Second, it aggregates nodes belonging to the same community and builds a new network whose nodes are the communities. These steps are repeated iteratively until a maximum of modularity is attained and a hierarchy of communities is produced.

# Chapter 4

# Results

According to the criteria mentioned in the previous chapter, patients were recruited for the study from the stroke clinic of the institute. The median age of the patients in the study was 54.5 and range (36,81). The median onset time of stoke patients recruited was 20 days. The median age of the control group is 48 with a range (28,65). The study was carried out after getting approval from the institute ethics committee. All the subjects were provided with an informed consent and information sheet. The subjects were explained about the nature of the data acquisition and signature in the consent was obtained. The patient data was also acquired for the second time after approximately 45 days to 60 days. The subject demographics are given table 4.1

Table 4.1 Patient Demographics and Information

| Sl.No. | Location of Insult | MRS/NIHSS | Onset (days) | Age (years) | Etiology of Stroke | Affected hand |
|---|---|---|---|---|---|---|
| 1 | Multiple infarcts in right MCA-ACA | NIHSS 2 | 25 | 46 | Large artery Atherosclerosis | Left |
| 2 | Left MCA minor stroke | MRS 3 | 10 | 61 | Lacunar | Right |
| 3 | LEFT MCA STROKE | NIHSS: 3,MRS-3 | 20 | 47 | Lacunar | Right |
| 4 | RIGHT MCA STROKE | MRS 2 | 20 | 66 | Large artery Atherosclerosis | Left |
| 5 | biHEMISPHERIC | MRS- 2 | 20 | 59 | Large artery Atherosclerosis | Right |
| 6 | RIGHT MCA STROKE M1area | MRS 2 | 11 | 36 | Undetermined | Left |
| 7 | RIGHT MCA STROKE M1area | MRS4/NIHSS 9 | 15 | 64 | Large artery Atherosclerosis | Left |
| 8 | RIGHT MCA STROKE | MRS 1/NIHSS1 | 28 | 38 | Lacunar | Left |
| 9 | RIGHT MCA STROKE | MRS2 | 25 | 64 | Large artery Atherosclerosis | Left |
| 10 | Left Frontal infarct | MRS 1/NIHSS 1 | 11 | 81 | undetermined | Right |
| 11 | RIGHT MCA STROKE M1area | MRS 2 | 40 | 42 | Large artery Atherosclerosis | Left |
| 12 | Left thalamocapsular infarct | MRS 1 | 20 | 52 | Lacunar | Right |
| 13 | LEFT MCA STROKE | MRS 3 | 60 | 66 | Lacunar | Right |
| 14 | Left Frontal infarct | MRS 2 | 20 | 45 | Large artery Atherosclerosis | Right |
| 15 | LEFT MCA STROKE | MRS 3 | 20 | 43 | Large artery Atherosclerosis | Right |
| 16 | LEFT MCA STROKE | MRS 3 | 10 | 56 | Lacunar | Right |
| 17 | Right MCA Stroke | NIHSS 7 | 60 | 65 | Large artery Atherosclerosis | Left |
| 18 | Left MCA | NIHSS 4 | 11 | 55 | Lacunar | Right |
| 19 | RIGHT MCA Stroke | MR3 | 20 | 48 | undetermined | Left |
| 20 | Right MCA Stroke. | NIHSS 5/MRS3 | 20 | 54 | undetermined | Left |

## *4.1 Task based Analysis*

The initial analysis of the study was concentrated on the task-based experiments. The finger/hand grasping task performed by a healthy group showed noticeable changes in oxyhemoglobin and to a lesser extent in the deoxyhemoglobin. The task phase and rest phase could be identified distinctly from the hemodynamic response curves obtained. The results from the healthy group were in line with previous studies (Leff et al., 2011). The subjects were able to perform left hand and right-hand finger movement and the average HbO response showed increased activation in the contralateral hemisphere. Fig 4.1 shows the hemodynamic response of one of the subjects in which the channel 5 from the left hemisphere and channel 16 from the right hemisphere are shown. The dominant hand movement (right hand) resulted in increased activation in channel 5 which is the contralateral channel. The non-dominant hand activation was seen similar in both the hemisphere.

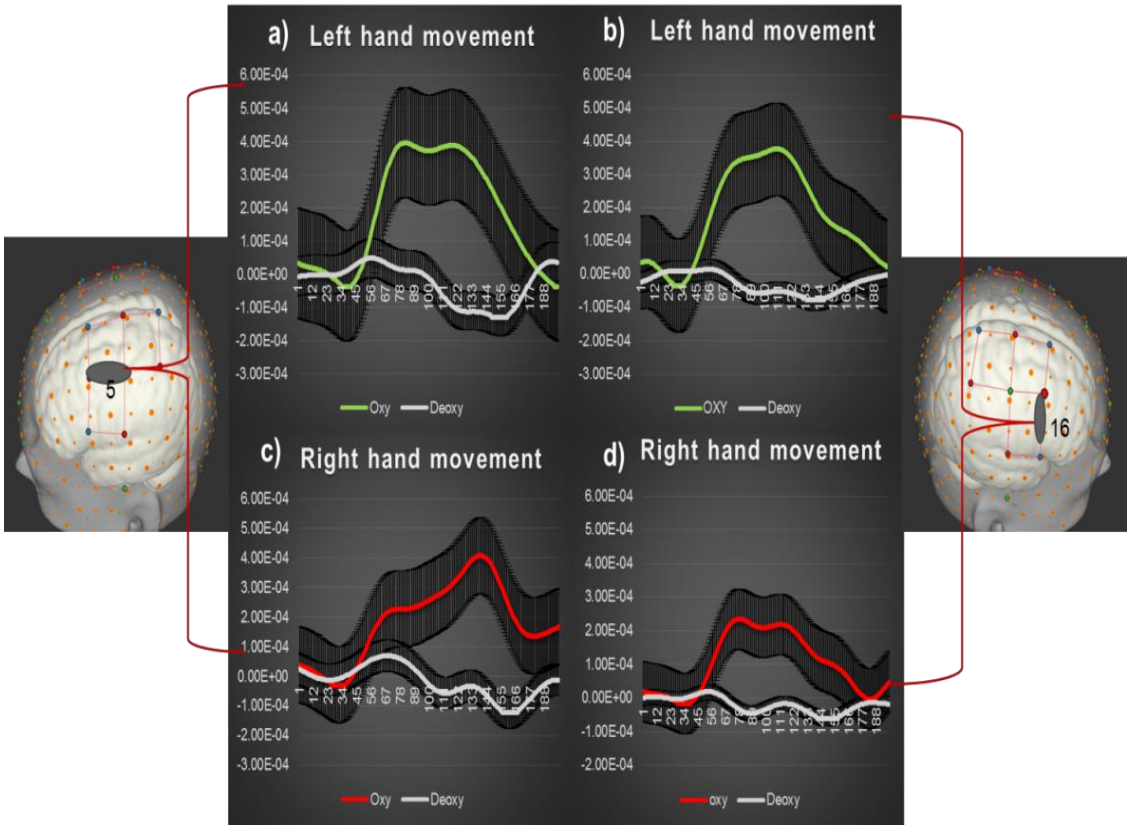


Figure 4.1: The hemodynamic response from one channel from the left hemisphere (Channel 5) and one channel from the right hemisphere (Channel 16). a & c represent the HbO and HbR response for the left and right hand movement from Channel 5 respectively. b & d represent the HbO and HbR response for the left and right hand movement from channel 16 respectively

### 4.1.1 Healthy Group Task based Results

Group analysis of the healthy group also confirmed the contralateral activation patterns. Fig 4.2 shows the increase in HbO values for left-hand movement in the right hemisphere and a similar increase for right-hand movement in the left hemisphere. The HbR variation is very small when compared to the HbO variation.

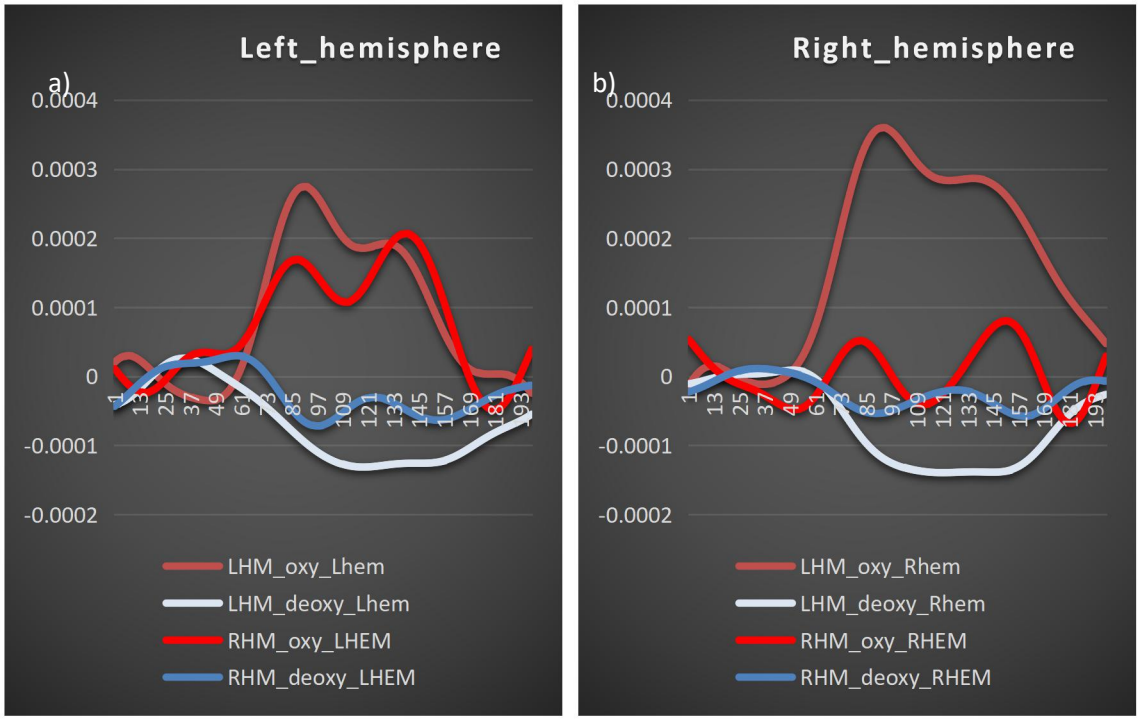


Figure 4.2 a) The task-based group average response for a healthy group for 25 s task window in the left hemisphere. b) The task-based group average response for a healthy group for 25 s task window in the right hemisphere. LHM- Left-hand movement, RHM – Right-hand movement

The GLM analysis is performed to extract the task-based activation for the left-hand task (LHT) and right-hand task (RHT). For RHT, M1 area (Channel 3) and premotor and supplementary cortical area ( Channel 1) in the left hemisphere have shown a significant increase ($p<0.05$,FDR corrected) in activation after the GLM analysis when the main effect of RHT was studied by giving full weight to RHT (contrast [RHT -1 LHT-0]). Similarly for LHT, M1 area (Channel 13) and premotor and supplementary cortical area (Channel 11,14 and 15 ) in the right hemisphere. The paired t-test revealed that channel 1($p<0.05$) and channel 3($p<0.02$) for the right-hand task and

channel 12 ($p<0.02$) and channel 14 ($p<0.05$) for the left-hand task showed a significant increase after the false discovery rate(FDR) correction. A decrease in activation is seen in the contralateral M1 area (Channel 13) for the RHT task. The fig 4.3 and 4.4 show the T stat plot for all the channels.

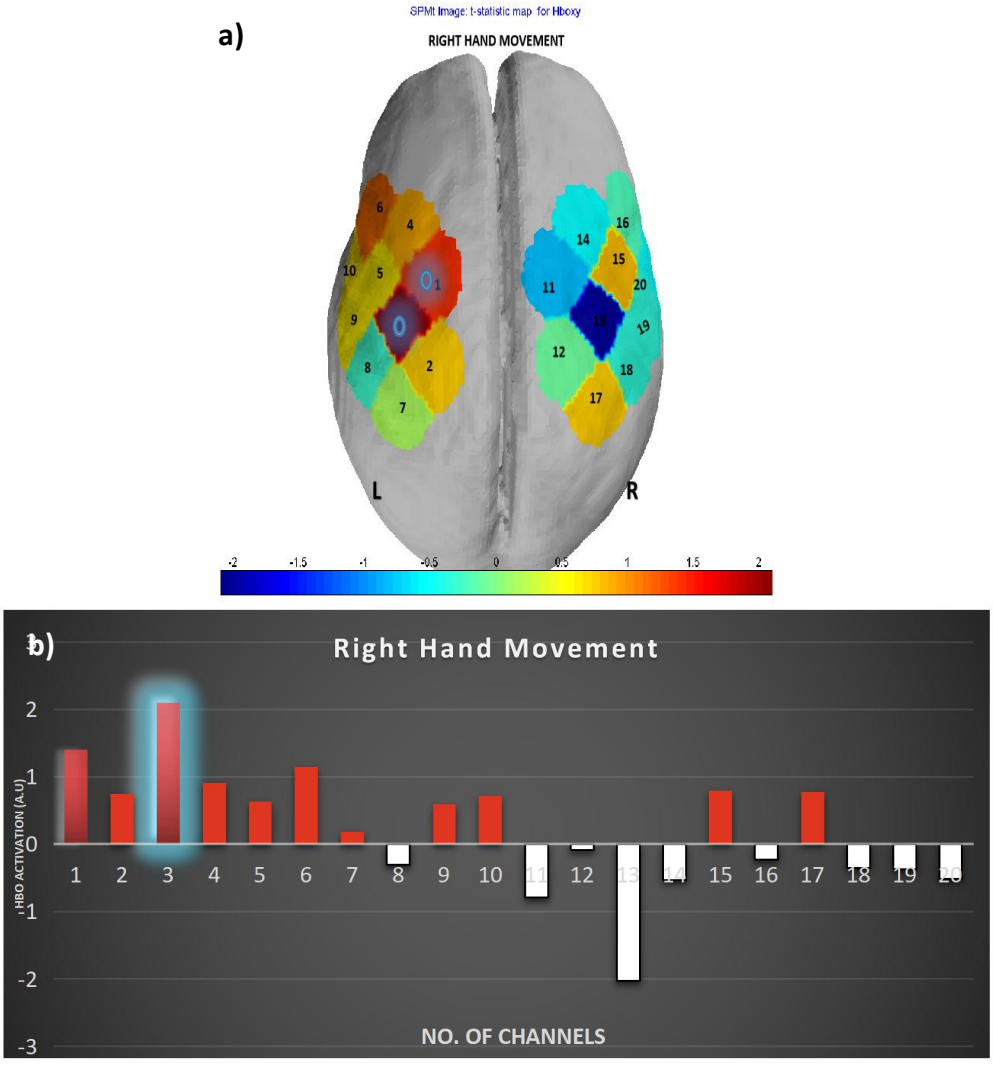


Figure 4.3 a) Task-based activation for all the channels is shown in the picture for the main effect of the right hand movement for a healthy group. The blue rings indicate the most activated channels in the healthy group. b) The graph represents the task activation in terms of T-stat values. The statistically significant ($p<0.05$,FDR corrected) channels are highlighted.

.

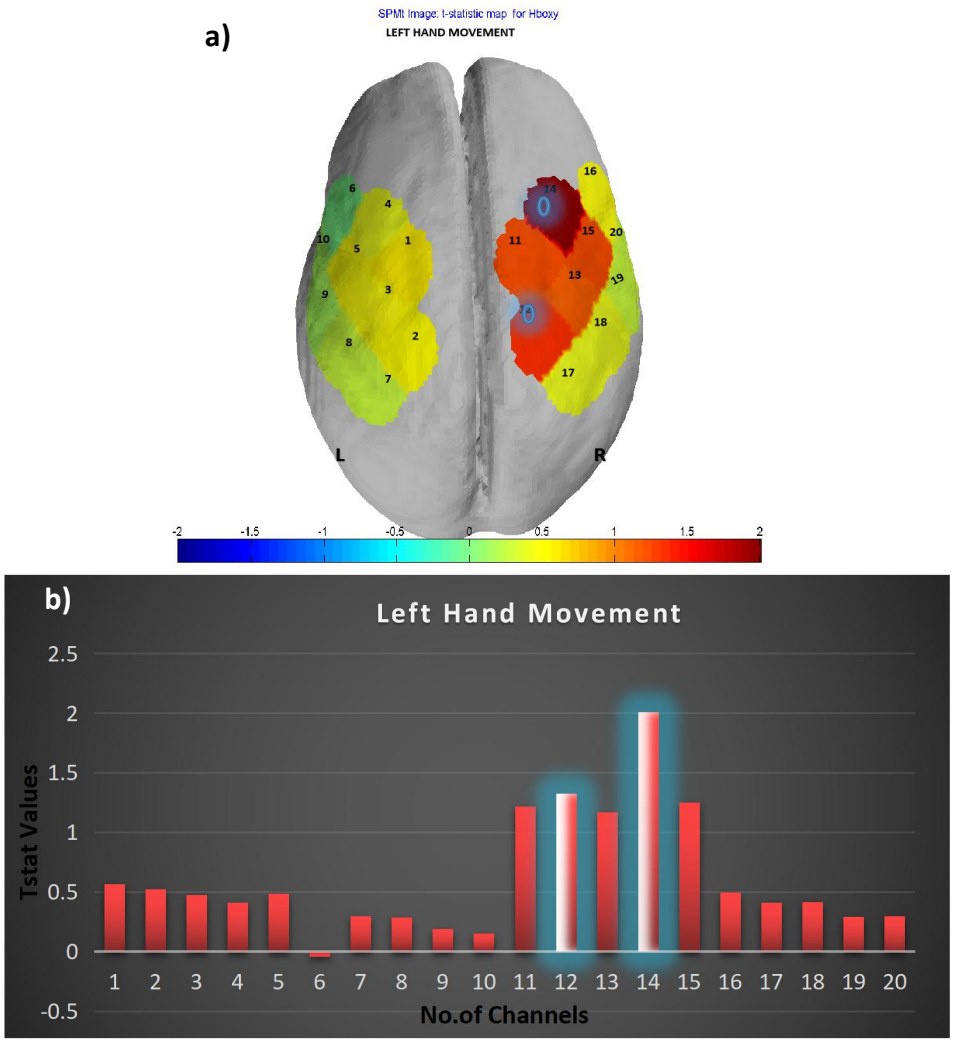


Figure 4.4 a) Task-based activation for all the channels is shown in the picture for the main effect of the left-hand movement for a healthy group. The blue rings indicate the most activated channels in the healthy group and b) The graph represents the task activation in terms of T-stat values. The statistically significant ($p<0.05$,FDR corrected) channels are highlighted

GLM analysis was done for identifying the activations in the motor areas for RHT >LHT condition and the contralateral M1 area and supplementary area activations were observed as shown in fig 4.5.

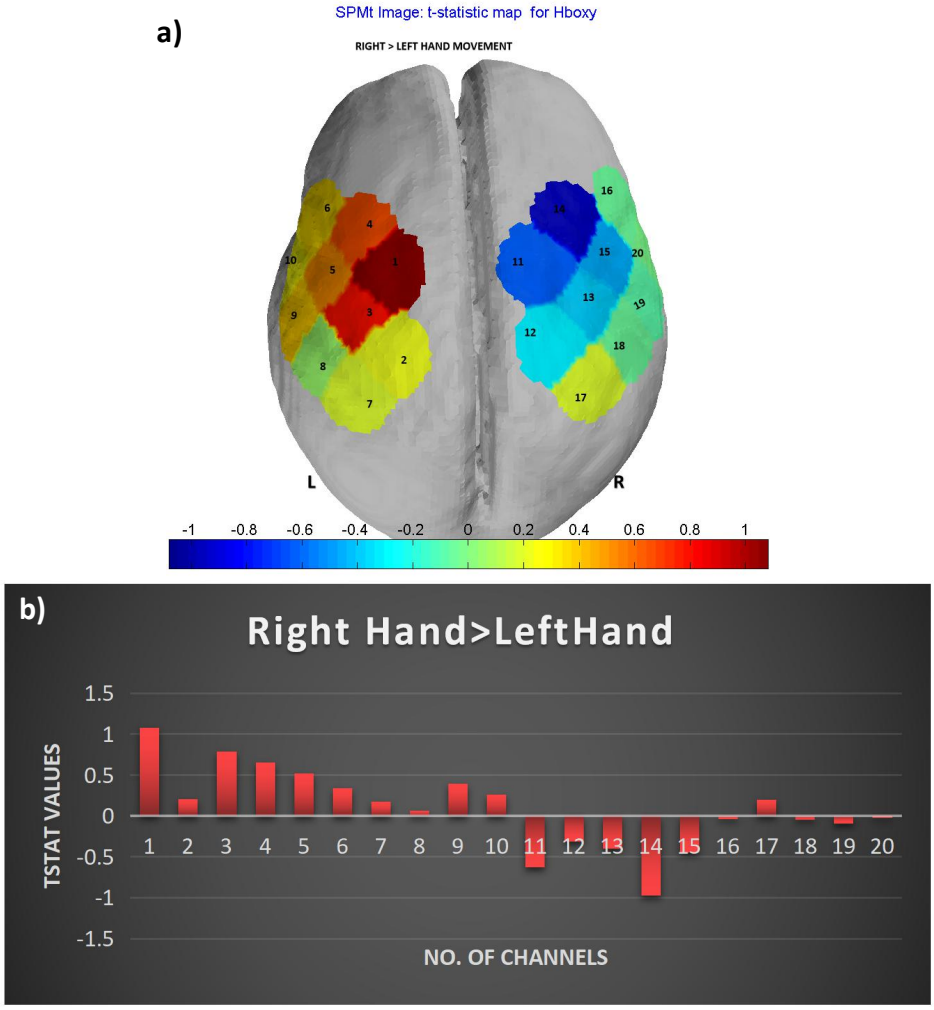


Figure 4.5a) Task-based activation for all the channels is shown in the picture for the effect of comparison of right-hand task over the left-hand task for a healthy group and b) The graph represents the task activation in terms of T-stat values.

### 4.1.2 Patient Group Task based Results.

The patient group was grouped into the left hemisphere affected stroke group and the right hemisphere affected the group. When the patient group was considered as a whole and the difference of left hand and right-hand movement did not yield any significant activation($p<0.05$) in any of the channels after FDR correction. Hence the

group analysis was performed for both the left affected and right affected group separately and also between the groups. Individual analysis of hemodynamic changes for both the tasks was done as explained in section 4.1. The response curve was indicative of some patients with difficulty in doing the task. Fig 4.6 shows the response of a subject who had difficulty in performing the task along with the response of a subject who could perform the task. The average HbO response of both hemispheres for both the tasks in Fig 4.6a and fig 4.6.b has been seen declining. The Fig 4.6c and 4.6d show that when the subject performs the task relatively better, the response is close to normal. The significant difference in HbO response in premotor and associated areas was seen patients while HbR response was minimal.

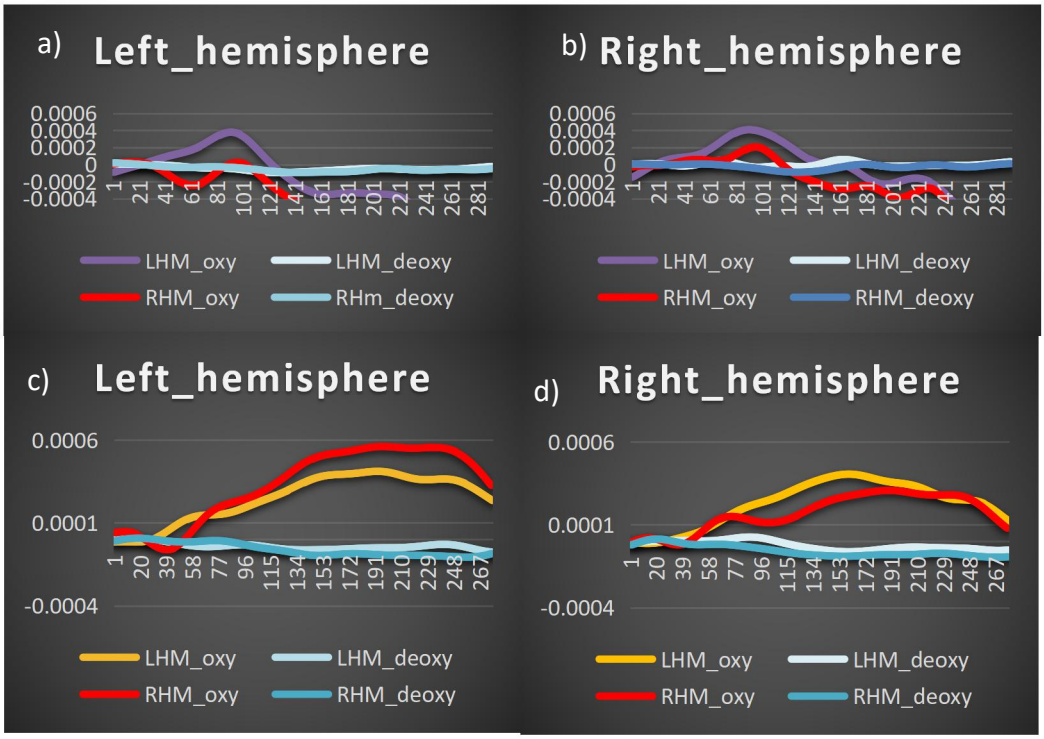


Fig 4.6a) and b) shows the average response from both hemisphere of the subject who had difficulty in moving the right hand. The HbO response (red line) of the right hand movement is having lesser

amplitude when compared to the left hand (yellow line). c) and d) shows the average response from both hemispheres of a subject who could perform a task and had left hemiparesis.

But most of the subjects performed the task in a way such that the hemodynamic response shows little difference in the task. Individual analyses of the subjects were performed. The analysis was performed for two sets of data. As shown in table 4.1 the initial data was acquired two to four weeks after the onset of stroke. The second set of data is acquired for assessing the recovery from the insult.

#### *4.1.2.1 Task Based result for Left Hemisphere Affected group*

The task-related response from the patient group whose left hemisphere areas were affected showed a difference from that of the normal group as detailed in 4.1.1. This group of subjects had difficulty in the right hand after stroke. Fig 4.7 shows the average response from different areas for a left hemisphere affected the subject. The subject performed the task. The response shows that the affected hand movement causes low response from M1 areas when compared to the premotor and supplementary areas. The premotor areas showed contralateral activation for the affected hand (right hand). GLM analysis was performed at the subject level and the activation for each task was compared statistically. Fig 4.8 shows the T statistic for each of the channel activations representing the HbO activations from each channel. The right-hand task yields a bilateral activation pattern from the M1 areas and somatosensory areas with significant ($p<0.05$, FDR corrected) activation in ipsilateral/contra-lesional areas. The left/normal hand activation shows a unilateral pattern with significant ($p<0.05$,FDR corrected) activation in the contralateral M1 areas. Fig 4.7 and 4.8 represent one subject from the

group. Group analysis was performed among the subjects with stroke whose left hemisphere was affected.

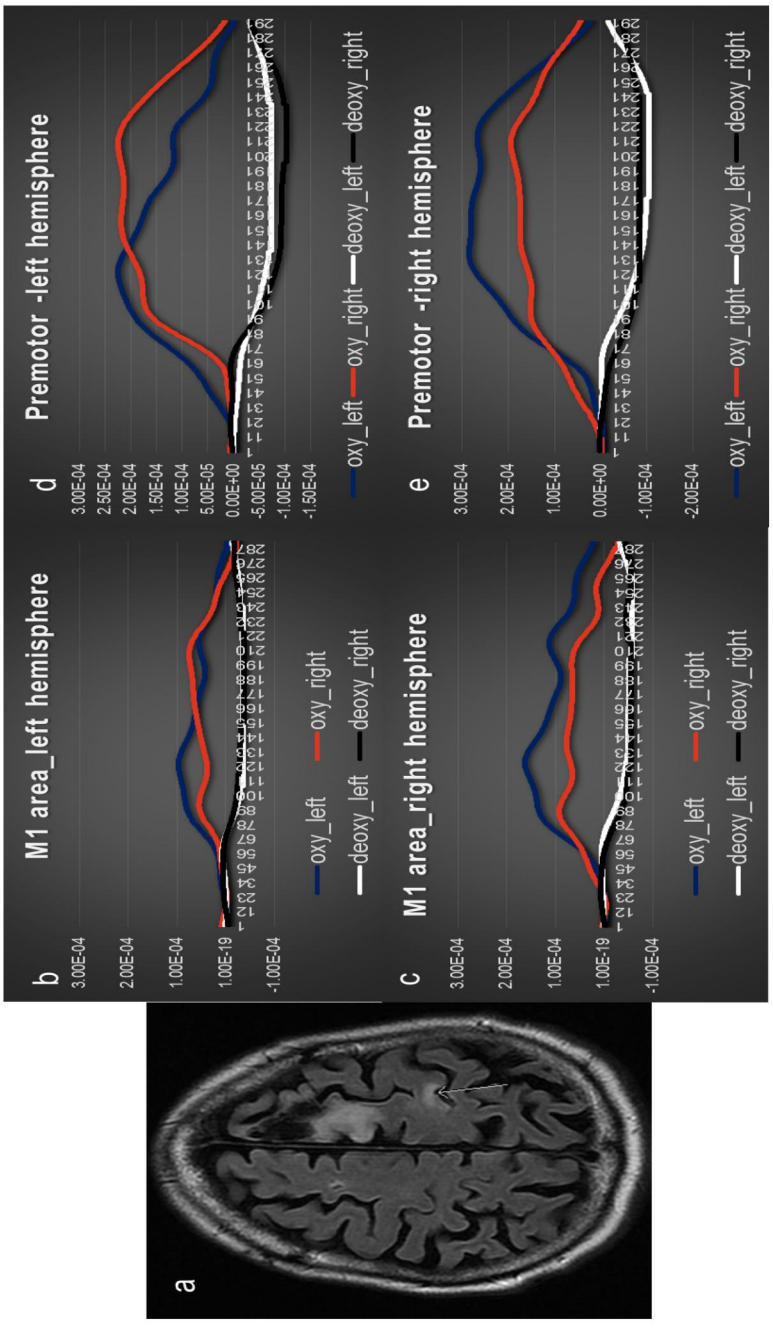


Figure 4.7a shows the MRI of the subject with left hemisphere stroke affected areas indicated in hyper intensity and arrow indicate the motor cortex b) and c) show the response from the primary motor cortex channels for both hemisphere. d) and e) show the response from the pre-motor and supplementary cortex channels for both hemisphere.

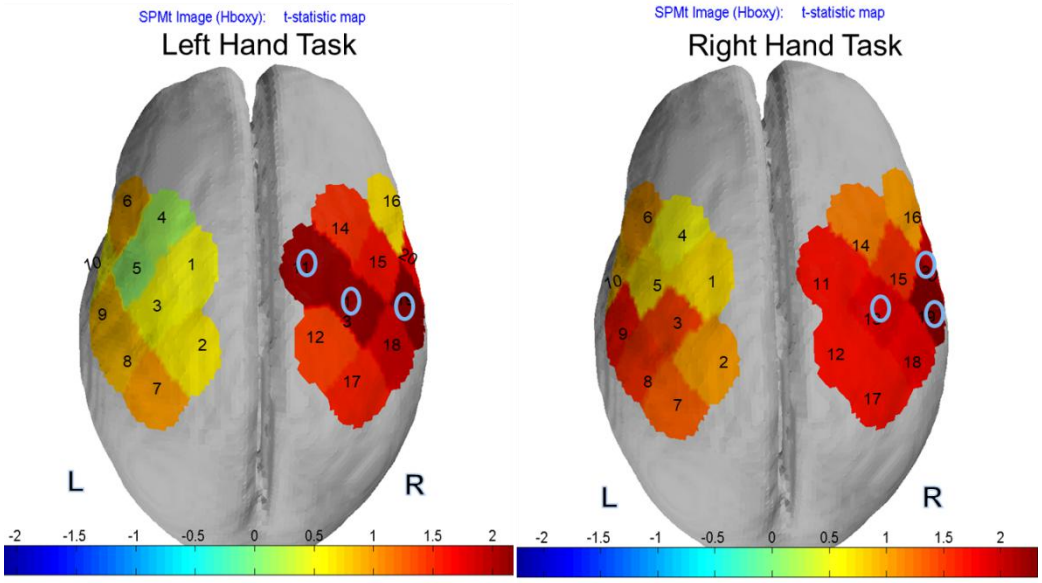


Figure 4.8 Task-based activation for all the channels is shown in the picture for the main effect of the left-hand movement and right hand movement for the Left hemisphere affected the subject. The blue rings indicate the significantly ($p<0.05$,FDR corrected) activated channels.

The group analysis results are given in fig 4.9. The results showed contralateral activation for the normal (left) hand movement task. The affected (right) hand movement task yielded a contra-lesional motor and premotor activation. The ipsilesional hemisphere produced deactivation in the M1 area while activations were observed in supplementary and premotor areas. GLM analysis revealed statistically significant channels for each task when compared to the rest period. Left-hand task produced significant ($p<0.05$,FDR corrected) activations in contralateral M1 areas(Channel 13). Right-hand task produced significant ($p<0.05$,FDR corrected) activations in the ipsilateral M1 and premotor areas.

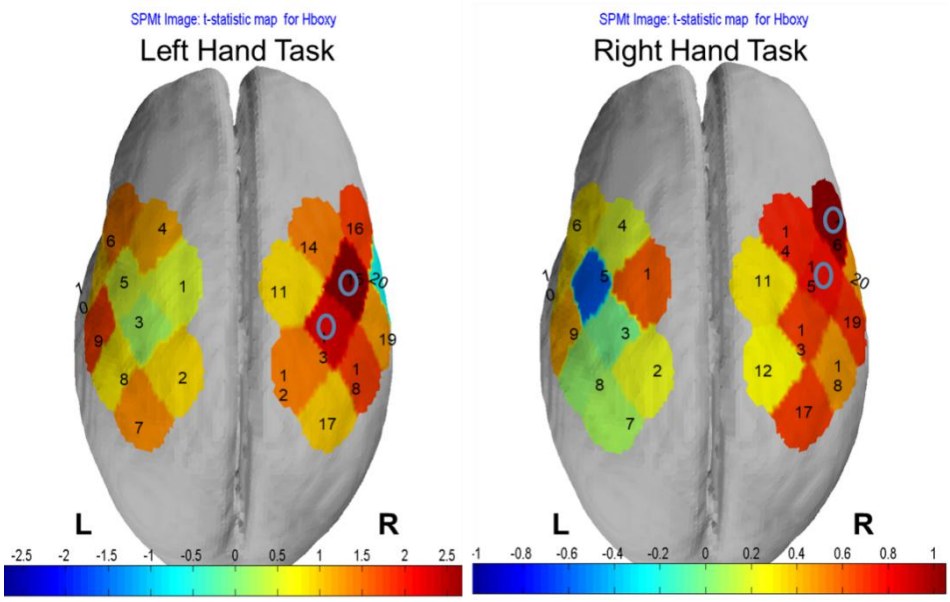


Figure 4.9 Task-based activation for all the channels is shown in the picture for the effect of the left-hand movement and right hand movement over rest, for the Left hemisphere affected group. The blue rings indicate the significantly ($p<0.05$,FDR corrected) activated channels.

#### *4.1.2.2 Task Based result for Right Hemisphere Affected group*

The task-related response from the patient group whose right hemisphere areas were affected showed a difference from that of the normal group as detailed in 4.1.1. This group of subjects had difficulty in the left hand after stroke. Fig 4.10 shows the average response from different areas for the right hemisphere affected subject. The subject could perform the task. The response shows that the affected hand movement causes responses in bilateral M1 areas, premotor and supplementary areas. GLM analysis was performed at the subject level and the activation for each task was compared statistically. Fig 4.11 shows the T statistics for each of the channel activations representing the HbO activation from each channel. The affected (left) hand task yields a significant ($p<0.05$,FDR corrected) bilateral activation pattern from the premotor areas.

The right/normal hand activation shows a unilateral pattern with significant ($p<0.05$,FDR corrected) activation in the contralateral M1 areas. The fig 4.10 and 4.11 represent one subject from the group.

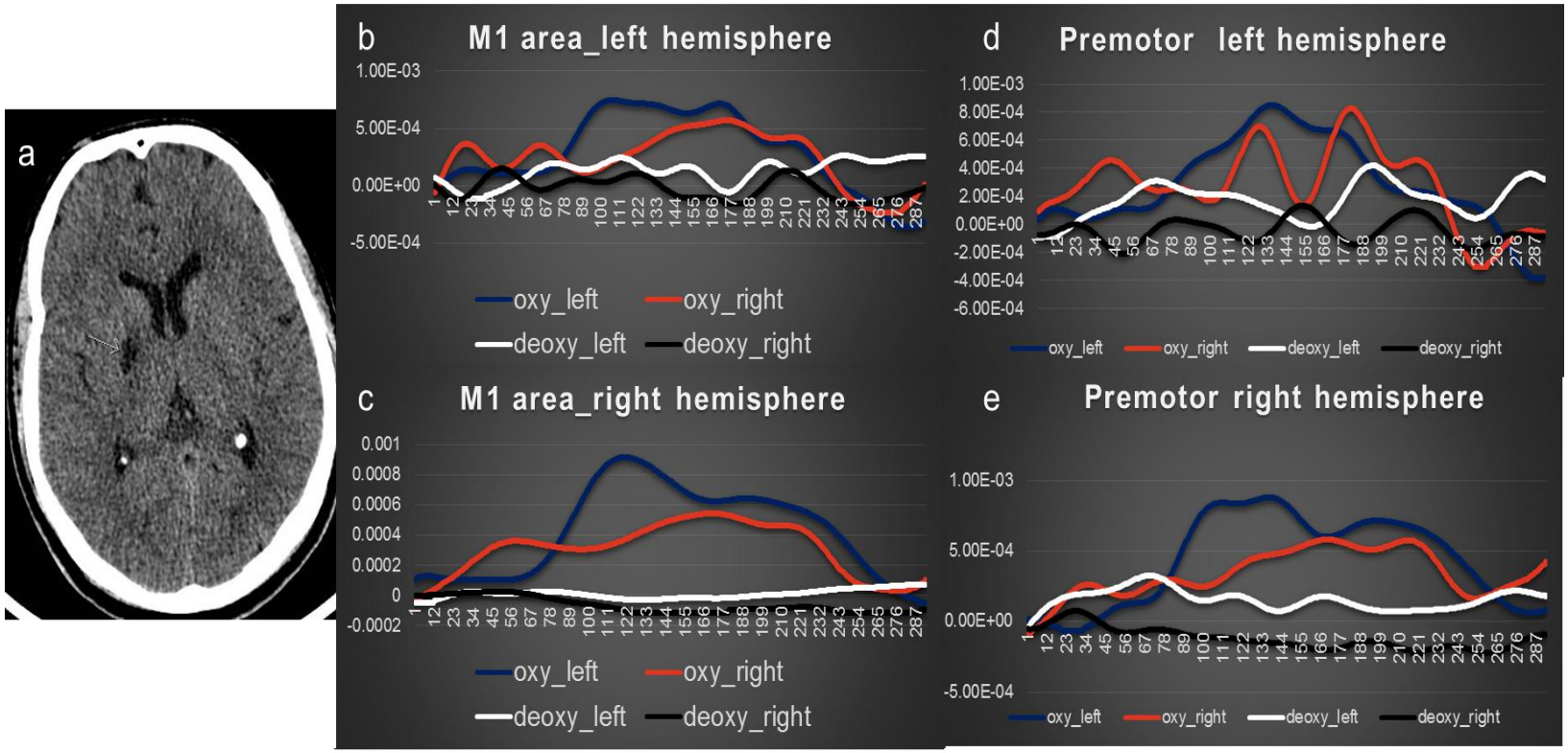


Figure 4.10a shows the MRI of the subject with right hemisphere stroke affected areas indicated in hypo intensity and arrow indicate the location b) and c) show the response from the primary motor cortex channels for both hemisphere. d) and e) show the response from the pre-motor and supplementary cortex channels for both hemisphere.

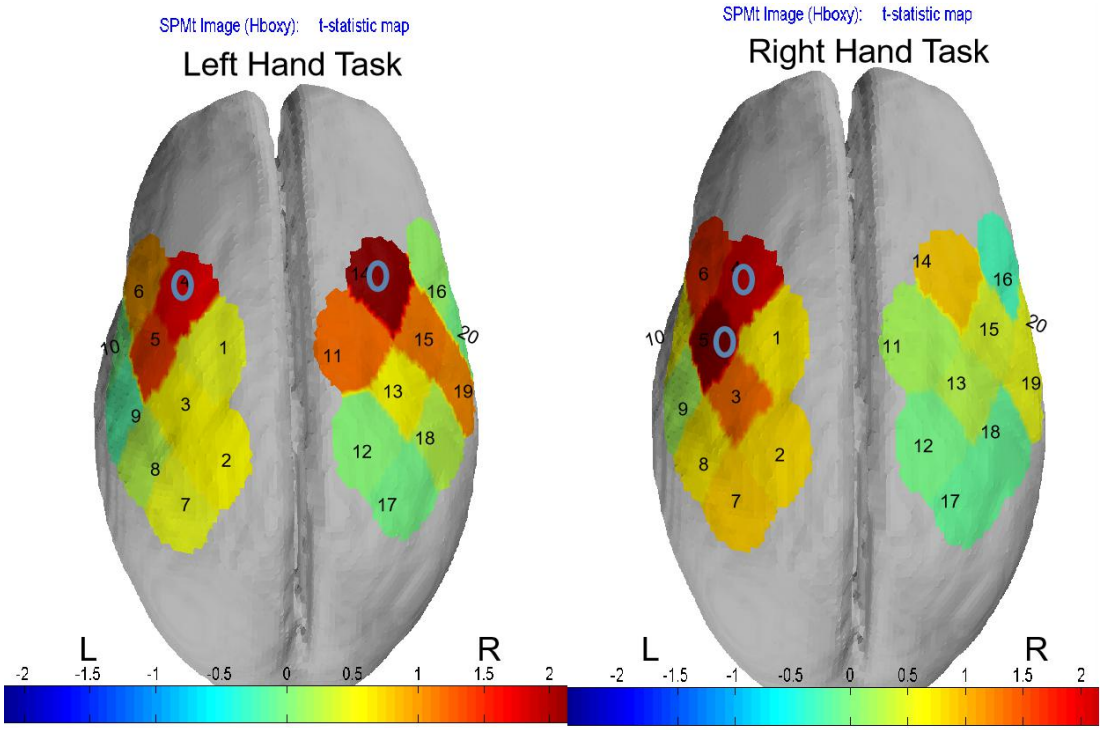


Figure 4.11 Task-based activation for all the channels is shown in the picture for the main effect of the left-hand movement and right hand movement for the right hemisphere affected subject. The blue rings indicate the significantly ($p<0.05$,FDR corrected) activated channels.

The group analysis results are given in fig 4.12. The results showed bilateral activation for the affected (left) hand movement task. The normal (right) hand movement task also yielded a bilateral motor and premotor activation. GLM analysis revealed statistically significant channels for each task when compared to the rest period. Left-hand task produced significant ($p<0.05$,FDR corrected) activations in contralateral M1 areas and ipsilateral supplementary motor areas. Right-hand task produced significant ($p<0.05$,FDR corrected) activations in the ipsilateral M1 and premotor areas as well as ipsilateral M1 and supplementary motor areas.

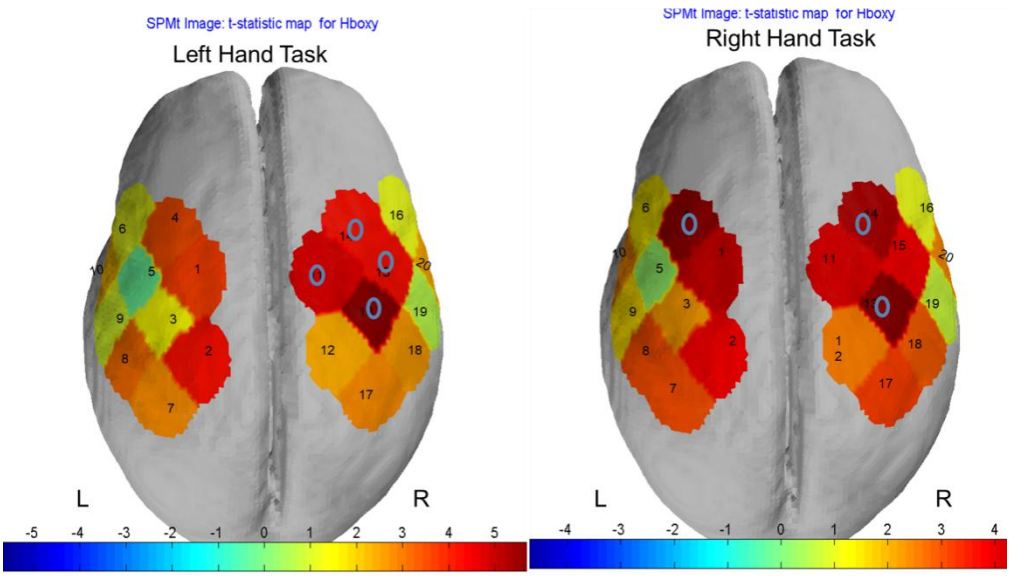


Figure 4.12 Task-based activation for all the channels is shown in the picture for the effect of the left-hand movement and right hand movement over rest, for the right hemisphere affected group. The blue rings indicate the significantly ($p<0.05$,FDR corrected) activated channels.

### *4.1.2.3 Task based results for post-recovery data*

The post-recovery data acquired for each subject were analyzed with the same processing steps as explained in section 3.5.1. The data acquisition took place on an average of two months from the day of first acquisition. Fig 4.13 shows the HbO activations for the right hemisphere affected patients. The bilateral activations shown in figure 4.12 has been changed over the recovery phase. The significant ($p<0.05$,FDR corrected) increases in HbO activation are present in the contralateral M1 areas for the affected (left) hand. The normal (right) hand movement results indicate a unilateral pattern. Significant ($p<0.05$ FDR corrected) activations are seen in the contralateral premotor areas.

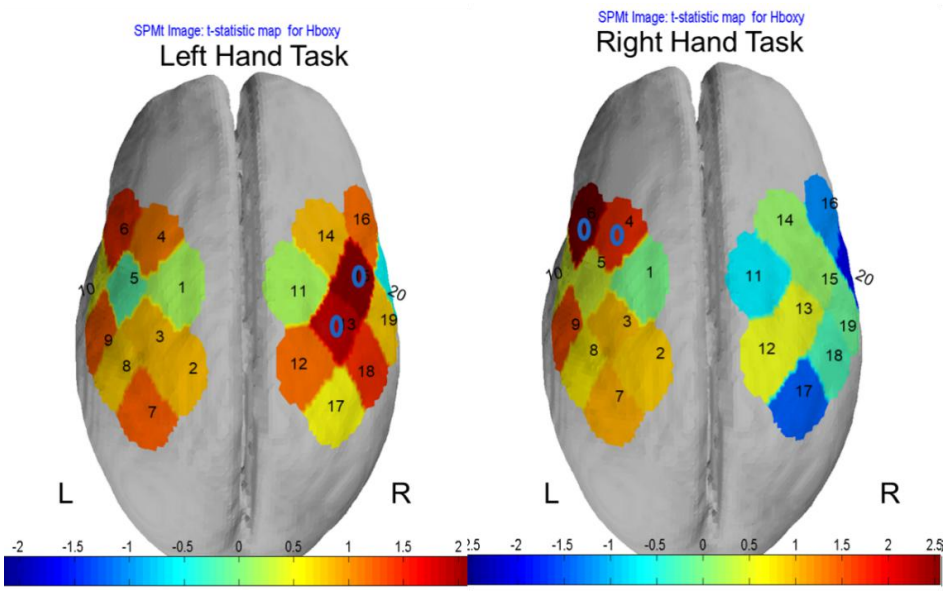


Figure 4.13 Task-based activation for all the channels is shown in the picture for the effect of the left-hand movement and right hand movement over rest, for the right hemisphere affected group for the recovered phase. The blue rings indicate the significantly ($p<0.05$,FDR corrected) activated channels.

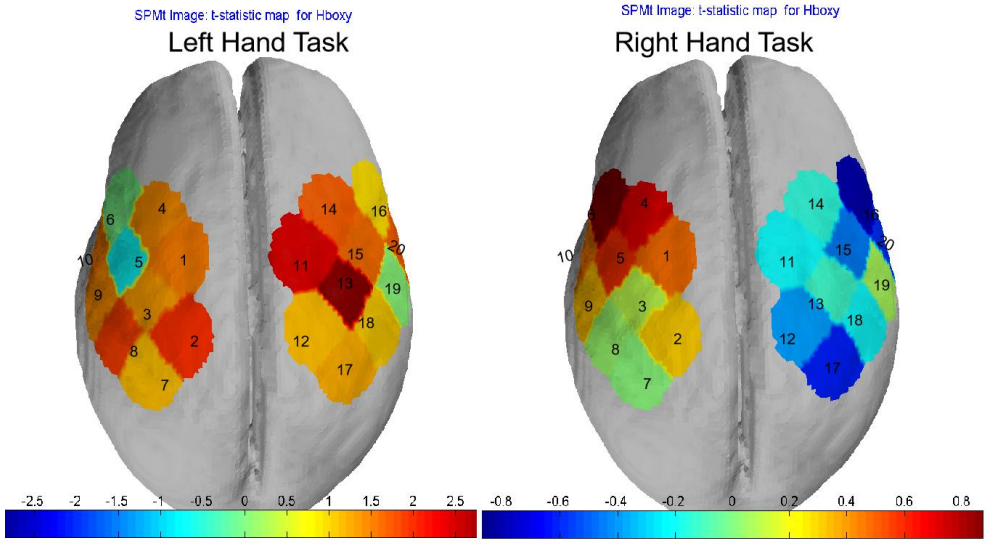


Figure 4.14 Task-based activation for all the channels is shown in the picture for the effect of the left-hand movement and right hand movement over rest, for the left hemisphere affected group for the recovered phase. There were no statistically significant channels

## *4.2 Resting state fNIRS results:*

### 4.2.1 Healthy Group RSFC

The resting-state data from the healthy subject group was processed and the correlation analysis was performed to obtain the RSFC. The average HbO activations from each channel were used for the correlation analysis. Fig 4.15 shows the connectivity matrix obtained from the correlation of HbO data from the healthy subject group.

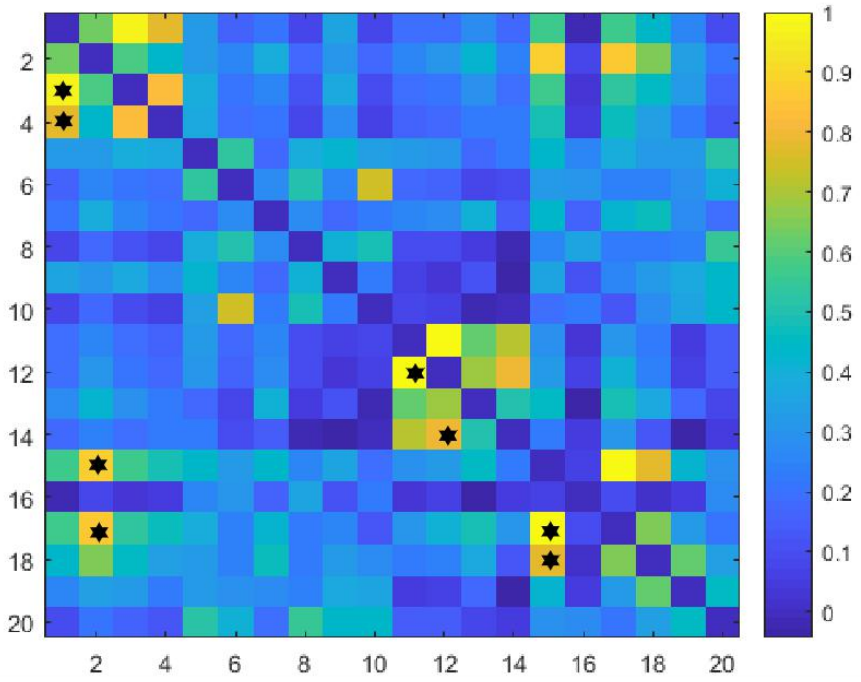


Figure 4.15 The figure shows the correlation coefficient values for oxyhemoglobin data from each of the 20 channels for healthy subjects. Channel 1 to 10 represent left hemisphere and channels 11 to 20 represent right hemisphere. The * represents the significant connections(P<0.05,FDR corrected).

The M1 area and premotor areas (Channels 3 and 4 and 11 to 14) of both left hemisphere and right hemisphere are shown to have a strong correlation indicating

strong intra-hemispheric connections. Inter-hemispheric connections are strong between the somatosensory regions and association cortex regions (Channels 2, 15 and 17). Fig 4.16 gives an idea of these stronger connections after thresholding the connectivity matrix. The thresholding leaves out connections that are not stronger than 50 % proportion of the correlation.

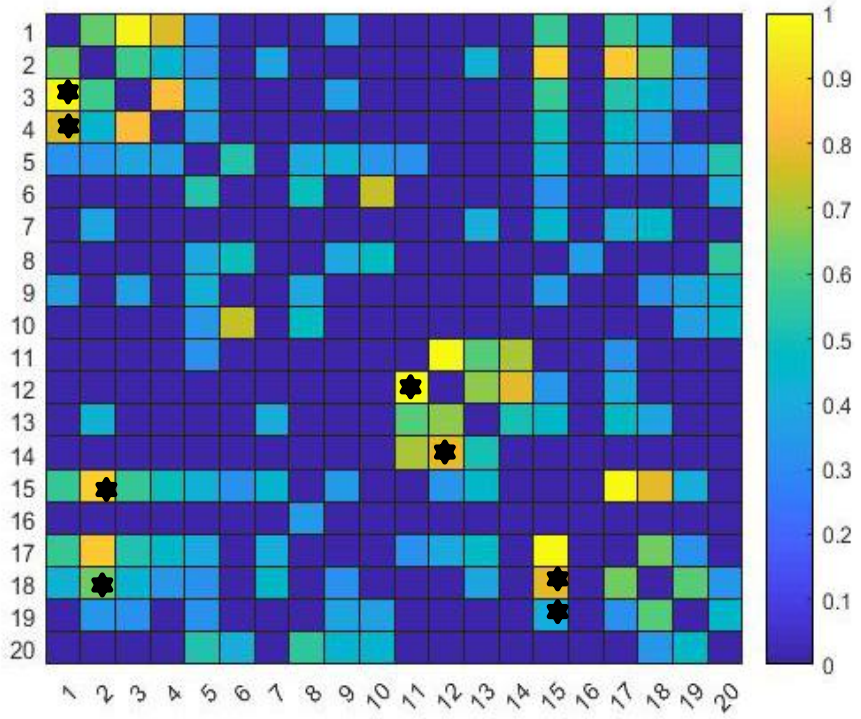


Figure 4.16 shows the thresholded RSFC for the healthy group. The correlation scores obtained in the matrix where r values are thresholded for a sparsity threshold of 0.5. The black star represents the significant connections(P<0.05,FDR corrected).

### 4.2.2 Healthy Group Network Analysis

Considering the channels as nodes and the connectivity strength as edges, network theory can be applied to the resting state data. As a measure for segregation modularity/community structure of the healthy group data was computed. Fig 4.17 shows the visualization of community structure in the thresholded RSFC network. The nodes (channels) are color-coded for the different modules. The degree of interaction between the nodes (channels) was studied using the modularity of the nodes. The fig 4.22a shows the channels divided into three modules. The green nodes represent the right hemispheric motor area channels. The red module includes the left-hemisphere motor area and right hemisphere supplementary areas. The golden yellow modules have somatosensory channels from both hemispheres. The edges represent the fisher transformed correlation coefficients between the channels. The inter-modular and inter-hemispheric patterns were also looked upon. The connections between modules were negligible.

The network properties like efficiency and clustering coefficient were calculated. Fig 4.17a shows that the primary motor, supplementary area and somatosensory areas (Channel no. 1, 3, 4, 7, 11) in the left hemisphere and premotor areas (Channel no. 14) in the right hemisphere have the maximum clustering coefficient. These areas tend to form a maximum cluster around and give the nature of network which can form specialized regions. The average clustering coefficient of the network is 0.716. Fig 4.17b indicates the efficiency of the nodes/channels. Higher efficiency means shorter the path length for

the nodes and thereby efficient information flow. For a healthy group, most of the nodes have high local efficiency indicating an intact network system for healthy volunteers. The global efficiency of the group was 0.738.

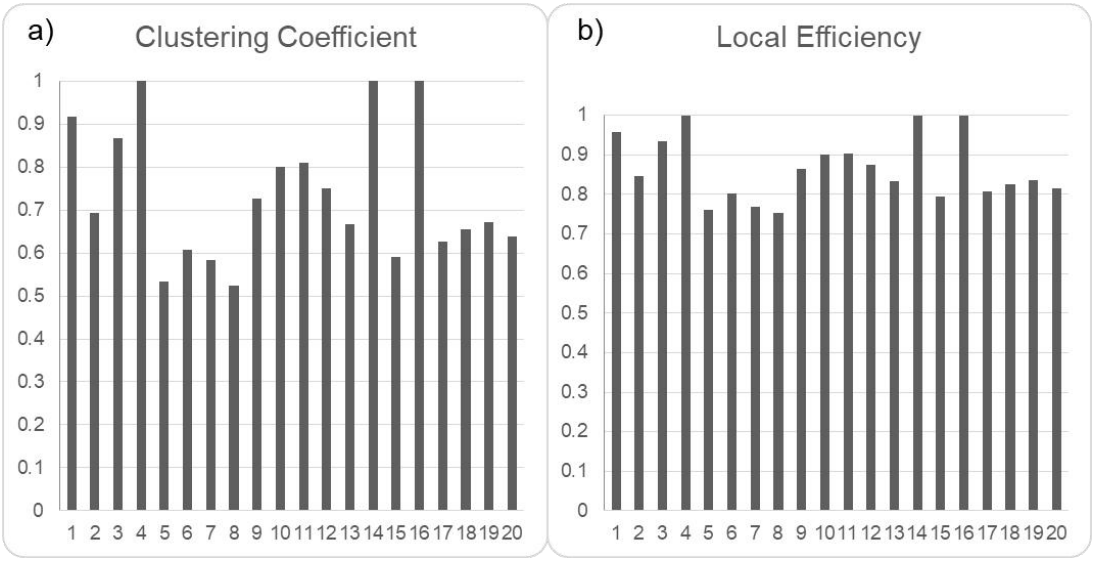


Figure 4.17 a) shows the clustering coefficient of all the nodes/channels for the healthy volunteer group. b) shows the efficiency of all the nodes/channel for the healthy volunteer group

### 4.2.3 Resting State Results For Left Hemisphere Affected Group.

As in the case of task-based analysis, the data of the patient group were divided into the left hemisphere affected and the right hemisphere affected group. These data were also examined for the network comparison of the modular/community structure and compared with the healthy control group. Fig 4.18a explains the RSFC for the left hemisphere affected group. For comparison with the healthy group, the thresholding parameters were kept the same (sparsity threshold of 0.5) and thresholded RSFC is obtained as shown in fig 4.18b. The RSFC strength in the left hemisphere areas was low compared to the RSFC in the contra-lesional hemisphere. The inter-hemispheric

connectivity also is disrupted in the left hemisphere affected group. Fig 4.22b shows the

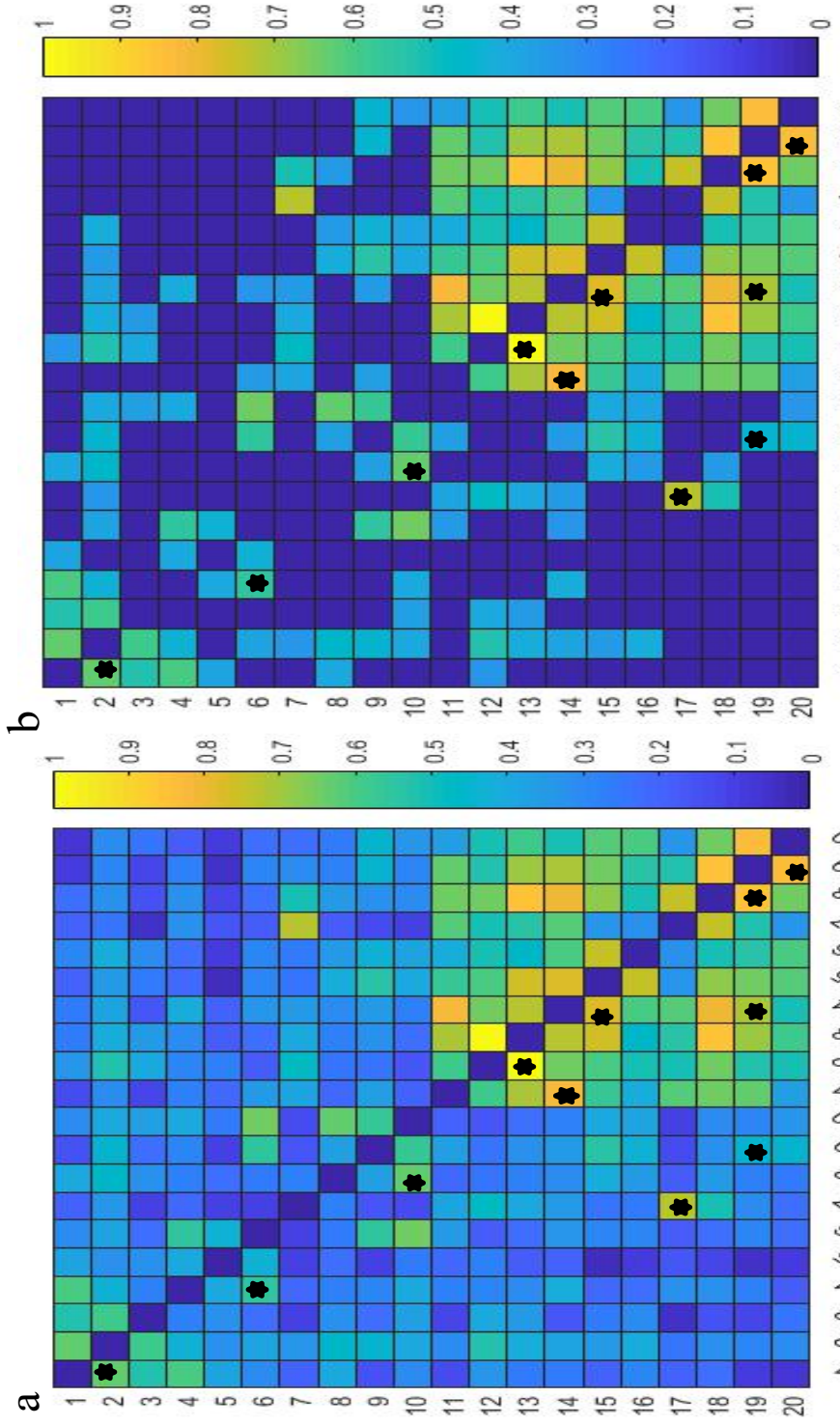


Figure 4.18 a) The figure shows the correlation coefficient values for oxy hemoglobin data from each of the 20 channels for left hemisphere affected subjects. Channel 1 to 10 represent left hemisphere and channels 11 to 20 represent right hemisphere. b) shows the thresholded RSFC for the left hemisphere affected group. The correlation scores seen in the matrix where r values are thresholded for a sparsity threshold of 0.5 The * represents the connections which are significant (P<0.05.FDR corrected)

community structure of the group. The areas are divided into two modules. The red nodes represent the ipsilesional areas and the green represents the contra-lesional areas except the somatosensory area (Channel 7) in the left hemisphere.

The clustering coefficients for each channel were calculated. The ipsilesional areas show less ability to form clusters when compared to the areas in the contralesional side as seen in fig 4.19a. The local efficiency of the areas though was high for most channels except the ipsilesional motor areas. The global efficiency of the group is 0.637.

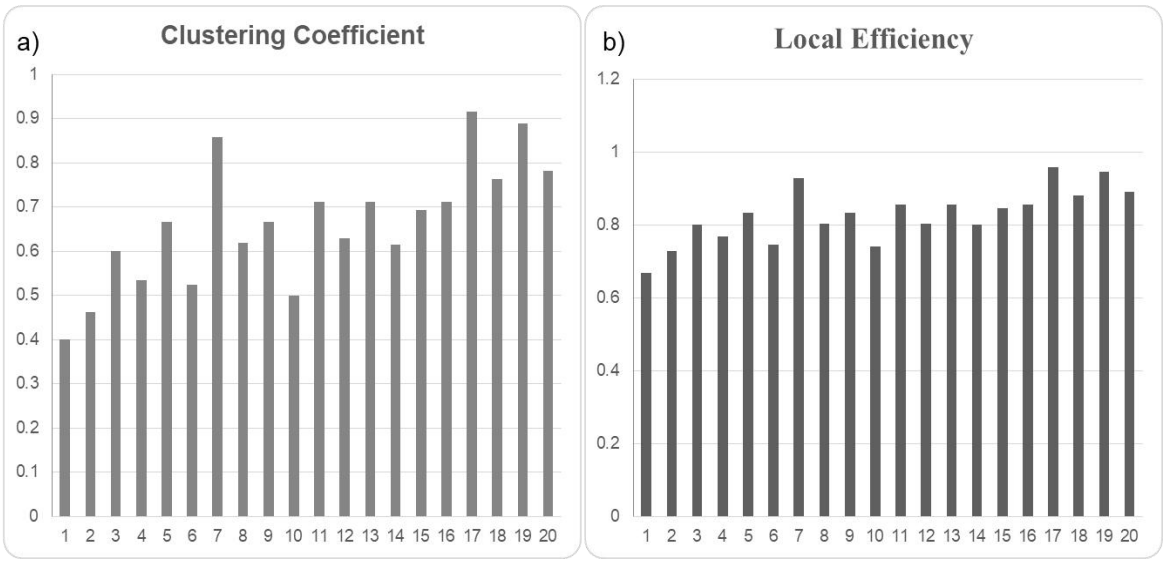


Figure 4.19a) shows the clustering coefficient of all the nodes/channels for the left hemisphere affected group. b) shows the local efficiency of all the nodes/channels

### 4.2.4 Resting State Results For Right Hemisphere Affected Group.

RSFC for the right hemisphere affected group was calculated. For comparison with the healthy group, the thresholding parameters were kept the same (sparsity threshold of 0.5) and thresholded RSFC is obtained as shown in fig 4.20b. The RSFC strength in both the hemisphere areas was seen high. The inter-hemispheric connectivity

is seen disrupted in the right hemisphere affected group. Fig 4.22d shows the community structure of the group. The areas are divided into three modules. The red nodes represent the somatosensory and primary sensory areas of both hemisphere, the dark green nodes represent the ipsilesional premotor and motor areas and the premotor areas of the contra-lesional. The light green nodes represent the ipsilesional somatosensory areas and contra-lesional motor areas and somatosensory areas.

The clustering coefficients for each channel were calculated. The ipsilesional areas and contra-lesional areas show a high ability to form clusters as seen in fig 4.21a. The somatosensory areas (Channel 9 and 20) at sparsity of 0.5 do not form clusters around. The local efficiency of the areas though was high for most channels except the somatosensory areas of both hemispheres. The global efficiency of the group is 0.623.

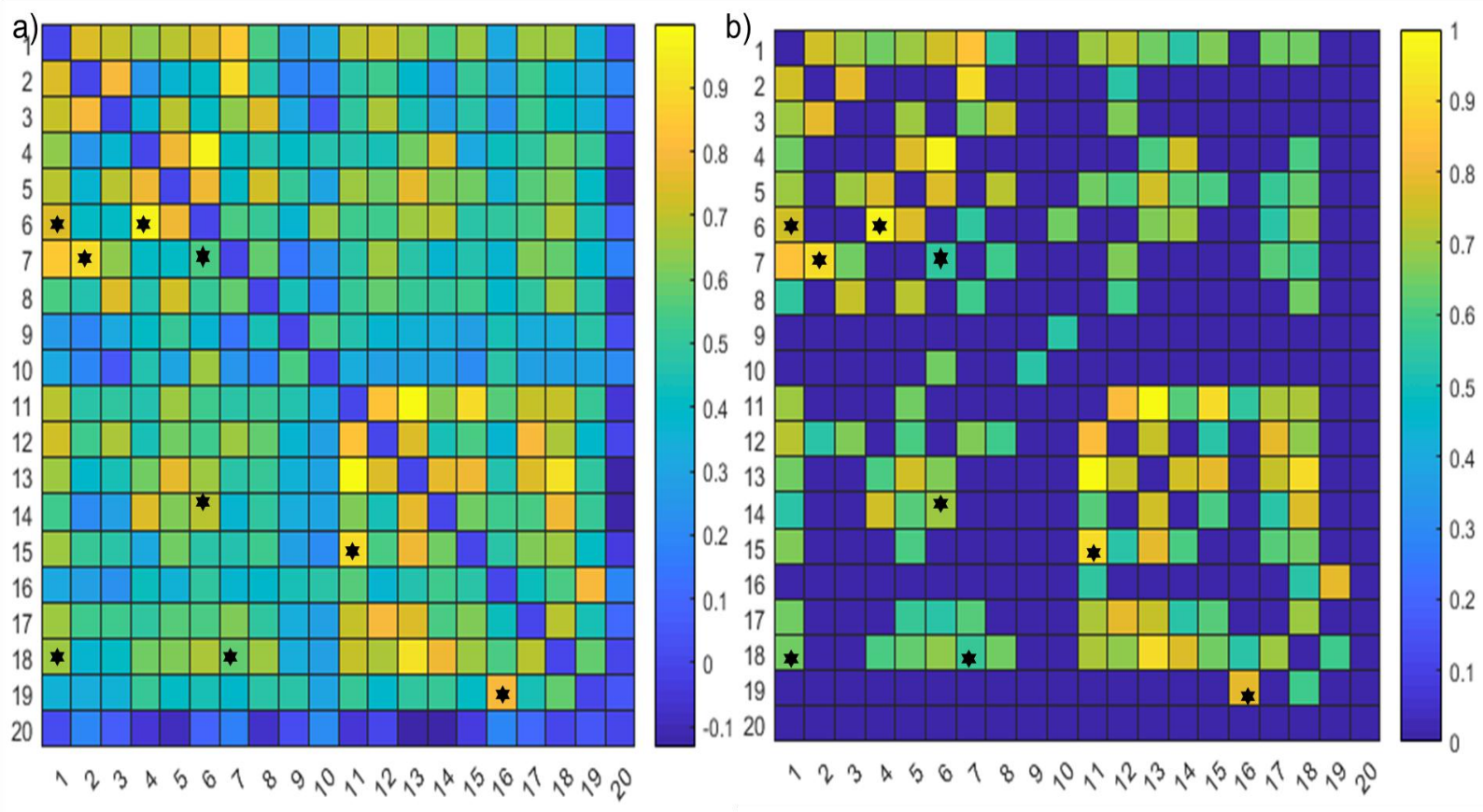


Figure 4.20 a) The figure shows the correlation coefficient values for oxy hemoglobin data from each of the 20 channels for the right hemisphere affected subjects. Channel 1 to 10 represent left hemisphere and channels 11 to 20 represent right hemisphere. b) shows the thresholded RSFC for the right hemisphere affected group. The correlation scores seen in the matrix where r values are thresholded for a sparsity threshold of 0.5. The * represents the connections which are significant (P<0.05,FDR corrected)

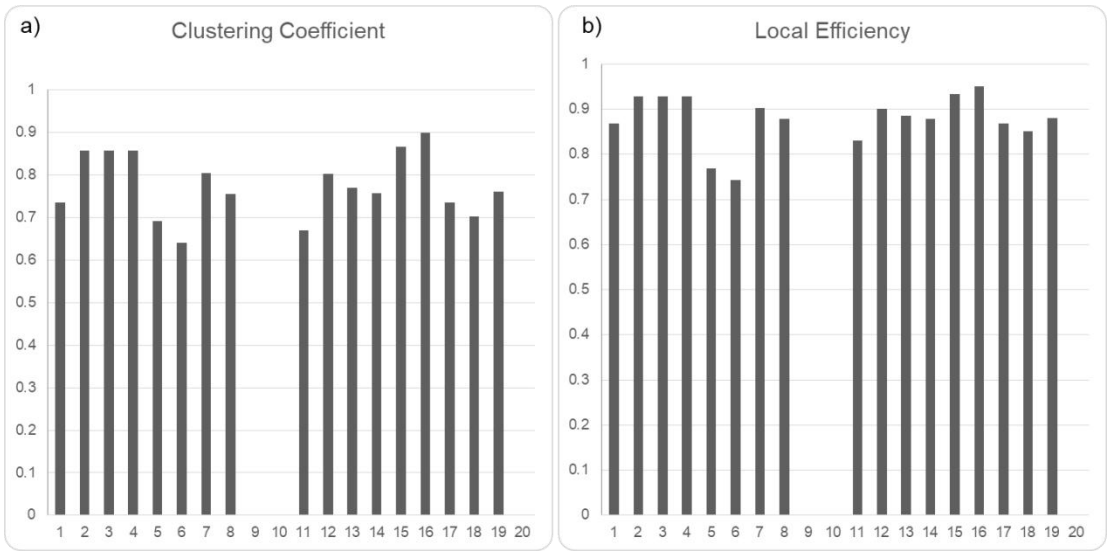


Figure 4.21a) shows the clustering coefficient of all the nodes/channels for the right hemisphere affected group. b) shows the local efficiency of all the nodes/channels

### 4.2.5 Comparison of Pre and Post Recovery

Since the main aim of the study is the identification of resting-state changes over the recovery from stroke, the resting state data acquired post-recovery were analyzed. The RSFC for both the patient groups is shown in fig 4.22 along with the healthy group. Fig 4.22 b) and c) is the RSFC of the left hemisphere thresholded for the sparsity of 0.5 for both the pre and post-recovery respectively. The inter-hemispheric connections have appeared more in the post-recovery analysis. The difference in RSFC is shown in the fig 4.23a and 4.23b for the patient groups. The premotor areas and supplementary areas show an increase in the inter-hemispheric RSFC for the left hemisphere affected the patient group. The ipsilesional hemisphere post-recovery has been shown to have

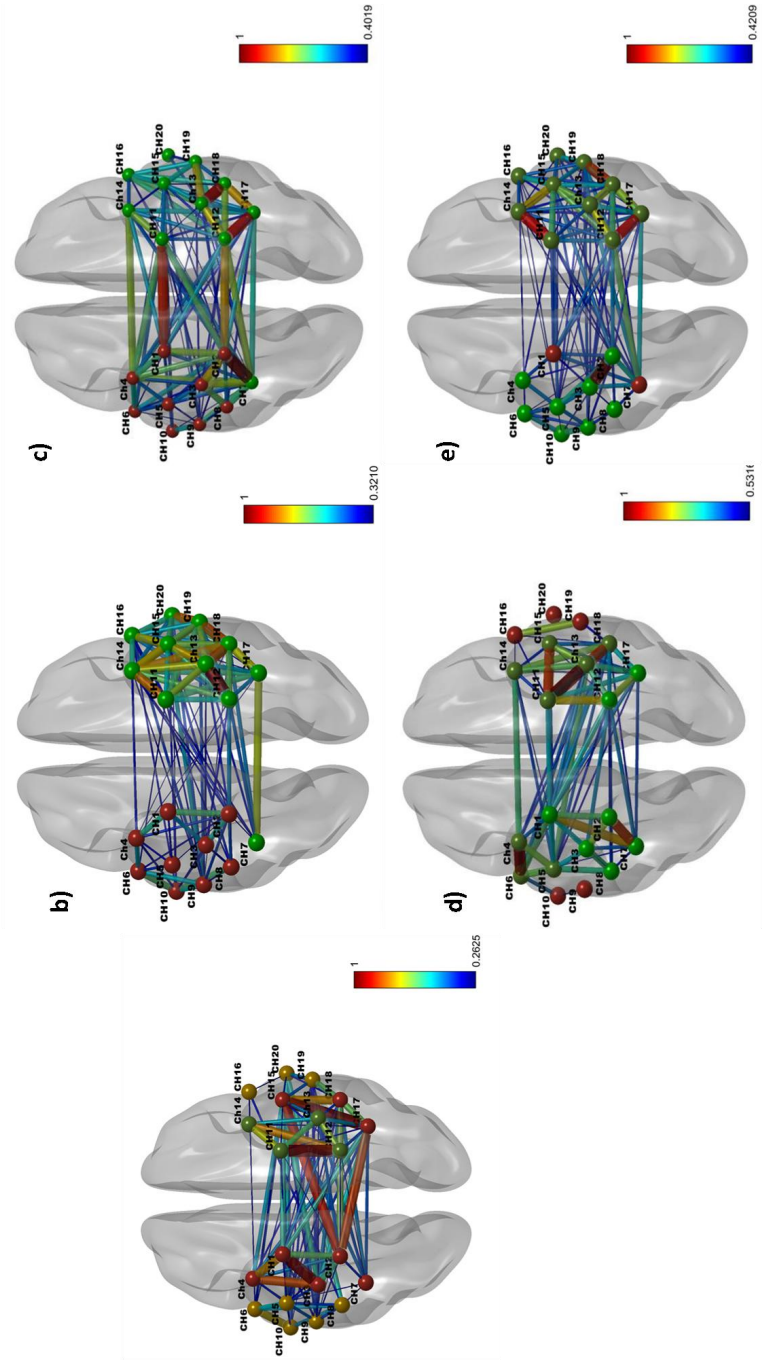


Figure 4.22 a) represent the modularity of the thresholded network of the motor cortex of the healthy group. b) and c) represent the modularity of the thresholded network of the motor cortex of the left hemisphere affected group for the pre and post recovery respectively.d) and e)represent the modularity of the thresholded network of the motor cortex of the right hemisphere affected group for the pre and post recovery respectively. The spheres represent the nodes/channels and the connection represent the RSFC strength between the channels.The color code of the nodes are based on the modularity of the nodes

increased RSFC in the M1 areas and connection to the ipsilesional premotor and somatosensory areas from the M1 area.

The contra-lesional side shows a decrease in the RSFC. For the right hemisphere affected patient group, the RSFC has increased over both the hemispheres. The inter-hemispheric connections are increased between the somatosensory cortex of the contra-lesional hemisphere and the premotor and supplementary areas and the somatosensory channels in the ipsilesional hemisphere.

.

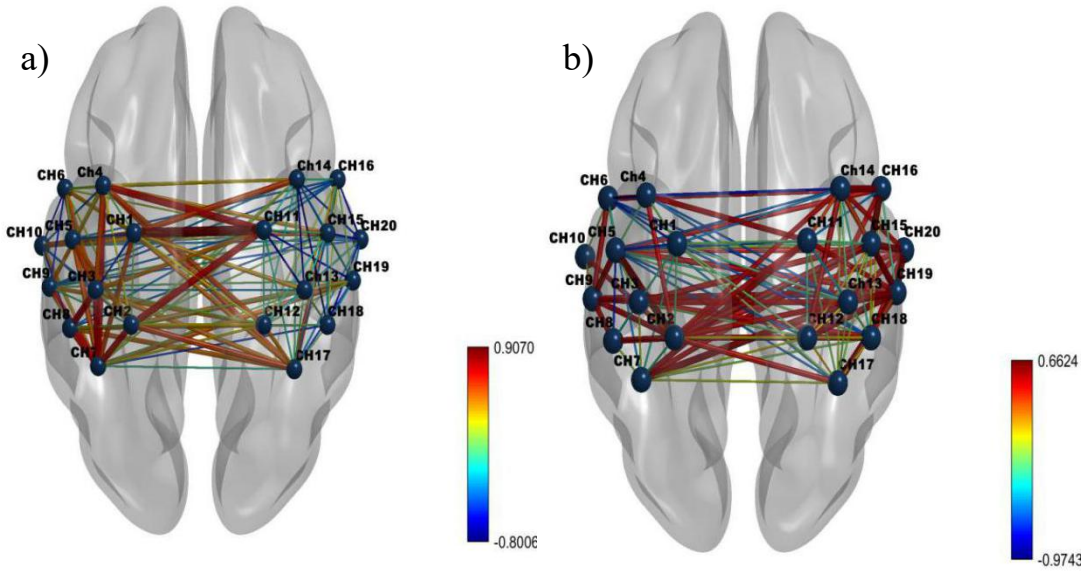


Figure 4.23 a) shows the difference in RSFC between the pre and post-recovery for the left hemisphere affected patient group b) shows the difference in RSFC between the pre and post-recovery for the right hemisphere affected the patient group. The nodes are represented in blue spheres.

### 4.2.6 Comparison of Network Measures

The network measures were calculated for a range (0,1) of sparsity thresholds. A significant difference ($p<0.05$,FDR corrected) was seen in the clustering coefficients of healthy groups when compared with both the left hemisphere affected patient group and

right hemisphere affected the patient group. Similarly, Global efficiency and Local efficiency (measures of integration) were compared among the groups. Global efficiency was not showing a significant difference among the groups. But the local efficiency is showing a significant difference ($p<0.05$,FDR corrected) in healthy and affected groups.

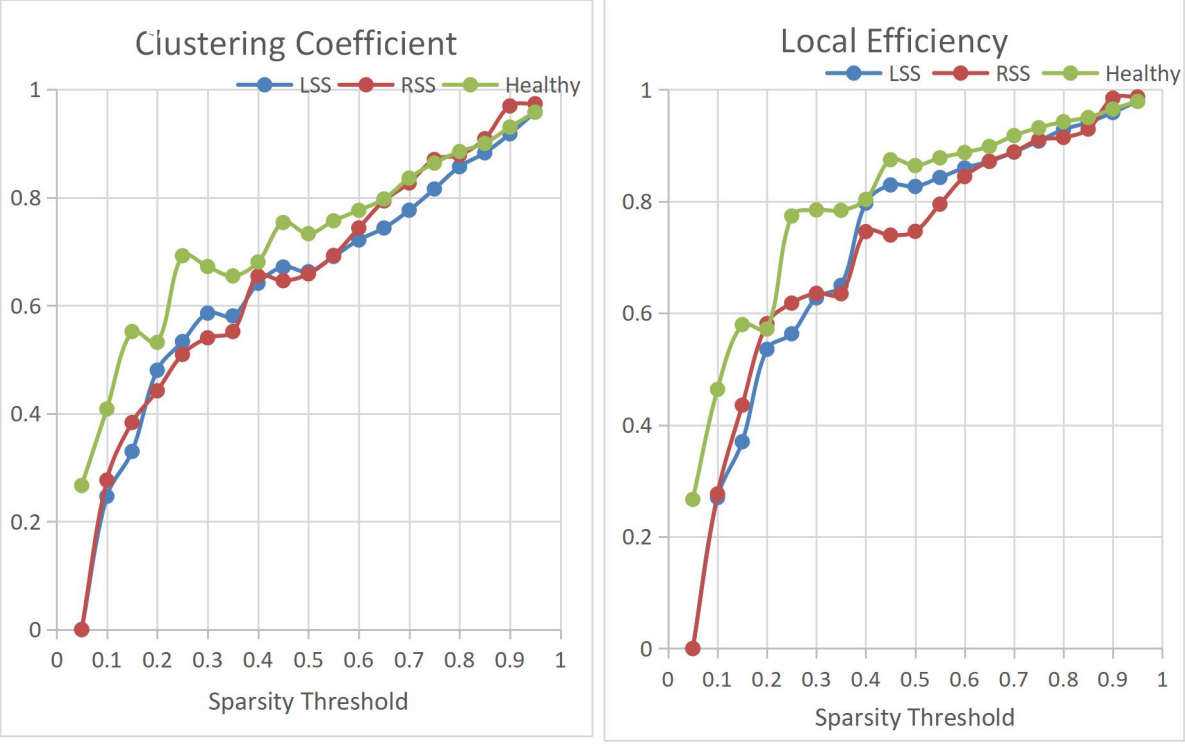


Figure 4.24 a) shows the comparison of clustering coefficient values for different sparsity thresholds for the healthy group and patient groups. b) shows the comparison of global efficiency values for different sparsity thresholds for the healthy group and patient groups.*$p<0.05$

# Chapter 5

# Discussion

The study utilized optical neuroimaging technique, fNIRS for examining the brain signals from the motor cortex and analyzing them for task-based and resting-state motor cortical activations in healthy controls and stroke-affected patients. The use of this modality is advantageous for such a population of patients due to its low restraint nature of data measurement and insensitiveness to small motion artifacts. The consistency of the method of fNIRS being used for neuroimaging studies has been validated in various applications. The fNIRS data mostly corresponds to functional neuroimaging data acquired using other methods, suggests that the technique reliably monitors brain activation. The upper limb recovery from stroke was studied here by analyzing the changes in both tasks related and resting-state based results. The individuality of the study lies in the fact that resting-state pattern changes for upper limb recovery from stroke are not reported heavily. The results from the resting state analysis for the patients in post-recovery will add more value to the rehabilitation research.

## *5.1 Normal Brain Response for Motor Tasks*

In a healthy group, the study investigated the brain response to the motor tasks, especially for the upper limb. The results agree to the common theory of the contralateral activation. There was a task-based increase in ΔHbO and the accompanying decrease in ΔHbR in the contralateral hemisphere during hand grasp by the healthy

subject. These are typical time courses in NIRS recording. For the normal brain, previous studies have reported that concomitant inhibition of the ipsilateral motor cortex associated with the contralateral activation during the motor tasks (Ocklenburg et al., 2015) as shown in fig 5.1. Results from this study could also show this phenomenon of ipsilateral inhibition for the healthy subject group. Channel 13 which is corresponding to the primary motor area in the right hemisphere is shown to have deactivation during the right-hand task while the left hemisphere motor areas are activated (Channel 3). Apart from the primary motor area, premotor (Channels 4, 6) and supplementary area (1, 5) were also activated contralaterally (though these areas failed to survive statistical significance). These areas are found out to have contralateral activation in the normal subject from the fMRI studies as well for the dominant hand.

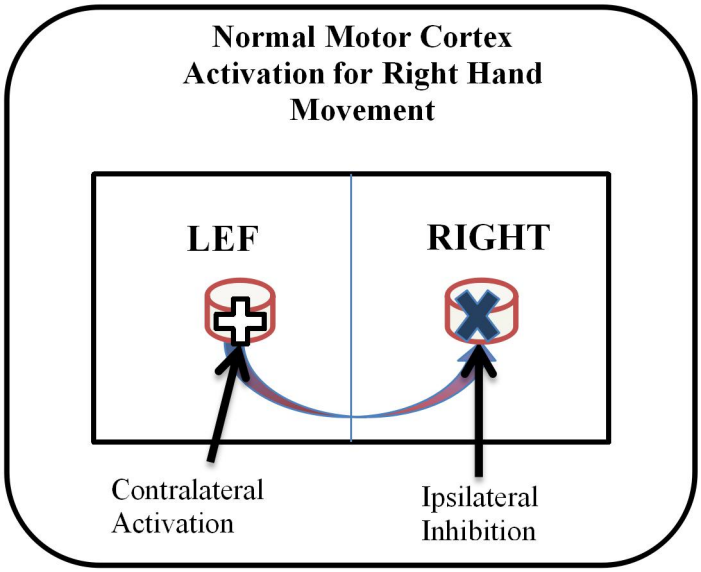


Figure 5.1 Model of normal motor cortex functioning during right-hand task showing contralateral activation.

## *5.2 Resting state activity of the normal motor cortex*

The main objective of the study was to assess the resting state activity of the motor cortex and its role in reorganization during recovery. For understanding this, it is essential to study the RSFC pattern for the normal brain. The current study shows there are strong connections between left M1 areas and ipsilateral premotor and supplementary motor areas. Similarly, for the right M1 area, there were strong functional connections towards the right premotor and supplementary motor areas. The right and left somatosensory areas showed strong inter-hemispheric correlation as well. This pattern of RSFC has been reported before using fMRI in other studies concerning brain motor assessment during resting state (B. Biswal et al., 1995; Bonzano et al., 2015; Saiote et al., 2016). The fMRI based studies also have the leverage of assessing the whole brain without depth restriction. For the current study, the RSFC is confined to the motor cortex and associated areas up to the cortical depth. A very large cohort study revealing similar insights from this result will be helpful in planning rehabilitation strategies for patients affected with stroke. The recovery from stroke due to the rehabilitation strategy used could be assessed by looking into information from RSFC measures of the patients. RSFC also possesses the advantage of being effortless for the patient as no task is involved in the measurement paradigm.

## *5.3 Stroke Affected Brain Response to Motor task*

The stroke affected brain activation in response to the upper limb task is different from the normal brain. Unlike the unilateral activation pattern seen in the healthy group,

the patient group largely exhibit bilateral activation pattern for the affected hand movement. The hand grasp task was used for the study. The left hemisphere affected patient group showed a bilateral increase in the activation for the affected (right) hand. This indicates a contra-lesional/ipsilateral activation in addition to the expected contralateral activation is present. The unaffected (left) hand, however, showed a significant increase in activation for the contralateral hemisphere only. In the case of the right hemisphere affected group also displayed bilateral activation especially in the premotor areas and SMA for the affected (left) hand movement. The unaffected (right) hand movement for this group, however, showed a close to the normal unilateral pattern of increase in activation in the contralesional hemisphere. Here the unaffected hand is the dominant hand for the patients and the unilateral activation could be attributed to this fact. A bilateral increase in HbO appears to cause a reduction in the contra-laterality in the patient group, unlike the clearer contralateral-dominant activations seen in previous fMRI studies during unilateral hand movement (Dodd et al., 2017). This also suggests that the ipsilesional primary motor area no longer inhibits the contra-lesional side causing an imbalance in the inter-hemispheric activities. It is also reported that the degree of this imbalance would be dependent on the severity of the impairment due to stroke (Murase et al., 2004).

Enhanced activity of contra-lesional activity has been studied by different groups using fMRI. The results of the current study also showed enhanced contra-lesional activity after the onset of stroke for both the group of patients. The median onset time for the study was about 20 days. Patients with earlier onset could not be recruited for the

study as acute stroke cases will be difficult to get the scanning done due to already sstressed out conditions. The increased contralesional activation may be linked to suggesting that motor regions in the unaffected cortex progressively pay costs for the damage. Evidence from the previous research using fNIRS modality also suggest the same (Calautti and Baron, 2003; Kato et al., 2002)

## *5.4 Resting State Pattern for the Stroke Affected Motor Cortex*

The RSFC analysis also revealed changes from a healthy pattern. It is always advantageous to be able to determine changes in the RSFC measures for the patient population from the healthy group. This can be a marker, indicative of the underlying physiology changes and could be appreciated without the struggle of doing the task for the patients. Asymmetry of the RSFC of the motor network has been reported after the onset of stroke (Carter et al., 2010; Park Chang-hyun et al., 2011). Sensory-motor RSFC is also seen to be disrupted in some studies using fMRI. The left hemisphere affected group showed disrupted ipsilesional connectivity and an increased contra-lesional RSFC. One of the objectives of the study was to study the correlation between the task and resting-state data analysis using the modality of fNIRS. The increased connectivity observed on the contra-lesional side correlates well with the increase in the contra-lesional activity during the motor task by the patient group.

## *5.5 Assessment of Recovery using fNIRS*

Longitudinal studies allow researchers to study the same group of subjects/patients, assess the changes in the stimulus-based activation pattern or RSFC in the course of the

recovery process. Longitudinal fMRI studies reported the role of the contra-lesional hemisphere in stroke recovery (Baron et al., 2004; Grefkes and Fink, 2011; Rehme et al., 2011). According to a recent comprehensive review by Yang et al, upper limb motor recovery using task-based fNIRS has been reported a few studies (Gobbo et al., 2017; Kato et al., 2001; Takeda et al., 2007; Yang et al., 2019). The task-based results of the study show an improvement in the responses from motor areas of the patient group over a period of time. The post-recovery data when analyzed reveals that during the affected hand movement the contra-lateral M1 area has increased significant activation unlike the bilateral increase activation seen in the pre-recovery analysis. This shows a reduction in activation ipsilateral hemisphere for the affected hand as reported by Takeda et al(Takeda et al., 2007). This is suggestive and consistent with the hypothesis that motor reorganization occurs during the recovery process.

Resting-state fNIRS based studies for assessment of the recovery of the upper limb from a stroke in adults has not been reported. One study reported RSFC using a wavelet coherence analysis of fNIRS for cerebral infarction. The results suggested a disruption in RSFC due to cerebral infarction(Tan et al., 2015). Another study used fNIRS for bedside monitoring of neonates to assess the prognosis longitudinally (White et al., 2012). The differences in the RSFC for the patient group in the pre and post-recovery period were analyzed. In the case of the right hemisphere affected group, the inter-hemispheric connections between somatosensory areas of the contralesional hemisphere and the premotor areas of the ipsilesional hemisphere are increased. (Channel 7-14). The Left hemisphere affected group showed improved connections in the ipsilesional hemisphere

between M1 area and somatosensory area and between somatosensory and premotor areas (Channel 7-3, 7-8, 7-1). A strong inter-hemispheric increase was seen between the premotor and supplementary areas of both hemispheres (Channel 1-11, 4-11). The ipsilesional disruption which was observed after the onset of stroke may be reorganized to strengthen the ipsilesional connections. The inter-hemispheric M1 connections were seen decreasing after the recovery suggestive of a more unilateral activation pattern (Channel 3-13). The study results are suggestive of detecting the disruption in the RSFC due to stroke and also the reorganisation of the connections during the recovery process.

Using the graph-theoretical methods the study tries to describe the changes network organization of the motor cortex. To understand this, topological features like the clustering coefficient, global efficiency, and local efficiency were explored. The brain network analysis concept identifies the brain as a network of specialized areas (nodes) that are interconnected functionally through RSFC (edges). The comparison of clustering coefficients between the groups yielded a significant difference for the healthy group when compared with both patient groups. This comparison was made using a range of thresholds from 0 to 0.50 as the clustering coefficient value may be dependent on the sparsity threshold. The value is seen increasing with increasing the density of connections. The patient group also showed an increase in values with an increase in threshold values. But there is a decrease in the value of the clustering coefficient for the patient groups when compared to the healthy group. This suggests the nodes in the patient group have less ability to form specialized clusters to process information.

The community structure of the three groups also differed significantly. This was analyzed by stratifying the RSFC based on the Louvain algorithm where the modularity of the division is optimized. For the healthy group, the RSFC between the nodes were divided into three modules after multiple iterative steps. The primary motor areas of both hemispheres were segregated into two different modules. This may be expected as contralateral hemispheres act for the corresponding tasks. Most of the somatosensory areas from both hemispheres constituted the third hemisphere. It is already reported that the somatosensory area can drive motor function with or without M1 activity (Borich et al., 2015). This independent nature may be attributed to the segregated community formation of the somatosensory module in normal healthy controls. In the case of the patient groups, the left hemisphere affected group showed a community structure with two modules. The nodes in the affected hemisphere formed one module and the nodes from the unaffected hemisphere were grouped into the second module. This structure is a deviation from the normal pattern. The right hemisphere affected group also showed deviation from the normal pattern.

## *5.6 Limitations of the Study and Future Directions*

The study focused on the motor cortex activations and the RSFC of the limited area. This restriction of the study comes from the fact that the fNIRS equipment for the measurement is a device with eight sources and eight detectors; hence the coverage of the brain area is limited to the motor cortex. This limited the assessment of RSFC from other parts of the brain which may contribute to stroke recovery. A direct comparison of

the patient response obtained using fNIRS with that of fMRI would have been ideal. The study did not have the leverage of recruiting the patient again for fMRI. The method of EEG location-based optode positioning is followed in the study. The optode positioning for the measurement was done without the help of a 3D digitizer or an MRI coregistration of the optode position using marker pills which are considered more advanced. Since no studies are reported for upper motor limb recovery assessment using RSFC fNIRS, the interpretations of the results require more support from larger cohort studies in the future. A more comprehensive motor functional network study using fNIRS is possible with a higher number of optodes to cover larger brain areas.

The future areas of research from the study are to translate the results into the patient domain. The RSFC parameters could be identified as markers for recovery from stroke if a larger population is studied. This, in turn, could be used to design machine learning-based classification of the patients on the basis of chances of recovery. Another encouraging future research using fNIRS in the rehabilitation domain can be the use of a brain-computer interface to design subject-specific rehabilitation strategies for stroke survivors.

# CHAPTER 6

## Summary and Conclusion

The main aim of the study was to study the role of cortical functional connectivity in the motor cortex reorganization in the recovery and how far we can compare the task and resting-state results using fNIRS. The results from the study can be summarized in the following lines. The task-based responses from the healthy group aligned with previously reported results from fMRI and a few fNIRS studies. The contralateral activation pattern for the healthy subjects and ipsilateral inhibition were obtained individually and in the group analysis. The patient group showed deviation in the task-based response from the healthy group. There were significant bilateral responses from the M1 areas and the premotor areas after the onset of the stroke. The task-related responses shifted to a unilateral activation of M1 areas, SMA and premotor areas.

The RSFC analysis yielded a symmetric correlation pattern for the M1 areas and SMA for the healthy group. Stroke causes a disruption of this symmetry in the RSFC as is seen for the patient group. The same patient group when assessed over time and in due course of recovery, the RSFC pattern has changed towards normalcy. The cortical functional connectivity changes indicating the reorganization of functional connections could be seen in the post-recovery assessment. The motor area connections were seen

increasing in the affected hemisphere and the inter-hemispheric somatosensory connections also improved.

In this study, with the help of fNIRS modality, the task-based results and the RSFC results indicate a change in the cortical activations and functional connections occur over a period of time in the process of recovery. The fNIRS modality could be used in such assessments, as the measurement of the patient's response is obtained at the bedside (the convenient place for the subject). The major implication of the study will be the potential of fNIRS being used as a marker for upper limb recovery using the RSFC results. This information from a larger cohort can be used in designing the prediction of recovery from a stroke when applied to a robust classification algorithm. This may be useful in planning subject-specific rehabilitation strategies for stroke survivors using a brain-computer interface. The portable nature of the neuroimaging modality used will be an added advantage when used in such systems.

# Bibliography

Arenth, P.M., Ricker, J.H., Schultheis, M.T., 2007. Applications of Functional Near-Infrared Spectroscopy (fNIRS) to Neurorehabilitation of Cognitive Disabilities. The Clinical Neuropsychologist 21, 38–57. https://doi.org/10.1080/13854040600878785

Baron, J.-C., Black, S.E., Butler, A.J., Carey, J., Chollet, F., Cohen, L.G., Corbetta, M., Cramer, S.C., Dobkin, B.H., Frackowiak, R., Heiss, W.D., Johansen-Berg, H., Krakauer, J.W., Lazar, R.M., Lennihan, L.L., Loubinoux, I., Marshall, R.S., Matthews, P., Mohr, J.P., Nelles, G., Pascual-Leone, A., Pomeroy, V., Rijntjes, M., Rossini, P.M., Rothwell, J.C., Seitz, R.J., Small, S.L., Sunderland, A., Ward, N.S., Weiller, C., Wise, R.J.S., 2004. Neuroimaging in Stroke Recovery: A Position Paper from the First International Workshop on Neuroimaging and Stroke Recovery. Cerebrovasc Dis 18, 260–267.

Biswal, Bharat, Yetkin, F.Z., Haughton, V.M., Hyde, J.S., 1995. Functional connectivity in the motor cortex of resting human brain using echo-planar mri. Magnetic Resonance in Medicine 34, 537–541. https://doi.org/10.1002/mrm.1910340409

Biswal, B., Yetkin, F.Z., Haughton, V.M., Hyde, J.S., 1995. Functional connectivity in the motor cortex of resting human brain using echo-planar MRI. Magn Reson Med 34, 537–541. https://doi.org/10.1002/mrm.1910340409

Boas, D.A., Dale, A.M., Franceschini, M.A., 2004. Diffuse optical imaging of brain activation: approaches to optimizing image sensitivity, resolution, and accuracy. Neuroimage 23 Suppl 1, S275-288. https://doi.org/10.1016/j.neuroimage.2004.07.011

Bonzano, L., Palmaro, E., Teodorescu, R., Fleysher, L., Inglese, M., Bove, M., 2015. Functional connectivity in the resting-state motor networks influences the kinematic processes during motor sequence learning. Eur J Neurosci 41, 243–253. https://doi.org/10.1111/ejn.12755

Borich, M.R., Brodie, S.M., Gray, W.A., Ionta, S., Boyd, L.A., 2015. Understanding the role of the primary somatosensory cortex: Opportunities for rehabilitation. Neuropsychologia 79, 246–255. https://doi.org/10.1016/j.neuropsychologia.2015.07.007

Brunetti, M., Morkisch, N., Fritzsch, C., Mehnert, J., Steinbrink, J., Niedeggen, M., Dohle, C., 2015. Potential determinants of efficacy of mirror therapy in stroke patients--A pilot study. Restor. Neurol. Neurosci. 33, 421–434. https://doi.org/10.3233/RNN-140421

Buetefisch, C.M., 2015. Role of the Contralesional Hemisphere in Post-Stroke Recovery of Upper Extremity Motor Function. Front Neurol 6. https://doi.org/10.3389/fneur.2015.00214

Calautti, C., Baron, J.-C., 2003. Functional Neuroimaging Studies of Motor Recovery After Stroke in Adults: A Review. Stroke 34, 1553–1566. https://doi.org/10.1161/01.STR.0000071761.36075.A6

Cao Y., D'Olhaberriague L., Vikingstad E. M., Levine S. R., Welch K. M. A., 1998. Pilot Study of Functional MRI to Assess Cerebral Activation of Motor Function After Poststroke Hemiparesis. Stroke 29, 112–122. https://doi.org/10.1161/01.STR.29.1.112

Carter, A.R., Astafiev, S.V., Lang, C.E., Connor, L.T., Rengachary, J., Strube, M.J., Pope, D.L.W., Shulman, G.L., Corbetta, M., 2010. Resting interhemispheric functional magnetic resonance imaging connectivity predicts performance after stroke. Ann. Neurol. 67, 365–375. https://doi.org/10.1002/ana.21905

Carter, A.R., Shulman, G.L., Corbetta, M., 2012. Why use a connectivity-based approach to study stroke and recovery of function? NeuroImage, Connectivity 62, 2271–2280. https://doi.org/10.1016/j.neuroimage.2012.02.070

Chance, B., Zhuang, Z., UnAh, C., Alter, C., Lipton, L., 1993. Cognition-activated low-frequency modulation of light absorption in human brain. Proc Natl Acad Sci U S A 90, 3770–3774.

Damoiseaux, J.S., Rombouts, S. a. R.B., Barkhof, F., Scheltens, P., Stam, C.J., Smith, S.M., Beckmann, C.F., 2006. Consistent resting-state networks across healthy subjects. Proc. Natl. Acad. Sci. U.S.A. 103, 13848–13853. https://doi.org/10.1073/pnas.0601417103

Davies, D.J., Clancy, M., Lighter, D., Balanos, G.M., Lucas, S.J.E., Dehghani, H., Su, Z., Forcione, M., Belli, A., 2017. Frequency-domain vs continuous-wave near-infrared spectroscopy devices: a comparison of clinically viable monitors in controlled hypoxia. J Clin Monit Comput 31, 967–974. https://doi.org/10.1007/s10877-016-9942-5

Dodd, K.C., Nair, V.A., Prabhakaran, V., 2017. Role of the Contralesional vs. Ipsilesional Hemisphere in Stroke Recovery. Front Hum Neurosci 11. https://doi.org/10.3389/fnhum.2017.00469

Duan, L., Zhang, Y.-J., Zhu, C.-Z., 2012. Quantitative comparison of resting-state functional connectivity derived from fNIRS and fMRI: A simultaneous recording study. NeuroImage 60, 2008–2018. https://doi.org/10.1016/j.neuroimage.2012.02.014

fNIRS Analysis [WWW Document], n.d. URL https://nirx.net/fnirs-analysis (accessed 8.26.19).

Fox, M.D., Raichle, M.E., 2007. Spontaneous fluctuations in brain activity observed with functional magnetic resonance imaging. Nat. Rev. Neurosci. 8, 700–711. https://doi.org/10.1038/nrn2201

Franceschini, M.A., Fantini, S., Thompson, J.H., Culver, J.P., Boas, D.A., 2003. Hemodynamic evoked response of the sensorimotor cortex measured noninvasively with near-infrared optical imaging. Psychophysiology 40, 548–560.

Frías, I., Starrs, F., Gisiger, T., Minuk, J., Thiel, A., Paquette, C., 2018. Interhemispheric connectivity of primary sensory cortex is associated with motor impairment after stroke. Sci Rep 8, 1–10. https://doi.org/10.1038/s41598-018-29751-6

Gobbo, M., Gaffurini, P., Vacchi, L., Lazzarini, S., Villafane, J., Orizio, C., Negrini, S., Bissolotti, L., 2017. Hand Passive Mobilization Performed with Robotic Assistance: Acute Effects on Upper Limb Perfusion and Spasticity in Stroke Survivors [WWW Document]. BioMed Research International. https://doi.org/10.1155/2017/2796815

Grefkes, C., Fink, G.R., 2011. Reorganization of cerebral networks after stroke: new insights from neuroimaging with connectivity approaches. Brain 134, 1264–1276. https://doi.org/10.1093/brain/awr033

Hara, Y., Obayashi, S., Tsujiuchi, kazuhito, Muraoka, Y., 2013. The effects of electromyography-controlled functional electrical stimulation on upper extremity function and cortical perfusion in stroke patients. - PubMed - NCBI [WWW Document]. URL https://www.ncbi.nlm.nih.gov/pubmed/23706813 (accessed 9.19.19).

Hirth, C., Obrig, H., Villringer, K., Thiel, A., Bernarding, J., Mühlnickel, W., Flor, H., Dirnagl, U., Villringer, A., 1996. Non-invasive functional mapping of the human motor cortex using near-infrared spectroscopy. Neuroreport 7, 1977–1981.

Homae, F., Watanabe, H., Otobe, T., Nakano, T., Go, T., Konishi, Y., Taga, G., 2010. Development of Global Cortical Networks in Early Infancy. J. Neurosci. 30, 4877–4882. https://doi.org/10.1523/JNEUROSCI.5618-09.2010

Hoshi, Y., Tamura, M., 1993. Detection of dynamic changes in cerebral oxygenation coupled to neuronal function during mental work in man. Neuroscience Letters 150, 5–8. https://doi.org/10.1016/0304-3940(93)90094-2

Imai, M., Watanabe, H., Yasui, K., Kimura, Y., Shitara, Y., Tsuchida, S., Takahashi, N., Taga, G., 2014. Functional connectivity of the cortex of term and preterm infants and infants with Down's syndrome. NeuroImage 85, 272–278. https://doi.org/10.1016/j.neuroimage.2013.04.080

Jang, S.H., 2011. A review of diffusion tensor imaging studies on motor recovery mechanisms in stroke patients. NeuroRehabilitation 28, 345–352. https://doi.org/10.3233/NRE-2011-0662

Jenkinson, M., Chappell, M., 2017. Introduction to Neuroimaging Analysis, Oxford Neuroimaging Primers. Oxford University Press, Oxford, New York.

Jiang, L., Xu, H., Yu, C., 2013. Brain connectivity plasticity in the motor network after ischemic stroke. Neural Plast. 2013, 924192. https://doi.org/10.1155/2013/924192

Kato, H., Izumiyama, M., Koizumi, H., Takahashi, A., Itoyama, Y., 2002. Near-infrared spectroscopic topography as a tool to monitor motor reorganization after hemiparetic stroke: a comparison with functional MRI. Stroke 33, 2032–2036. https://doi.org/10.1161/01.str.0000021903.52901.97

Kato, H., Izumiyama, M., Shiga, Y., Saito, N., Koizumi, H., Takahashi, A., Itoyama, Y., 2001. [Hand motor cortical area reorganization following cerebral infarction evaluated with functional MRI, near infrared spectroscopic imaging, and transcranial magnetic stimulation]. No To Shinkei 53, 869–874.

Kato, T., Kamei, A., Takashima, S., Ozaki, T., 1993. Human visual cortical function during photic stimulation monitoring by means of near-infrared spectroscopy. J. Cereb. Blood Flow Metab. 13, 516–520. https://doi.org/10.1038/jcbfm.1993.66

Kim, S.G., Ashe, J., Hendrich, K., Ellermann, J.M., Merkle, H., Uğurbil, K., Georgopoulos, A.P., 1993. Functional magnetic resonance imaging of motor cortex: hemispheric asymmetry and handedness. Science 261, 615–617. https://doi.org/10.1126/science.8342027

Kohl, M., Nolte, C., Heekeren, H.R., Horst, S., Scholz, U., Obrig, H., Villringer, A., 1998. Determination of the wavelength dependence of the differential pathlength factor

from near-infrared pulse signals. Phys. Med. Biol. 43, 1771–1782. https://doi.org/10.1088/0031-9155/43/6/028

LaManna, J.C., 2007. In situ measurements of brain tissue hemoglobin saturation and blood volume by reflectance spectrophotometry in the visible spectrum. JBO 12, 062103. https://doi.org/10.1117/1.2804184

Leff, D.R., Orihuela-Espina, F., Elwell, C.E., Athanasiou, T., Delpy, D.T., Darzi, A.W., Yang, G.-Z., 2011. Assessment of the cerebral cortex during motor task behaviours in adults: A systematic review of functional near infrared spectroscopy (fNIRS) studies. NeuroImage 54, 2922–2936. https://doi.org/10.1016/j.neuroimage.2010.10.058

Lu, C.-M., Zhang, Y.-J., Biswal, B.B., Zang, Y.-F., Peng, D.-L., Zhu, C.-Z., 2010. Use of fNIRS to assess resting state functional connectivity. J. Neurosci. Methods 186, 242–249. https://doi.org/10.1016/j.jneumeth.2009.11.010

MacLellan, C.L., Keough, M.B., Granter-Button, S., Chernenko, G.A., Butt, S., Corbett, D., 2011. A critical threshold of rehabilitation involving brain-derived neurotrophic factor is required for poststroke recovery. Neurorehabil Neural Repair 25, 740–748. https://doi.org/10.1177/1545968311407517

Meer, M.P.A. van, Marel, K. van der, Wang, K., Otte, W.M., Bouazati, S. el, Roeling, T.A.P., Viergever, M.A., Sprenkel, J.W.B. van der, Dijkhuizen, R.M., 2010. Recovery of Sensorimotor Function after Experimental Stroke Correlates with Restoration of Resting-State Interhemispheric Functional Connectivity. J. Neurosci. 30, 3964–3972. https://doi.org/10.1523/JNEUROSCI.5709-09.2010

Mihara, M., Miyai, I., 2016. Review of functional near-infrared spectroscopy in neurorehabilitation. Neurophotonics 3. https://doi.org/10.1117/1.NPh.3.3.031414

Miyai, I., Tanabe, H.C., Sase, I., Eda, H., Oda, I., Konishi, I., Tsunazawa, Y., Suzuki, T., Yanagida, T., Kubota, K., 2001. Cortical Mapping of Gait in Humans: A Near-Infrared Spectroscopic Topography Study. NeuroImage 14, 1186–1192. https://doi.org/10.1006/nimg.2001.0905

Miyai, I., Yagura, H., Oda, I., Konishi, I., Eda, H., Suzuki, T., Kubota, K., 2002. Premotor cortex is involved in restoration of gait in stroke. Annals of Neurology 52, 188–194. https://doi.org/10.1002/ana.10274

Mukherjee, P., 2005. Diffusion Tensor Imaging and Fiber Tractography in Acute Stroke. Neuroimaging Clinics of North America 15, 655–665. https://doi.org/10.1016/j.nic.2005.08.010

Murase, N., Duque, J., Mazzocchio, R., Cohen, L.G., 2004. Influence of interhemispheric interactions on motor function in chronic stroke. Ann. Neurol. 55, 400–409. https://doi.org/10.1002/ana.10848

Nakano, T., Watanabe, H., Homae, F., Taga, G., 2009. Prefrontal cortical involvement in young infants' analysis of novelty. Cereb. Cortex 19, 455–463. https://doi.org/10.1093/cercor/bhn096

Niu, H., He, Y., 2014. Resting-state functional brain connectivity: lessons from functional near-infrared spectroscopy. Neuroscientist 20, 173–188. https://doi.org/10.1177/1073858413502707

Niu, H., Khadka, S., Tian, F., Lin, Z.-J., Lu, C., Zhu, C., Liu, H., 2011. Resting-state functional connectivity assessed with two diffuse optical tomographic systems. J Biomed Opt 16, 046006. https://doi.org/10.1117/1.3561687

Obrig, H., Hirth, C., Junge-Hülsing, J.G., Döge, C., Wolf, T., Dirnagl, U., Villringer, A., 1996. Cerebral oxygenation changes in response to motor stimulation. J. Appl. Physiol. 81, 1174–1183. https://doi.org/10.1152/jappl.1996.81.3.1174

Ocklenburg, S., Ball, A., Wolf, C.C., Genç, E., Güntürkün, O., 2015. Functional cerebral lateralization and interhemispheric interaction in patients with callosal agenesis. Neuropsychology 29, 806–815. https://doi.org/10.1037/neu0000193

Park Chang-hyun, Chang Won Hyuk, Ohn Suk Hoon, Kim Sung Tae, Bang Oh Young, Pascual-Leone Alvaro, Kim Yun-Hee, 2011. Longitudinal Changes of Resting-State Functional Connectivity During Motor Recovery After Stroke. Stroke 42, 1357–1362. https://doi.org/10.1161/STROKEAHA.110.596155

Rao, S.M., Binder, J.R., Bandettini, P.A., Hammeke, T.A., Yetkin, F.Z., Jesmanowicz, A., Lisk, L.M., Morris, G.L., Mueller, W.M., Estkowski, L.D., 1993. Functional magnetic resonance imaging of complex human movements. Neurology 43, 2311–2318. https://doi.org/10.1212/wnl.43.11.2311

Reddy, H., Matthews, P.M., Lassonde, M., 2000. Functional MRI cerebral activation and deactivation during finger movement. Neurology 55, 1244–1244. https://doi.org/10.1212/WNL.55.8.1244

Rehme, A.K., Fink, G.R., von Cramon, D.Y., Grefkes, C., 2011. The role of the contralesional motor cortex for motor recovery in the early days after stroke assessed with longitudinal FMRI. Cereb. Cortex 21, 756–768. https://doi.org/10.1093/cercor/bhq140

Remy, P., Zilbovicius, M., Leroy-Willig, A., Syrota, A., Samson, Y., 1994. Movement-and task-related activations of motor cortical areas: a positron emission tomographic study. Ann. Neurol. 36, 19–26. https://doi.org/10.1002/ana.410360107

Saiote, C., Tacchino, A., Brichetto, G., Roccatagliata, L., Bommarito, G., Cordano, C., Battaglia, M., Mancardi, G.L., Inglese, M., 2016. Resting-state functional connectivity and motor imagery brain activation. Human Brain Mapping 37, 3847–3857. https://doi.org/10.1002/hbm.23280

Saitou, H., Yanagi, H., Hara, S., Tsuchiya, S., Tomura, S., 2000. Cerebral blood volume and oxygenation among poststroke hemiplegic patients: Effects of 13 rehabilitation tasks measured by near-Infrared spectroscopy. Archives of Physical Medicine and Rehabilitation 81, 1348–1356. https://doi.org/10.1053/apmr.2000.9400

Scholkmann, F., Kleiser, S., Metz, A.J., Zimmermann, R., Mata Pavia, J., Wolf, U., Wolf, M., 2014. A review on continuous wave functional near-infrared spectroscopy and imaging instrumentation and methodology. NeuroImage 85, 6–27. https://doi.org/10.1016/j.neuroimage.2013.05.004

Seidler, R.D., Bernard, J.A., Burutolu, T.B., Fling, B.W., Gordon, M.T., Gwin, J.T., Kwak, Y., Lipps, D.B., 2010. Motor control and aging: links to age-related brain structural, functional, and biochemical effects. Neurosci Biobehav Rev 34, 721–733. https://doi.org/10.1016/j.neubiorev.2009.10.005

Smitha, K., Akhil Raja, K., Arun, K., Rajesh, P., Thomas, B., Kapilamoorthy, T., Kesavadas, C., 2017. Resting state fMRI: A review on methods in resting state connectivity analysis and resting state networks. Neuroradiol J 30, 305–317. https://doi.org/10.1177/1971400917697342

Smitha, K.A., Akhil Raja, K., Arun, K.M., Rajesh, P.G., Thomas, B., Kapilamoorthy, T.R., Kesavadas, C., 2017. Resting state fMRI: A review on methods in resting state connectivity analysis and resting state networks. Neuroradiol J 30, 305–317. https://doi.org/10.1177/1971400917697342

Son, S.M., Park, S.H., Moon, H.K., Lee, E., Ahn, S.H., Cho, Y.W., Byun, W.M., Jang, S.H., 2009. Diffusion tensor tractography can predict hemiparesis in infants with high

risk factors. Neuroscience Letters 451, 94–97. https://doi.org/10.1016/j.neulet.2008.12.033

Stormtrooper, 2014. An Updated Definition of Stroke for the 21st Century: A Statement for Healthcare professionals from the American Heart Association/American Stroke Association [WWW Document]. URL https://www.cns.org/guidelines/updated-definition-stroke-21st-century-statement-healthcare-professionals-american-hear-0 (accessed 8.26.19).

Strangman, G., Goldstein, R., Rauch, S.L., Stein, J., 2006. Near-Infrared Spectroscopy and Imaging for Investigating Stroke Rehabilitation: Test-Retest Reliability and Review of the Literature. Archives of Physical Medicine and Rehabilitation, Neuroplasticity and Brain Imaging Research: Implications for Rehabilitation 87, 12–19. https://doi.org/10.1016/j.apmr.2006.07.269

Takeda, K., Gomi, Y., Imai, I., Shimoda, N., Hiwatari, M., Kato, H., 2007. Shift of motor activation areas during recovery from hemiparesis after cerebral infarction: A longitudinal study with near-infrared spectroscopy. Neuroscience Research 59, 136–144. https://doi.org/10.1016/j.neures.2007.06.1466

Tan, Q., Zhang, Ming, Wang, Yi, Zhang, Manyu, Wang, Yan, Xin, Q., Wang, B., Li, Z., 2015. Frequency-specific functional connectivity revealed by wavelet-based coherence analysis in elderly subjects with cerebral infarction using NIRS method. Medical Physics 42, 5391–5403. https://doi.org/10.1118/1.4928672

Tombari, D., Loubinoux, I., Pariente, J., Gerdelat, A., Albucher, J.-F., Tardy, J., Cassol, E., Chollet, F., 2004. A longitudinal fMRI study: in recovering and then in clinically stable sub-cortical stroke patients. Neuroimage 23, 827–839. https://doi.org/10.1016/j.neuroimage.2004.07.058

Torricelli, A., Contini, D., Pifferi, A., Caffini, M., Re, R., Zucchelli, L., Spinelli, L., 2014. Time domain functional NIRS imaging for human brain mapping. NeuroImage 85, 28–50. https://doi.org/10.1016/j.neuroimage.2013.05.106

Villringer, A., Planck, J., Hock, C., Schleinkofer, L., Dirnagl, U., 1993. Near infrared spectroscopy (NIRS): a new tool to study hemodynamic changes during activation of brain function in human adults. Neurosci. Lett. 154, 101–104. https://doi.org/10.1016/0304-3940(93)90181-j

Ward, N.S., Brown, M.M., Thompson, A.J., Frackowiak, R.S.J., 2003. Neural correlates of motor recovery after stroke: a longitudinal fMRI study. Brain 126, 2476–2496. https://doi.org/10.1093/brain/awg245

Watts, D.J., Strogatz, S.H., 1998. Collective dynamics of "small-world" networks. Nature 393, 440–442. https://doi.org/10.1038/30918

White, B.R., Liao, S.M., Ferradal, S.L., Inder, T.E., Culver, J.P., 2012. Bedside optical imaging of occipital resting-state functional connectivity in neonates. Neuroimage 59, 2529–2538. https://doi.org/10.1016/j.neuroimage.2011.08.094

White, B.R., Snyder, A.Z., Cohen, A.L., Petersen, S.E., Raich-le, M.E., Schlaggar, B.L., Culver, J.P., 2009. Resting-state functional connectivity in the human brain revealed with diffuse optical tomography. Neuroimage 47, 148–156. https://doi.org/10.1016/j.neuroimage.2009.03.058

Xia, M., Wang, J., He, Y., 2013. BrainNet Viewer: A Network Visualization Tool for Human Brain Connectomics. PLOS ONE 8, e68910. https://doi.org/10.1371/journal.pone.0068910

Xu, H., Qin, W., Chen, H., Jiang, L., Li, K., Yu, C., 2014. Contribution of the resting-state functional connectivity of the contralesional primary sensorimotor cortex to motor recovery after subcortical stroke. PLoS ONE 9, e84729. https://doi.org/10.1371/journal.pone.0084729

Xu, J., Liu, X., Zhang, J., Li, Z., Wang, X., Fang, F., Niu, H., 2015. FC-NIRS: A Functional Connectivity Analysis Tool for Near-Infrared Spectroscopy Data [WWW Document]. BioMed Research International. https://doi.org/10.1155/2015/248724

Xu, Y., Xu, Y., Graber, H.L., Graber, H.L., Barbour, R.L., Barbour, R.L., 2014. nirsLAB: A Computing Environment for fNIRS Neuroimaging Data Analysis, in: Biomedical Optics 2014 (2014), Paper BM3A.1. Presented at the Biomedical Optics, Optical Society of America, p. BM3A.1. https://doi.org/10.1364/BIOMED.2014.BM3A.1

Yang, M., Yang, Z., Yuan, T., Feng, W., Wang, P., 2019. A Systemic Review of Functional Near-Infrared Spectroscopy for Stroke: Current Application and Future Directions. Front. Neurol. 10. https://doi.org/10.3389/fneur.2019.00058

Ye, J.C., Tak, S., Jang, K.E., Jung, J., Jang, J., 2009. NIRS-SPM: statistical parametric mapping for near-infrared spectroscopy. Neuroimage 44, 428–447. https://doi.org/10.1016/j.neuroimage.2008.08.036

Zhang, H., Zhang, Y.-J., Lu, C.-M., Ma, S.-Y., Zang, Y.-F., Zhu, C.-Z., 2010. Functional connectivity as revealed by independent component analysis of resting-state fNIRS measurements. Neuroimage 51, 1150–1161. https://doi.org/10.1016/j.neuroimage.2010.02.080

# Appendices

# I.List of Publications

**Arun KM**, Smitha KA, Sylaja P N, Kesavadas C "Identifying Resting-State Functional Connectivity Changes in the Motor Cortex Using fNIRS During Recovery from Stroke" Brain Topogr 33, 710–719 (2020). https://doi.org/10.1007/s10548-020-00785-2

**Arun KM**, Smitha KA, Rajesh PG, Kesavadas C. "Functional near-infrared spectroscopy is in moderate accordance with functional MRI in determining lateralization of frontal language areas". Neuroradiol J. 2017 Oct pp 133-141

Dr. Sujesh Sreedharan, **Arun KM**, Dr. Chandrasekaran Kesavadas, Dr. Sylaja P N, and Dr. Rangantha Sitaram. "Functional Connectivity of Language Regions of Stroke patients with Expressive Aphasia during Real-time fMRI Neurofeedback "Brain Connectivity,http://doi.org/10.1089/brain.2019.0674

Smitha K A, **Arun KM**, Rajesh PG, Bejoy Thomas, Ashalatha Radhakrishnan, Sankara Sarma, C Kesavadas. "Resting fMRI as an alternative for task-based fMRI for language lateralization in temporal lobe epilepsy patients: a study using independent component analysis". Neuroradiology (2019) 61: 803. https://doi.org/10.1007/s00234-019-02209-w

Smitha K A, **Arun KM**, Rajesh PG, Ramesh Venkateshan, Suresh Joel, Kesavadas C, "Multiband fMRI as a Plausible, Time-saving Technique for Resting-state Data Acquisition: Study on Functional Connectivity Mapping using Graph Theoretical Measures". Magnetic Resonance Imaging. 2018 Nov; 53:1-6.

Smitha K A, **Arun KM**, Rajesh PG, Bejoy Thomas, C Kesavadas. "Resting-state seed-based analysis: an alternative to task-based language fMRI and its laterality Index". AJNR Am J Neuroradiol. 2017 Jun;38(6):1187-1192

Smitha KA, Akhil Raja K, **Arun KM**, Rajesh PG, Thomas B, Kapilamoorthy TR, Kesavadas C. "Resting-state fMRI: A review on methods in resting-state connectivity analysis and resting-state networks". Neuroradiol J. 2017 Aug;30(4):305-317

## II.List of Presentations

"Functional near infra-red spectroscopy (fNIRS) - a potential brain monitoring tool", oral presentation at the technical conference, SYNAPSES' 14 held at TKMIT, Kollam, Kerala

"fNIRS based BCI and Its Applications" -oral presentation at BrainConn 2018, a national level conference held at Sree Chitra Tirunal Institute for Medical Sciences and Technology, Trivandrum, December 2018

"Functional Connectivity changes during Real-time fMRI based Neuro-rehabilitation of post stroke Aphasic Patients". Sujesh Sreedharan, Arun K. M., Sylaja P. N., Ranaganatha Sitaram, and Kesavadas C. Proc. Intl. Soc. Mag. Reson. Med. 26 (2018) (Digital Poster)

"Identifying Resting Pattern in Stroke Using fNIRS: A Pilot Study", Arun K M, P N Sylaja, C Kesavadas, Salzburg Mind-Brain Annual Meeting( SAMBA) 2019 (Poster Abstract accepted)